Stony Brook University

Structure and Assembly of *Saccharomyces cerevisiae* Outer Spore Wall

A Dissertation Presented

by

Pei-Chen Coney Lin

To

The Graduate School

In Partial Fulfillment of the

Requirements

for the Degree of

Doctor of Philosophy

in

Biochemistry and Structural Biology

Stony Brook University

August 2013

The Graduate School

Pei-Chen Coney Lin

We, the dissertation committee for the above candidate for the
Doctor of Philosophy degree,
hereby recommend acceptance of this dissertation.

Dr. Aaron Neiman- Dissertation Advisor
Associate Professor, Department of Biochemistry and Cell Biology

Dr. Steven O. Smith - Chairperson of Defense
Professor, Department of Biochemistry and Cell Biology

Dr. Nancy Goroff
Associate Professor, Department of Chemistry

Dr. Erwin London
Professor, Department of Biochemistry and Cell Biology

Dr. Rolf Sternglanz
Professor, Department of Biochemistry and Cell Biology

This dissertation is accepted by the Graduate School

Charles Taber
Interim Dean of the Graduate School

Abstract of the Dissertation

Structure and Assembly of *Saccharomyces cerevisiae* Outer Spore Wall

by

Pei-Chen Coney Lin

Doctor of Philosophy

in

Biochemistry and Structural Biology

Stony Brook University

2013

In *Saccharomycs cerevisiae*, spores are a quiescent, stress-resistant cell type, which can survive for extended periods of time in unfavorable conditions until nutrient conditions are suitable. The outer layers of the spore wall contain chitosan and dityrosine, which are macromolecules specific for the spore. These layers are critical for resistance of the spores to adverse environmental stresses. The dityrosine layer is an unique polymer component of cross-linked N, N'-bisformyl dityrosine. This layer provides a shield from protein-sized attack such as lytic enzymes.

For structural studies, we took advantage of the insolubility of the spore wall materials by using solid-state NMR to examine the components of the spore wall outer layers and the cross-linkage among these components. These studies identified a previously unknown component, which we term χ.

To reveal the proteins involved in dityrosine layer assembly, a synthetic genetic array approach was performed. The study uncovers a highly redundant genetic network, and also identifies new genes involved in outer spore wall formation. Several of the genes have paralogs in the yeast genome. Deletion of the paralog sets cause dityrosine layer defects. Taken together, we conclude that there are different levels of redundancy

to regulate the synthesis of dityrosine layer. The first aspect of redundancy is the genes listed in the network, which may play parallel roles in the alternative pathways of dityrosine layer assembly. The other level of redundancy is the paralogs from the network, which may function on the same pathway of dityrosine layer synthesis.

Table of Contents

List of Abbreviations

ECM, extracellular matrix

GPI, glycosylphosphatidylinositol

Ime1, inducer of meiosis

LDs, lipid droplets

MAPK, Mitogen-Activated Protein Kinase

MOP, meiosis II outer plaque

MSE, middle sporulation element

NMR, nuclear magnetic resonance

PrM, prospore membrane

RTG, return to growth

SEs, sterol esters

SPB, spindle pole body

TAGs, triacylglycerols

TM, transmembrane domain

URS1, upstream repression sequence 1

Chapter 1

Introduction

1.1 Overview of the life cycle of *Saccharomyces cerevisiae*

1.1.1 Life cycle of *S. cerevisiae*

In response to varied environmental conditions, yeast cells can change their physiological status and switch to different developmental pathways. In rich medium, the budding yeast *S. cerevisiae* can grow vegetatively as haploid or diploid cells and exist as stable cultures for repeated rounds of the mitotic cycle. Diploid cells are derived from the mating of haploid cells of opposite mating type, MAT **a** and MAT α. The mating response is triggered by the release of small peptide mating hormones that act on cell surface receptors of the opposite mating type.

When nutrients are absent, both haploid and diploid cells enter stationary phase. Incomplete nutrient depletion may cause diploid cells to grow with an elongated morphology called pseudohyphae or haploids invasive filaments as to explore nutrient sources. Under nitrogen starvation and in the presence of a nonfermentable carbon source, such as acetate, diploid *MAT**a**/MATα* cells can undergo the sequential processes of meiosis and spore formation. The result of meiosis and sporulation is the production of haploid **a** and α gametes which are packaged as spores within the ascus and can lie dormant until environmental conditions become favorable for growth. Nutrients reintroduced allow spore germination and begin the life cycle as haploid cells (Figure 1.1).

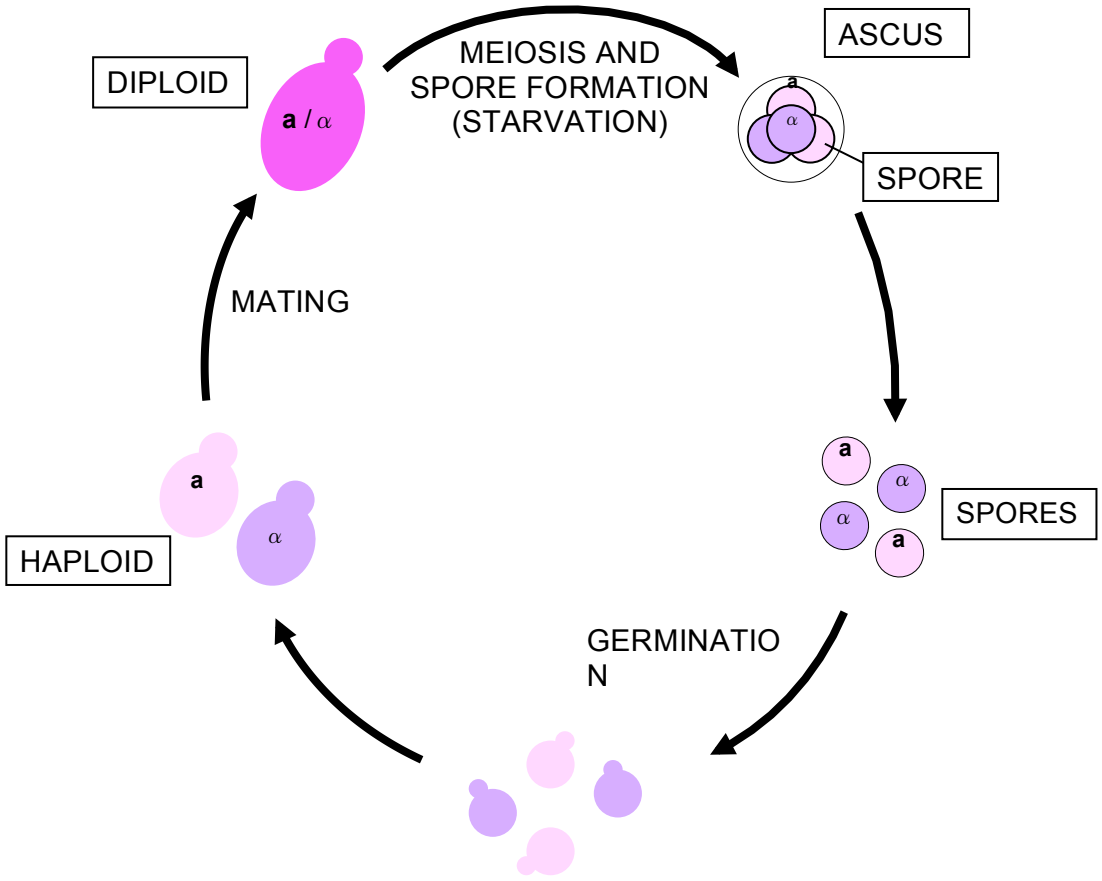

Figure 1.1. The life cycle of *Saccharomyces cerevisiae*. Given appropriate nutrients, yeast cells can grow vegetatively either haploid or diploid form and maintain stable growth with repeated mitotic cycle. Haploids of opposite mating type can mate to each other with the intermediate cell type, shmoo, to form diploids. When nutrients are limited, specifically under nitrogen deficient and with the presence of non-fermentable carbon source, diploid cells can undergo meiosis and sporulation to produce haploid ascospores. Spores have better resistance to tough environmental conditions than stationary cells. If nutrients are reintroduced to the environment, spores can germinate as haploid cells.

1.1.2 Meiosis and sporulation

Only diploid ***a/α*** cells with no defect in the respiratory chain can enter meiosis and sporulation program. In other words, haploids, ***a/a*** or *α/α* diploid cells, and petites wouldn't be able to. Sporulation is induced by starvation. The key nutritional factors for cells to decide to enter this program is a lack of nitrogen and glucose as well as the presence of a non-fermentable carbon source. In addition, sporulation-competent cells have to be in the G1 phase of the cell cycle and have reached a minimum size (DICKINSON 2004).

In meiosis, a single round of DNA replication during premeiotic S phase is followed by two cycles of meiotic divisions. In meiosis I, the spindle pole body (SPB) duplicates, and both chromatids of homologous chromosomes segregate to opposite spindle poles. The individual daughter cell in this stage therefore contains homologous chromosomes comprising two chromatids. The sporulation program starts from meiosis II. During meiosis II, SPBs duplicate again, and the chromatids of each chromosome segregate to opposite spindle poles to produce four haploid nuclei. The meiosis II SPBs are modified and therefore can dock and recruit vesicles to the cytosolic side of SPBs. There, the vesicles under SNARE mediated fusion to form prospore membranes (PrMs) (NEIMAN 1998; JANTTI *et al.* 2002).

In meiosis II, sporulation specific proteins including Mpc54p, Spo21p, Spo74p and Ady4p along with constitutively expressed Cnm67p and Nud1p form the meiosis II outer plaque (MOP) complex layered on the top of the central plaque Spc42p(KNOP and STRASSER 2000; NICKAS *et al.* 2003; MATHIESON *et al.* 2010). The MOP components serve as the platform for vesicle docking (RIEDEL *et al.* 2005; NAKANISHI *et al.* 2006). For vesicle fusion process during prospore membrane formation, a SNARE complex comprised of the t-SNARE Sso1p/Spo20p and v-SNARE Snc1/2p are needed (NEIMAN 1998; JANTTI *et al.* 2002; YANG *et al.* 2008). By the end of meiosis II, each of the four

prospore membranes completely engulfs a newly formed haploid nucleus and closes. The final process of sporulation is spore wall assembly by depositing spore wall components in the lumen between two layers of the prospore membrane (Figure 1.2) (LYNN and MAGEE 1970; NEIMAN 2005).

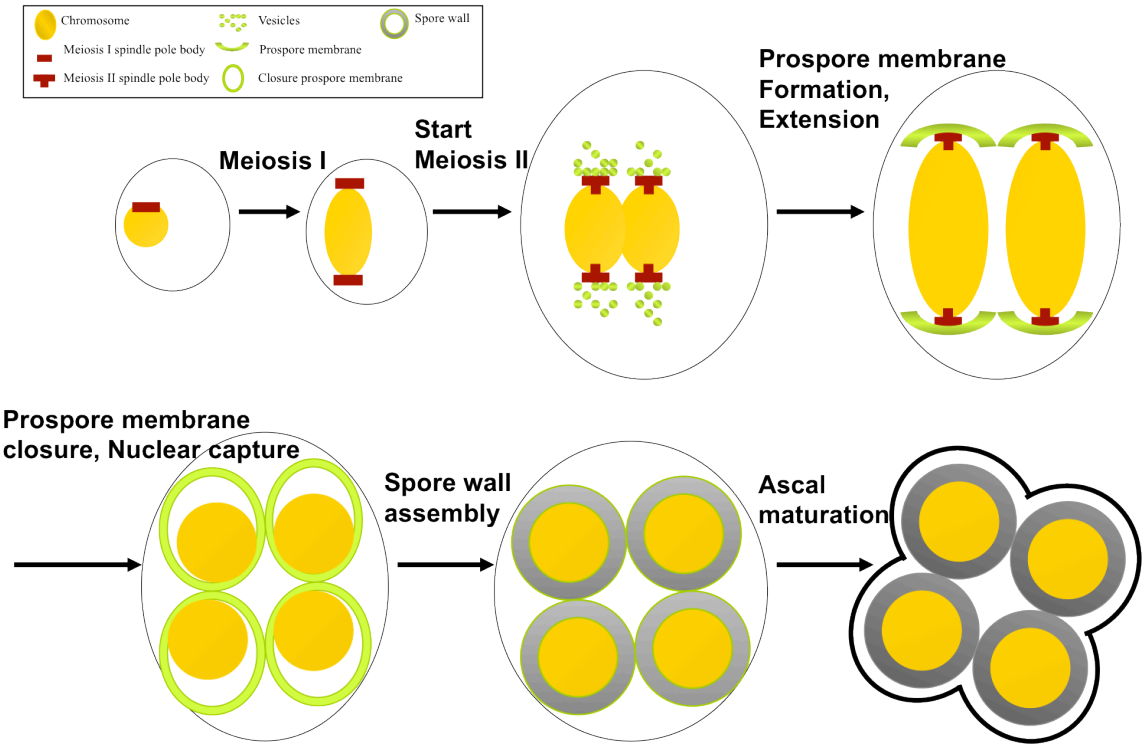

Figure 1.2. The sporulation process of *S. cerevisiae*. (Modified from (NEIMAN 2005) Sporulation starts from meiosis II: two spindle pole bodies duplicate and the chromatids of one chromosome segregate to opposite spindle poles to produce four haploid nuclei. SPBs are modified and can dock and recruit vesicles to form prospore membranes. By the end of meiosis II, each prospore membrane engulfs haploid nucleus and closes. The final process of sporulation is spore wall assembly. Spore wall materials are deposited in the lumen of prospore membrane.

1.1.3 Transcriptional regulation during sporulation

Entering sporulation is strictly regulated by environmental nutrient conditions. However, even cells that have reached the early stages of meiosis can resume vegetative growth if nutrients are reintroduced, termed return to growth (RTG). The stage which cells couldn't return to growth, called commitment (to meiosis), occurs when cells exit from meiotic prophase and enter meiosis I nuclear division(FRIEDLANDER *et al.* 2006). After the "commitment point", cells will still continue sporulation process even though nutrients exist. Based on microarray analysis, during sporulation, there are approximately 1,000 specifically expressed genes and can be classified into three main classes, termed early, middle, and late genes(CHU and HERSKOWITZ 1998; PRIMIG *et al.* 2000). In the program time frame, early genes are induced in the beginning of meiotic prophase, middle genes are expressed around later stage of meiosis and in the beginning of spore formation, and late genes are activated during spore formation.

Regulation of early genes expression

The initiation of meiosis and expression of early genes are triggered by the transcription factor Ime1 (inducer of meiosis 1)(KASSIR *et al.* 1988; SMITH *et al.* 1990). The regulatory element URS1 (upstream repression sequence 1) serves as promoter of most early genes and associates with Ume6 which functions as a repressor but also can be an activator depending on the binding partners (STRICH *et al.* 1994; ANDERSON *et al.* 1995; STEBER and ESPOSITO 1995; WILLIAMS *et al.* 2002). As shown in Figure 1.3, when Ume6 interacts with Sin3-Rpd3 and Isw2 repressor complex, it acts as a repressor (KADOSH and STRUHL 1998; GOLDMARK *et al.* 2000; VERSHON and PIERCE 2000; FAZZIO *et al.* 2001), while the binding of Ime1 to Ume6 activates the early sporulation genes by relieving the interactions between the repressor complex and Ume6. The early gene set is involved in pre-meiotic DNA replication, chromosome recombination, synaptonemal

complex formation, sister chromatids, centromere cohesion (PRIMIG *et al.* 2000), and the induction of subsequent middle genes, including Ndt80 and Ime2. Both Ndt80 and Ime2 are important regulators for the middle genes expression.

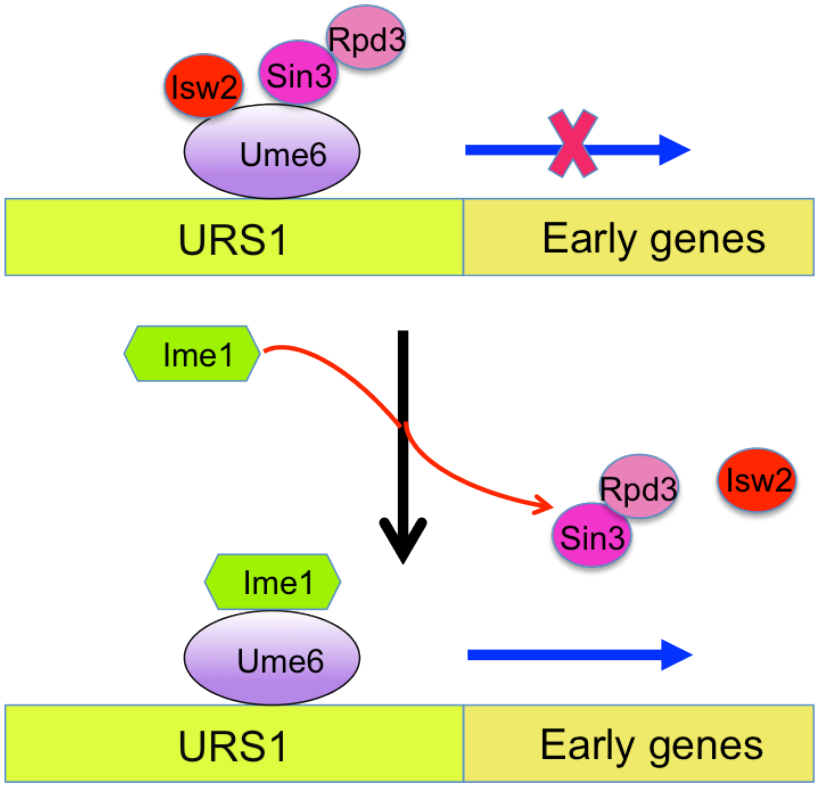

Figure 1.3 Regulation of early gene expression through Ume6p/Ime1p.

Regulation of middle genes expression

Middle genes expression starts from the first meiotic division and the master regulator for this stage is the Ndt80 transcription factor. The middle gene set can either be repressed or activated by the binding of Sum1 or Ndt80 to MSE (middle sporulation element)

sequence, respectively (Figure 1.4). As shown in the diagram of Figure 1.4, two promoter elements, URS1 and MSE are located upstream of NDT80 as well as middle genes coding sequence and regulate the transient activation by different combination of regulatory proteins. Similar to the regulatory of URS1 and early genes set, the binding of Ime1/Ume6 to URS1 is the first step to induce the activation of the successive process. Both Sum1 and Ndt80 have binding affinity to the MSE sequence. The phosphorylation of Sum1 by Ime2/Cdk1/Cdc7 causes the release of Hst1 (from Sum1) and weakens the binding affinity with MSE element (SHIN *et al.* 2010). Further phosphorylation of Ndt80 by Ime2 and the accumulation hyperphosphorylated of Ndt80 leads to high binding affinity of Ndt80 for the MSE and also promote even higher expression level of Ndt80p (PAK and SEGALL 2002; PIERCE *et al.* 2003; AHMED *et al.* 2009).

Regulation of mid-late and late genes expression

The mid-late genes set is activated around the end of meiosis. The mid-late and late genes are involved in post-meiotic differentiation and encode proteins required for spore maturation. There is relatively little known about the regulatory mechanisms at this step. Among the mid-late genes, *DIT1* is needed for spore wall maturation (PRIMIG *et al.* 2000). The expression of late genes set can be repressed by a Tup1/Ssn6 complex. Ndt80 and Sum1 may also be involved in the regulatory of *DIT1* expression (FRIESEN *et al.* 1997; MIZUNO *et al.* 1998). The transcription factor Gis1 is required for the induction of *DIT1* (COLUCCIO *et al.* 2004a). So far, no transcription factor for the late genes has been identified.

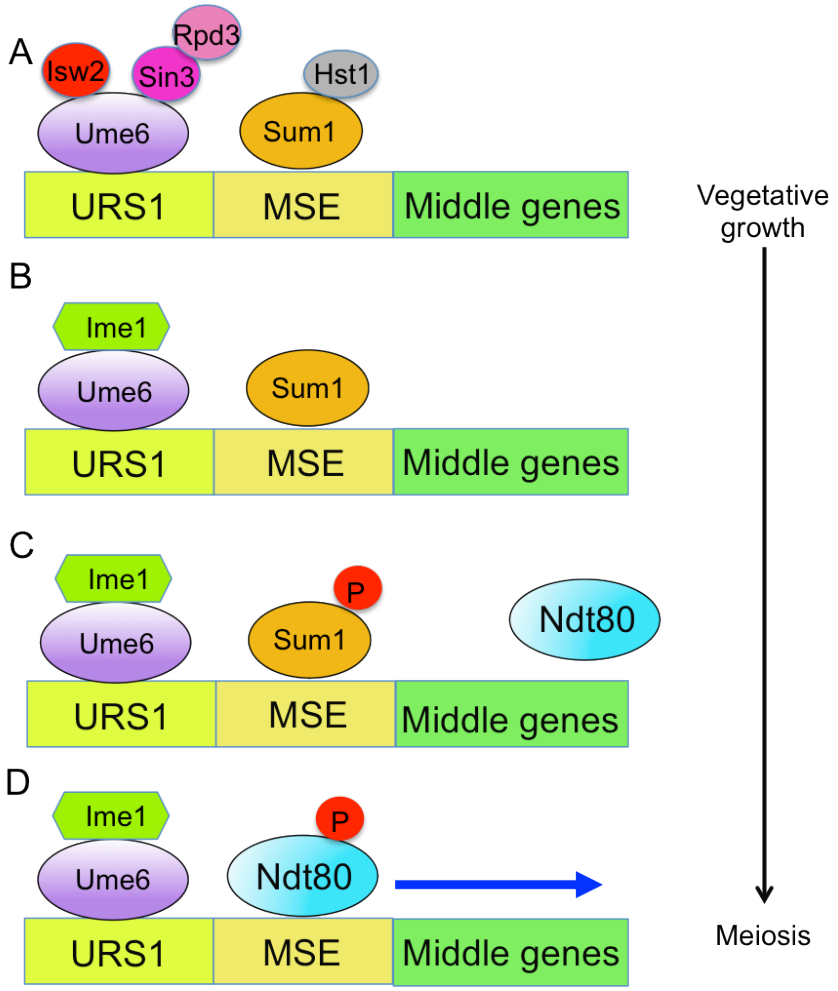

Figure 1.4 Regulation of middle gene expression through Ndt80.

1.2 Yeast spore wall assembly

1.2.1 Significance of spore wall

Outside of the cell plasma membrane, the extracellular matrix (ECM) is the structural component that provides not only a physical scaffold for the cell but also gives biochemical and biomechanical cues for cell morphogenesis and developmental processes (FRANTZ *et al.* 2010). In fungi, the extracellular matrix contains both polysaccharides and protein complexes and is referred to as the cell wall. As cell walls are essential for cellular integrity, and the virulence of a diverse group of pathogenic fungi such as *Candida*, *Cryptococcus neoformans*, and *Aspergillus fumigatus* for immune-compromised patients, fungal cell walls are an attractive target for antifungal drug development. *S. cerevisiae* vegetative cell wall has been extensively studied as a model for understanding fungal walls. Studying the spore wall can be considered an expansion of this theme. Actually, spore walls are similar to cell walls in some ways in terms of a partial overlap in composition. More importantly, the spore wall also contains components that aren't found in *S. cerevisiae* vegetative walls, but exist in certain morphogenetic stages of pathogenic yeasts. From the physiological and biochemical point of view, the spore wall serves protective function with physical rigidity to sustain tough environmental conditions. These unique properties drive the strong motivation for studying the spore wall.

1.2.2 Overview of yeast spore wall

The spore wall consists of four layers, mannan, β-1,3-glucan, chitosan, and dityrosine (Figure 1-5A). The inner two layers are composed of mannan and β-1,3-glucan, which are also the major components of the vegetative cell wall (Figure 1-5B).The outer two layers are specific to the spore wall. The third layer consists mainly of chitosan, a β-1,4-

linked glucosamine polymer, and the outermost layer is the dityrosine layer, which is enriched in an insoluble macromolecule containing cross-linked N, N'-bisformyl dityrosine (BRIZA *et al.* 1996). The outer two layers are essential for the resistance of the spores to adverse environmental conditions, such as to elevated temperature, to certain organic solvents, and to hydrolysis by lytic enzymes, and is necessary to allow passage through the gut of *Drosophila* (BRIZA *et al.* 1990b; SMITS *et al.* 2001; COLUCCIO *et al.* 2008).

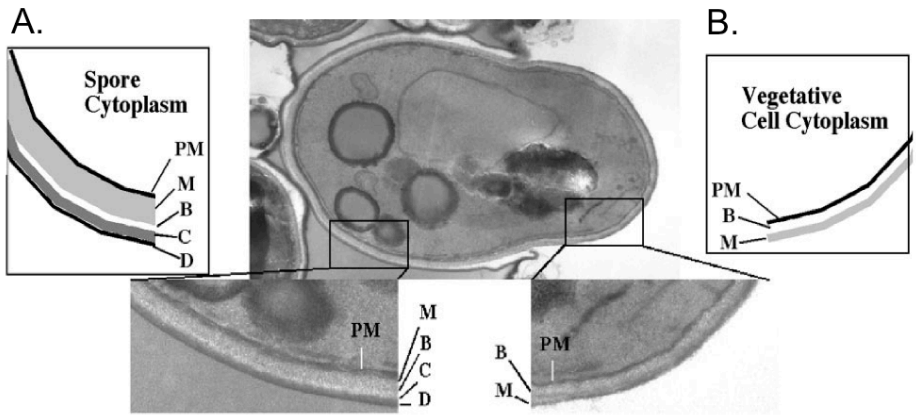

Figure 1.5 The composition of (A) spore wall and (B) vegetative cell wall. (A) From inside (PM, plasma membrane) to outside: M=mannan; B=β-glucan; C=chitosan; D=dityrosine. (B) From inside to outside: B=β-glucan; M= mannan. (Reproduced from (NEIMAN 2005)).

1.2.3 The order of spore wall assembly

Spore wall assembly begins in the lumen of the two membranes derived from the closure of the prospore membrane (LYNN and MAGEE 1970; NEIMAN 2011). The layers of spore wall materials are deposited in a temporal order matching with the final order from the innermost mannan layer, β-glucan layer, chitosan layer, and then, the dityrosine layer (TACHIKAWA *et al.* 2001).

Mannan and β-glucan layers: Glucose and mannose are the major constituents of spore wall represent 55% and 17% of total dry weight, respectively (Table 1.1) (BRIZA *et al.* 1988). Both glucan and mannan are bound to structural proteins (BARTNICKI-GARCIA 1968; FARKAS 1979). Mannoproteins can be linked to β-1,6-glucose chains through a glycosylphosphatidylinositol (GPI) anchor or to β-1,3-glucan through an alkali-sensitive bond. The glucan layer is composed of a degree of polymerization of around 1,500 glucose units per chain. In the wall extracts, β-1,3-glucan is found as a branched polymer with β-1,6-interchain linkages as well as β-1,4-linkages to the other wall components. (KOLLAR *et al.* 1995; KOLLAR *et al.* 1997; MRSA *et al.* 1997; DIJKGRAAF *et al.* 2002).

Table 1.1 (BRIZA *et al.* 1988)
Chemical composition of vegetative cell wall and spore wall

	Spore wall	Cell wall
	wt %	wt %
Glucose	55	45
Mannose	17	40
Glucosamine	9	2
Protein	11	8
Phosphate	0.2	not determined

The *GIP1* gene is suggested to link the onset of spore wall synthesis to closure of the prospore membrane. The "prospore wall" in *gip1*Δ mutants contains only the mannoproteins present during prospore membrane formation; no additional spore wall material is deposited after the completion of prospore membrane closure(TACHIKAWA *et al.* 2001). *spo73*Δ mutant shows no visible spores under light microscope and only present a subtle deposition of mannan layer under electron microscope. The phenotype of

*spo*73 mutants is further confirmed by FITC-ConA stain for mannan under fluorescence microscope and biochemical analysis for (other) spore wall components (COLUCCIO *et al.* 2004a). Actually, mannoproteins are deposited as early as the prospore membrane forms (TACHIKAWA *et al.* 2001). As the further β-glucans, chitosan, or dityrosine formation is arrested in *spo73*Δ spores, this may indicate that additional deposition is necessary before the β-1,3-glucan deposition (COLUCCIO *et al.* 2004a).

In *S. cerevisiae*, three genes encode predicted β-1,3-glucan synthases: *FKS1*, *FKS2* and *FKS3*. *FKS1* is primarily expressed during vegetative growth, whereas *FKS2* is induced under starvation, sporulation as well as in response to mating pheromones (INOUE *et al.* 1995; MAZUR *et al.* 1995; MAZUR and BAGINSKY 1996). Fks3p, has similarity to β-1,3-glucan synthase catalytic subunits Fks1p and Fks2p, also contributes some function as *fks3*Δ mutants have been shown to have spore wall defects (ISHIHARA *et al.* 2007; SUDA *et al.* 2009).

Several genes are required to properly assemble/organize the β-glucan layer of the spore wall, including *SPO77*, *SPS2*, *SPS22* and *SSP2*. These gene deletion mutants form normal prospore membranes but do not produce spores visible in the light microscope. Although electron micrographs reveal deposition of wall materials, these mutants still cannot form an intact β-glucan layer (SARKAR *et al.* 2002; COLUCCIO *et al.* 2004a; COLUCCIO *et al.* 2004b).

Chitosan layer: Chitosan is made in a two-step process: polymerization of UDP-GlcNAc by chitin synthase to form chitin followed by a chitin deacetylase acting *in situ* on nascent chitin (BRIZA *et al.* 1988; PAMMER *et al.* 1992). In sporulating cells, Chs3p perform the function of chitin synthesis (PAMMER *et al.* 1992), followed by Cda1p and Cda2p function in the conversion of chitin to chitosan by deacetylation of N-acetyl

glucosamine residues and form the β-1,4-glucosamine polymer (CHRISTODOULIDOU *et al.* 1996; MISHRA *et al.* 1997; CHRISTODOULIDOU *et al.* 1999).

*chs3*Δ mutants cannot form a chitosan layer. Without the construction of chitosan layer, the dityrosine layer is not formed (COLUCCIO *et al.* 2004a). A *cda1*Δ*cda2*Δ mutant strain also fails to form a distinct chitosan layer although it contains 25% of total glucosamine compare to the WT strain (CHRISTODOULIDOU *et al.* 1996; CHRISTODOULIDOU *et al.* 1999). The defect in *cda1*Δ*cda2*Δ implies that without deacetylation, chitin cannot form a layer or incorporate into the wall with other layers.

Several genes have been shown to contribute to the organization of the chitosan layer, including *GIS1*, *MUM3* and *OSW1* (see below) (COLUCCIO *et al.* 2004a).

1.2.4 Inter-layer organization

Since wall components are deposited from innermost to outermost with respect to the spore cytoplasm, enzymatic activities must be necessary for the formation of cross-links between the spore wall polymers. The cross-linkage of different layers also contributes to a robust spore coat, which has been shown for several mutants having wall defects.

CRR1, encoding a putative transglycosidase, is involved in the cross-linking between β-glucan and chitosan layers. Because of the linkage defect, *crr1*Δ spores are sensitive to temperature shock (55°C), permeable for calcofluor staining, and display an unusual ruffle phenotype of the outer layers under electron microscope (GOMEZ-ESQUER *et al.* 2004).

1.2.5 Regulation of spore wall assembly

The sporulation-specific MAPK (Mitogen-Activated Protein Kinase), Smk1p, seems to be a critical regulator for spore wall assembly (KRISAK *et al.* 1994). Like other MAPKs, it is controlled by dual phosphorylation of the T-X-Y motif (SCHABER *et al.*

2002; HUANG *et al.* 2005), and increasing Smk1 activity sequentially coordinates spore wall assembly (WAGNER *et al.* 1999). As for the genetic interactions among Smk1 and other proteins: Swm1p, a nuclear-localized APC subunit during sporulation process, with Smk1p and Sps1p are required for full expression of the mid-late and late genes (NEIGEBORN and MITCHELL 1991; UFANO *et al.* 1999). *ssp2*Δ spores show reduced phosphorylation level of Smk1p (MCDONALD *et al.* 2005). Ime1 induces higher level of phosphorylated Smk1 (MCDONALD *et al.* 2009). The coordinator function of Smk1 that regulates the next layer assembly at the appropriate time as well as distinct Smk1p activity thresholds in distinct sporulation events indicate the key regulatory role (WAGNER *et al.* 1999; HUANG *et al.* 2005). There are several candidates that may function with Smk1 in the same pathway. *SSP2, CRR1, SPO77, OSW1*, and *MUM3* are required for the proper organization of the outer layers, and may work with or in parallel with Smk1 to regulate the transition between inner and outer spore wall deposition (HUANG *et al.* 2005).

1.3 Properties of dityrosine layer

1.3.1 Overview of dityrosine

Dityrosine was first recognized in 1955 and can be distinguished by a 420 nm fluorescence under excitation at either 284 nm (acidic solutions) or 315 nm (alkaline solutions) (GROSS and SIZER 1959). These properties enable the detection of dityrosine in fluorescence microscopy studies (Figure 1-6).

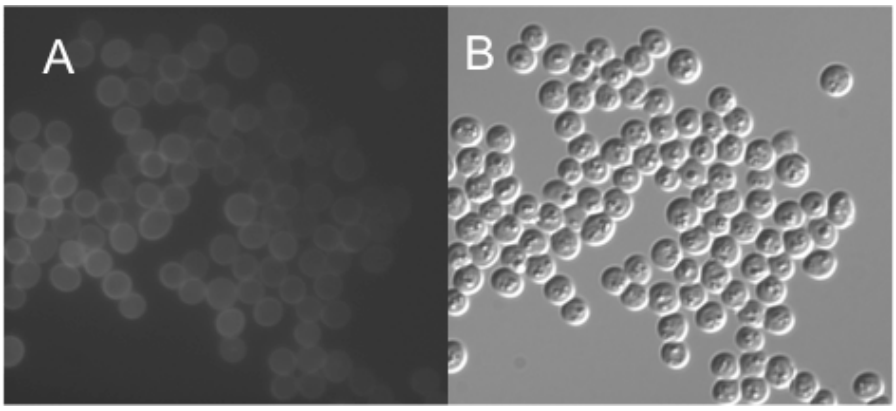

Figure 1-6. Dityrosine fluorescence of *S. cerevisiae* spores (A) Natural fluorescence image of purified wild-type spores in 5% ammonia solution under dityrosine filter set (B) Differential interference (DIC) image of (A).

Dityrosine can be found in many structures, including insect cuticle protein (ANDERSEN 1964), the spore coat of *Bacillus subtilis* (PANDEY and ARONSON 1979), and the fertilization membrane of the sea urchin egg (FOERDER and SHAPIRO 1977). In these cases, dityrosine crosslinks occur as a posttranslational modification of proteins and confer resistance and protective functions because of the stabilizing crosslink (GIULIVI *et al.* 2003). Dityrosine can also be found in non-structural proteins as a product of oxidative stress (AESCHBACH *et al.* 1976; GIULIVI and DAVIES 1993; GIULIVI and DAVIES 1994). Moreover, increased amount of dityrosine in urine has been found in aging and

patients with systemic inflammation (LEEUWENBURGH *et al.* 1999b; LEEUWENBURGH *et al.* 1999a; BHATTACHARJEE *et al.* 2001).

1.3.2 Uniqueness of *S. cerevisiae* dityrosine

In the *S. cerevisiae* spore wall, the dityrosine layer appears as a very thin layer in the electron microscope (Figure 1-5). However, unlike the dityrosine that serves as structural functions in other organisms, the dityrosine in the spore wall is not created by cross-linking between peptides but is synthesized directly from the amino acid L-tyrosine (BRIZA *et al.* 1994; BRIZA *et al.* 1996; NEIMAN 2005). The importance of the dityrosine layer is shown by the increased sensitivity of *dit1*Δ mutant spores, which lack the dityrosine layer, to lytic enzymes, ether vapor, elevated temperature (BRIZA *et al.* 1990a), and passage through the gut of *Drosophila* (COLUCCIO *et al.* 2008).

1.3.3 Proteins involved in dityrosine formation

In sea urchin eggs, a peroxidase was reported to function in the cross-linking of two tyrosine residues (DEITS *et al.* 1984). However, in the yeast spore wall, dityrosine monomers are synthesized by a two-step process (Figure 1-7) that takes place in the cytoplasm of the maturing spores (BRIZA *et al.* 1990a; BRIZA *et al.* 1994; FELDER *et al.* 2002). First, L-tyrosine is modified by Dit1p, resulting in the formation of N-formyl tyrosine. Next, two molecules of N-formyl tyrosine are cross-linked by Dit2p forming bisformyl dityrosine (Figure 1-7) (BRIZA *et al.* 1996). Dtr1p, which localizes in the prospore membrane, then serves as a transporter to transport bisformyl dityrosine through the prospore membrane. Finally, dityrosine monomers will be incorporated into the maturing spore wall (FELDER *et al.* 2002).

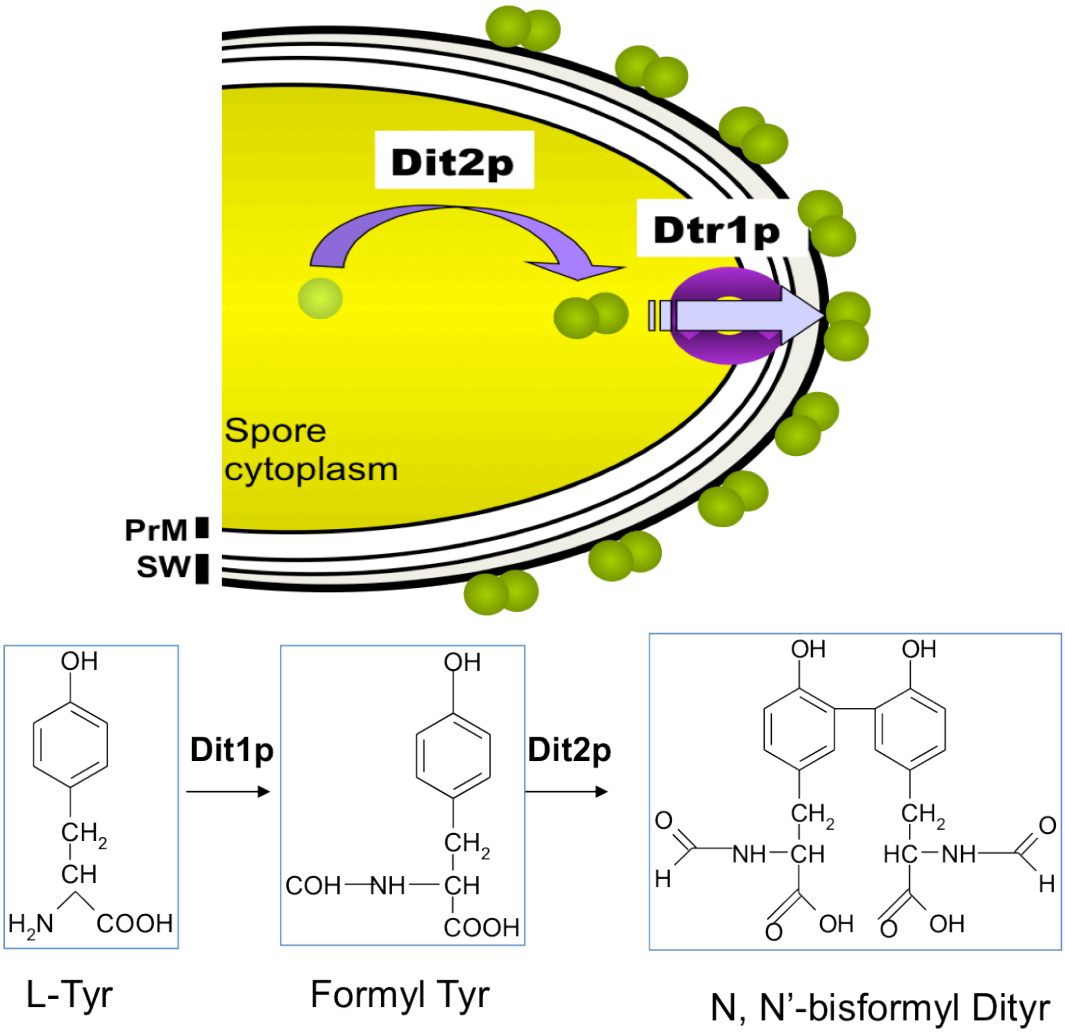

Figure 1-7. Yeast spore wall monomeric dityrosine synthesis process

1.3.4 Dityrosine common properties- from *Saccharomyces cerevisiae* to *Candida albicans*

The yeast *Candida albicans* is the most frequently isolated fungal pathogen in humans, causing systemic infection in immunocompromised patients (Odds 1998). Dityrosine fluorescence can be observed in the chlamydospores (Figure 1-8) (SMAIL *et al.* 1995). The genomic sequence of *C. albicans* reveals two genes homologous to *S.*

cerevisiae DIT1 and *DIT2* (SMAIL *et al.* 1995). *In vitro* analysis also demonstrated that *E. coli* overexpressed- *C. albicans CYP56* (Dit2p) catalyzed the conversion of formyl tyrosine into bisformyl dityrosine (MELO *et al.* 2008). The role of dityrosine in *C. albicans* cell wall metabolism is not clear. However, drug susceptibility testing of the *cyp56* mutant indicates that dityrosine may play a role in *C. albicans* cell wall structural dynamics (MELO *et al.* 2008). Therefore, the study of the structure and assembly mechanism of the dityrosine macromolecule in *S. cerevisiae* provides an attractive model to explore the biological function of the dityrosine in *C. albicans.*

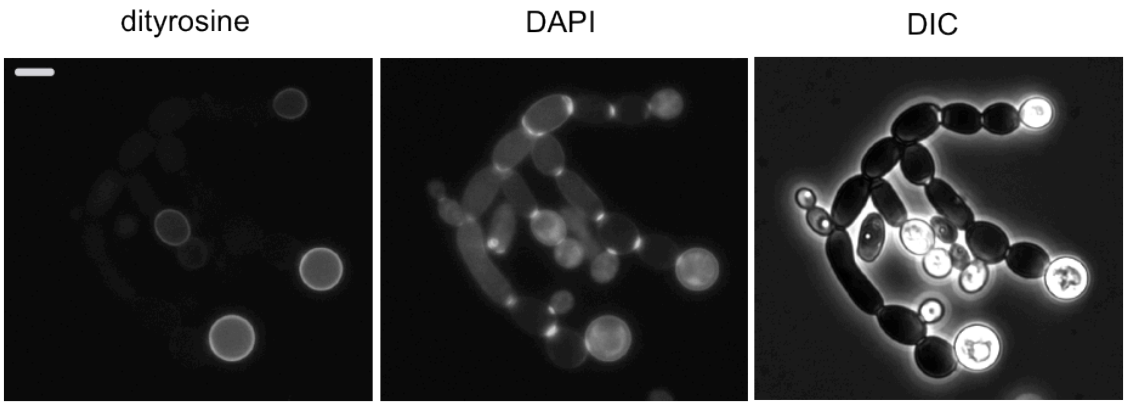

Figure 1-8. Dityrosine fluorescence of *C. albicans* can be seen at chlamydospores under dityrosine filter set. The fluorence signal under DAPI filter set at bud scars or budding sites are not dityrosine.

Chapter 2

Structural study of *Saccharomyces cerevisiae* spore wall dityrosine layer by solid-state nuclear magnetic resonance spectroscopy

2.1 Introduction

2.1.1 General introduction

Diploid MAT a/α cells of the budding yeast *Saccharomyces cerevisiae* under nitrogen starvation and in the presence of nonfermentable carbon source can enter meiosis and sporulation to produce an ascus which contains four haploid spores (KUPIEC *et al.* 1997). Spores are a quiescent, stress-resistant cell type protected by the spore wall that can survive for extended periods of time in unfavorable conditions until nutrient conditions are suitable (STERN *et al.* 1984). In particular, the outer layers of spore wall contribute physical rigidity as well as the property of low permeability which protects spores from chemical and enzymatical invasions (BRIZA *et al.* 1990a; NEIMAN 2005; NEIMAN 2011).

Prior to the deposition of spore wall materials, prospore membranes (PrM) are formed at the four spindle pole bodies. Secretory vesicles dock and fuse to each PrM. Each prospore membrane engulfs and fully encapsulates a haploid nucleus. After closure of the PrM, spore wall layers are assembled in the luminal space of the double-layered prospore membranes. The ascospore wall of *S. cerevisiae* contains four layers. Under transmission electron microscope with osmium tetroxide staining, the layered ultrastructure can be distinguished (KREGER-VAN RIJ 1978). The inner two layers of spore wall are composed of mannoproteins and glucans that are also the components of vegetative cell wall. However, the order of these two layers is reversed with respect to the vegetative cell wall

(KLIS *et al.* 2006; LESAGE and BUSSEY 2006). The first layer formed outside of spore plasma membrane (which was the inner membrane of the PrM) is composed of mannosylated secreted proteins and is referred to as the mannan layer. The second layer is the β-glucan layer, which consists of linear chains of β-1, 3-linked glucose residues branched by β-1, 6-linkages. The coiled spring-like β-1, 3-glucose chains confer elasticity and tensility to the wall structure (LESAGE and BUSSEY 2006). The outer layers are made of chitosan, the deacetylated form of chitin, and dityrosine, a polymerized form of N, N'-bisformyl dityrosine (BRIZA *et al.* 1988; BRIZA *et al.* 1996). Both components are macromolecules specific for the spore wall, serving critical roles for resistance of the spores to adverse environmental stresses.

2.1.2 Biochemical studies of spore wall dityrosine layer

Different biochemical approaches have been used to identify the components, intermediate molecules, and linkage information of the dityrosine layer. Reverse Phase High Performance Liquid Chromatography (RP-HPLC) separation combined with the fluorescence spectrum of spore wall acid hydrolysate (prepared with 6N HCl at 110°C for 14 hours) reveal two dityrosine fluorescence-containing fractions, peak 1 and peak 2 (Figure 2.1) (BRIZA *et al.* 1990b). Peak 1 contains just dityrosine representing exactly same elution time as LL-dityrosine standard (BRIZA *et al.* 1986). Peak 2 is broad and contains chitosan as well as dityrosine (BRIZA *et al.* 1988). Examination of the molecular mass of peak 1 and peak 2 by electrophoretic separation showing that both peaks are as a smear of bands containing dityrosine, ranging from 10 kDa to 100 kDa, with peak 2 distributed quite evenly while peak 1 is concentrated at around 10 kDa to 30 kDa. Isoelectric focusing analysis of peak 1 showed seven bands indicating an ionizable component with regular repeats (BRIZA *et al.* 1990b). Amino acid analysis by HPLC methods reveals the major amino acids of the macromolecules (BRIZA *et al.* 1990b).

Based on these results, dityrosine and glycine are the most abundant amino acids, around 53% and 31%, respectively, in the peak 1 fraction (BRIZA *et al.* 1990b). Analysis of results from infrared spectroscopy indicates that the components of peak 1 don't contain conventional peptide bonds (BRIZA *et al.* 1990b; JABS *et al.* 1999).

2.1.3 Genes involved in the synthesis of dityrosine precursors

Monomeric dityrosine is synthesized by a two-step process in the cytoplasm of spores. First, free L-tyrosine is converted to formyl tyrosine by Dit1p. In the second step, two molecules of formyl tyrosine are cross-linked by Dit2p, which is a protein of cytochrome P-450 peroxidase family, and form N, N'-bisformyl dityrosine (BRIZA *et al.* 1994). The precursor is then transported from the cytosol to outer spore wall by Dtr1p, which is a multidrug resistance transporter of the major facilitator superfamily. The mechanism of how soluble dityrosine precursor is incorporated to spore wall and form an intact layer remains unclear.

2.2 Materials and Methods

2.2.1 Yeast strains, growth media, and growth conditions

The yeast strains used in this study are AN120 and AN264, listed in Table 2.1. Both strains are in the SK-1 background. Unless otherwise noted, standard yeast media and growth conditions were used (BURKE *et al.* 2005).

Table 2.1 Yeast strains used in this study.

STRAIN	GENOTYPE	SOURCE
AN120	MATa/MATα ura3/ura3 leu2/leu2 his3ΔSK/his3ΔSK trp1Δ::hisG/trp1Δ::hisG ARG4/arg4 –NspI lys2/lys2 hoΔ::LYS2/hoΔ::LYS2 RME1/rme1Δ::LEU2	(NEIMAN *et al.* 2000)
AN264	MATa/MATα ura3/ura3 leu2/leu2 his3ΔSK/his3ΔSK trp1Δ::hisG/trp1Δ::hisG ARG4/arg4-NspI lys2/lys2 hoΔ::LYS2/hoΔ::LYS2 RME1/rme1Δ::LEU2 dit1Δ::HIS3MX6/dit1Δ::HIS3MX6	(COLUCCIO *et al.* 2004a)

2.2.2 Unlabeled spore wall sample preparation for NMR experiments

Around 25 g wet weight of AN120 sporulated cells were collected (around 2.5 L SPO media at 75% sporulation frequency), resuspended and washed with 0.1 M sodium phosphate buffer (pH 7.2) and then resuspended in 60 ml of 0.1 M sodium phosphate buffer (pH 7.2) containing 20 mg of Zymolyase (US Biologicals, Salem, MA) as well as 0.04 % ß-mercaptoethanol. Cells were incubated with shaking at 30ºC for 2 hr until spores were released from asci. Cells were washed three times in 0.5% Triton X-100 to remove ascal debris and zymolyase and then layered onto a Percol (MP Biomedicals, Santa Ana, CA)/TX-100/2.5 M Sucrose step gradient (0.8/ 0.0005/ 0.1 → 0.7/ 0.001/ 0.1 → 0.6/ 0.0015/ 0.1 → 0.5/ 0.002/ 0.1) to separate spores from vegetative cells or cell debris. Collected spores were then mixed with 20 ml of 0.5 % Triton X-100 solution and 20 ml of 0.5 mm zirconia/silica beads (BioSpec, Bartlesville, OK) for spore disruption by

bead beating. Spores were disrupted in in the cooling chamber of a BeadBeater device (BioSpec, Bartlesville, OK) with pulses of 20 sec ON/ 40 sec OFF until 80 % of spores were disrupted as determined by light microscopy. Spore wall fragments were separated from intact spores or spore cytoplasm by centrifugation through a 60% Percoll plus 2% TX-100/H_2O cushion at 23,000 rpm for 1hr. Spore wall materials were collected and washed three times with H_2O. For AN264 spore wall purification, the percoll gradient ratio of the first step was 0.4→0.3→0.2→0.1. The second separation was performed using 40% Percoll plus 2% TX-100/H_2O.

To eliminate the NMR signal from inner spore wall layers, collected spore wall materials were treated with the following lytic enzymes in order: 1mg of protease K (US Biologicals) in 50 mM Tris (pH 8.0) containing 1% SDS and 5mM DTT at 50ºC for 24 hr; 1.5 mg of zymolyase (US Biologicals) in 0.1 M sodium phosphate buffer (pH 7.2) containing 0.04 % of ß-mercaptoethanol for 24 hr. Before and after protease K reaction, samples were heated at 95ºC to stop the reaction. After zymolyase digestion, samples were washed by 0.5% TX-100 as well as H_2O, and then dried out by speed vacuum concentrator under low temperature.

2.2.3 Cell cultures of stable isotope-labeled spore wall materials for NMR experiments

AN120 and AN264 cells were cultured in synthetic complete (SC) media, which contains yeast nitrogen base w/o ammonium sulfate w/o amino acids (US Biologicals) (1.7 g/L), dropout amino acids <-Tyr-Gly> (2 g/L), ^{15}N2 ammonium sulfate (99%, Cambridge Isotope Laboratories) (5 g/L), U-^{13}C6-D-glucose (99%, Cambridge Isotope Laboratories) (20 g/L). A single colony taken from ^{12}C-YPD agar plates was patched onto another ^{12}C-YPD plate at 30ºC overnight and inoculated into 50 mL of ^{13}C, ^{15}N-SC broth until cells reach the stationary phase (OD_{660}~1.2-1.5). Cells were then harvested,

washed once with sterile water and diluted to OD_{660} ~ 1.0 into 2% KOAc medium for sporulation at 30ºC for two days before isolation of outer spore walls.

2.2.4 Solid-state NMR analysis

50-100 mg of speed vac. dried spore wall samples were packed into 4 mm rotors for solid-state NMR experiments. Unless otherwise indicated, measurements were carried out on either a 500, 600, or 750 MHz Bruker AVANCE spectrometer using an 4 mm HX magic-angle spinning (MAS) probe. All experiments were performed at room temperature. The MAS spinning speed was set between 10 to 13 kHz to eliminate overlap of MAS sidebands.

2.2.4.1 1D ^{1}H- ^{13}C cross polarization (CP) experiments

The ^{13}C chemical shift spectra were recorded by ramped-amplitude cross polarization experiments. The technique enhances sensitivity using polarization from abundant nuclei ^{1}H and transfer to dilute nuclei ^{13}C to increase signal to noise ratio (S/N). Also, since abundant nuclei are strongly dipolar coupled, the spin lattice relaxation is rapid. Therefore there is no need to wait for the slowly relaxation of rare nuclei (Figure 2.1)(HARTMANN and HAHN 1962; PINES *et al.* 1973; LEVITT 2008).

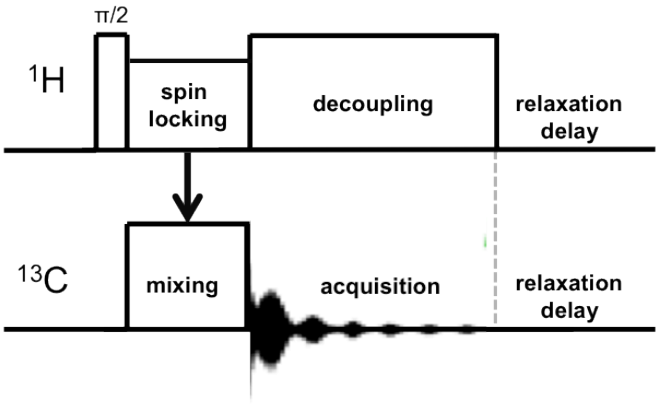

Figure 2.1 The NMR pulse sequence for 1D ^{13}C CP experiments

2.2.4.2 ^{13}C-observe Rotational-echo, double-resonance (REDOR) NMR

All REDOR experiments were performed on a 500 MHz Bruker AVANCE spectrometer using a 4 mm triple channel HXY MAS probe at room temperature. REDOR provides a direct measurement of heteronuclear spin pairs through dipolar interactions (GULLION and SCHAEFER 1989). ^{13}C magnetization is produced by the CP (cross-polarization) transfer from dipolar-coupled ^{1}H, and then ^{1}H is removed by resonant recoupling. Application of ^{15}N pulse trains causes a net dephasing of the ^{13}C that is dipole-coupled to ^{15}N. Figure 2.2 illustrates a typical REDOR pulse sequence. The number of rotor cycle applied in our experiments was 20.

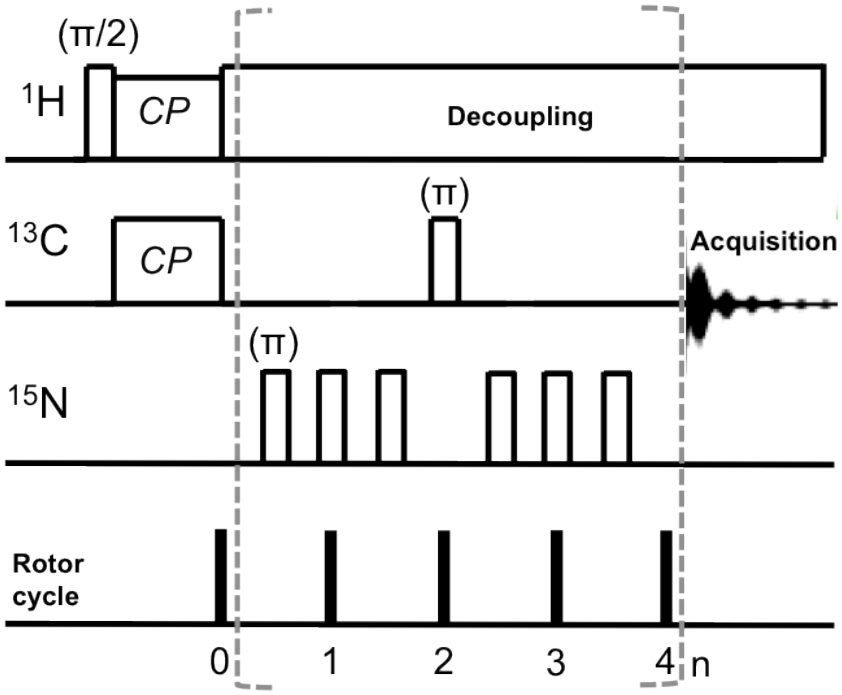

Figure 2.2 REDOR ^{13}C NMR pulse sequence. The initial ^{13}C magnetization is produced by cross polarization from ^{1}H to ^{13}C. The application of ^{15}N π pulses dephases ^{13}C signal and results in a reduced ^{13}C signal.

2.2.4.3 ^{13}C-^{13}C refocused INADEQUATE experiments

In solid-state NMR techniques, because through bond *J* coupling is usually much smaller than through space dipolar interaction between adjacent spin pairs, through bond correlation experiments are less commonly applied. However, in INADEQUATE experiments, the coherence transfer can be exclusively mediated by *J* interactions to identified through bond connectivity (LESAGE *et al.* 1999). The ^{13}C-^{13}C homonuclear dipolar couplings are removed by MAS, and the chemical shift is refocused by a π pulse. The diagram of INADEQUATE pulse sequence is shown in Figure 2.3.

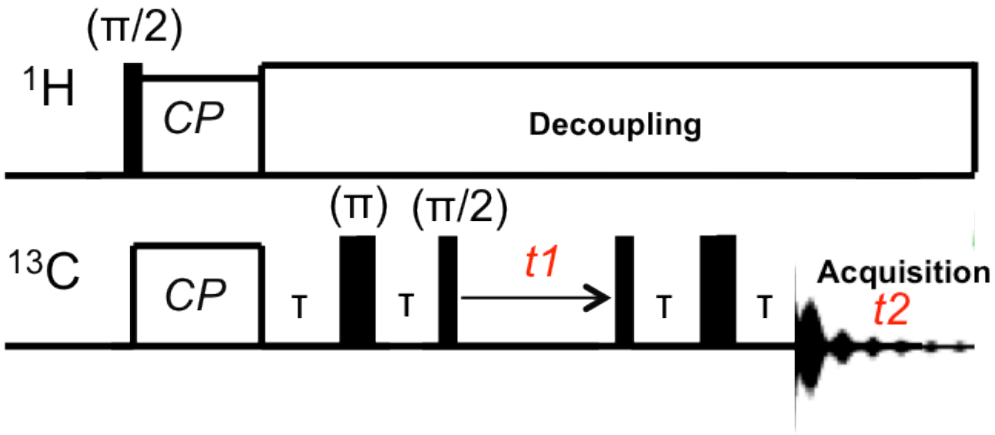

Figure 2.3 Pulse sequence of refocused INADEQUATE experiments. The double quantum coherence created by the first ^{13}C π/2 pulse evolves during *t1* at the sum frequency of the two spins and is converted back during the second τ- π -τ delay to in-phase signal before acquisition (LESAGE *et al.* 1999).

2.2.4.4 2D ^{13}C- ^{13}C dipolar-assisted rotational resonance (DARR) experiments

Figure 2.4 shows the diagram of 2D ^{13}C-^{13}C DARR experiments pulse sequence. In DARR experiments, magnetization is transferred from the abundant ^{1}H nuclei to directly bound ^{13}C nuclei, and then from the directly bound ^{13}C nuclei to other spacially close ^{13}C nuclei. During the evolution step, high power decoupling is applied on the ^{1}H channel. The ^{1}H decoupling increases resolution of the final spectrum by averaging the strong dipolar coupling between ^{1}H and ^{13}C nuclei. During mixing step, a recoupling pulse is applied to ^{1}H channel with a low power constant wave. This technique allows the measure of long range ^{13}C-^{13}C correlations between pairs of nuclei within 6 Å (TAKEGOSHI *et al.* 2001; TAKEGOSHI *et al.* 2003; LEVITT 2008).

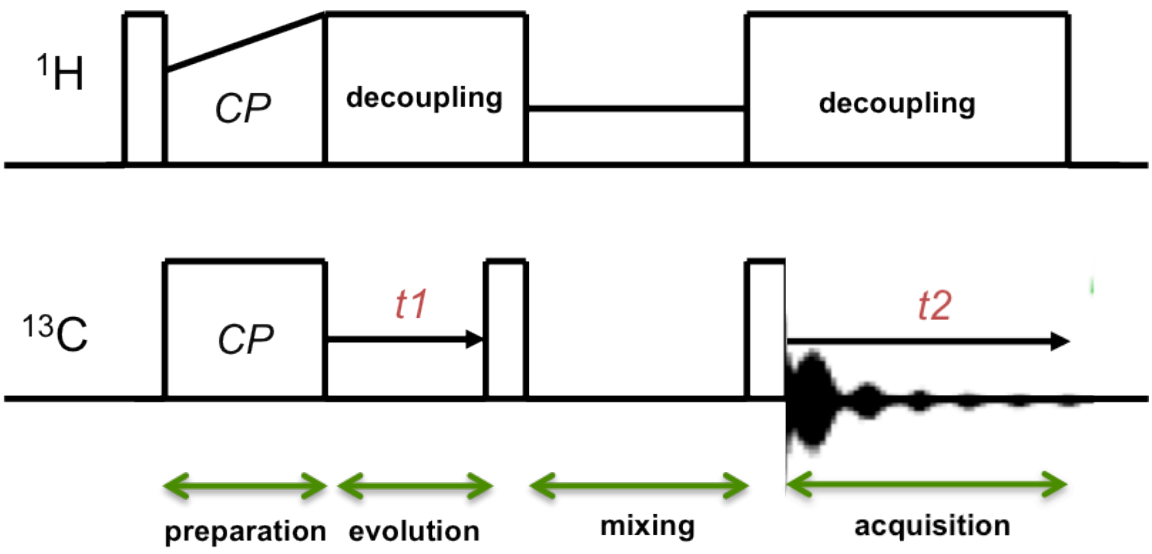

Figure 2.4 The NMR pulse sequence for 2D ^{13}C-^{13}C DARR experiments.

2.3 Results

2.3.1 Solid-state NMR 1D CP spectra reveal the components of spore wall samples

For the 1D CP experiments, unlabeled wild type spore wall samples were isolated and outer spore wall materials were enriched by enzymatic treatment. The ^{13}C spectra were collected from the natural abundance ^{13}C signal (Figure 2.5C). By comparing the chemical shift with chitosan (Figure 2.5A) and L-tyrosine (Figure 2.5B), we were able to unambiguously assign most of peaks (Figure 2.6A). There are three major classes of components from the spectrum: 1) Polysaccharides. The chemical shifts range from 54-110 ppm. The signal is produced by chitosan/chitin. The major signal of C=O peak located around 172 ppm is from chitin, the acetylated form of chitosan. This peak is relatively broad. Therefore, we assume that the "shoulder" signal is from carbonyl moiety of other components, such as dityrosine or other amino acids. 2) Dityrosine. Due to the relatively low content of dityrosine and disordered solid sample property, the dityrosine fraction is resolved into two major peaks at 128 and 151 ppm on ^{13}C spectrum (Figure 2.6A). By comparing with *dit1*Δ sample, we confirmed that those peaks are from dityrosine (Figure 2.6B, denoted by red arrows). 3) Unknown component, χ. There are around 7 peaks located at low chemical shift ranging from 15 to 38 ppm. From the CP spectra, χ component is relatively enriched in the spore wall samples (Figure 2.6). It seems that dityrosine is not required for the incorporation of χ as χ peaks are present in the *dit1*Δ spectrum (Figure2.6, *dit1*Δ) although the signal from χ is reduced.

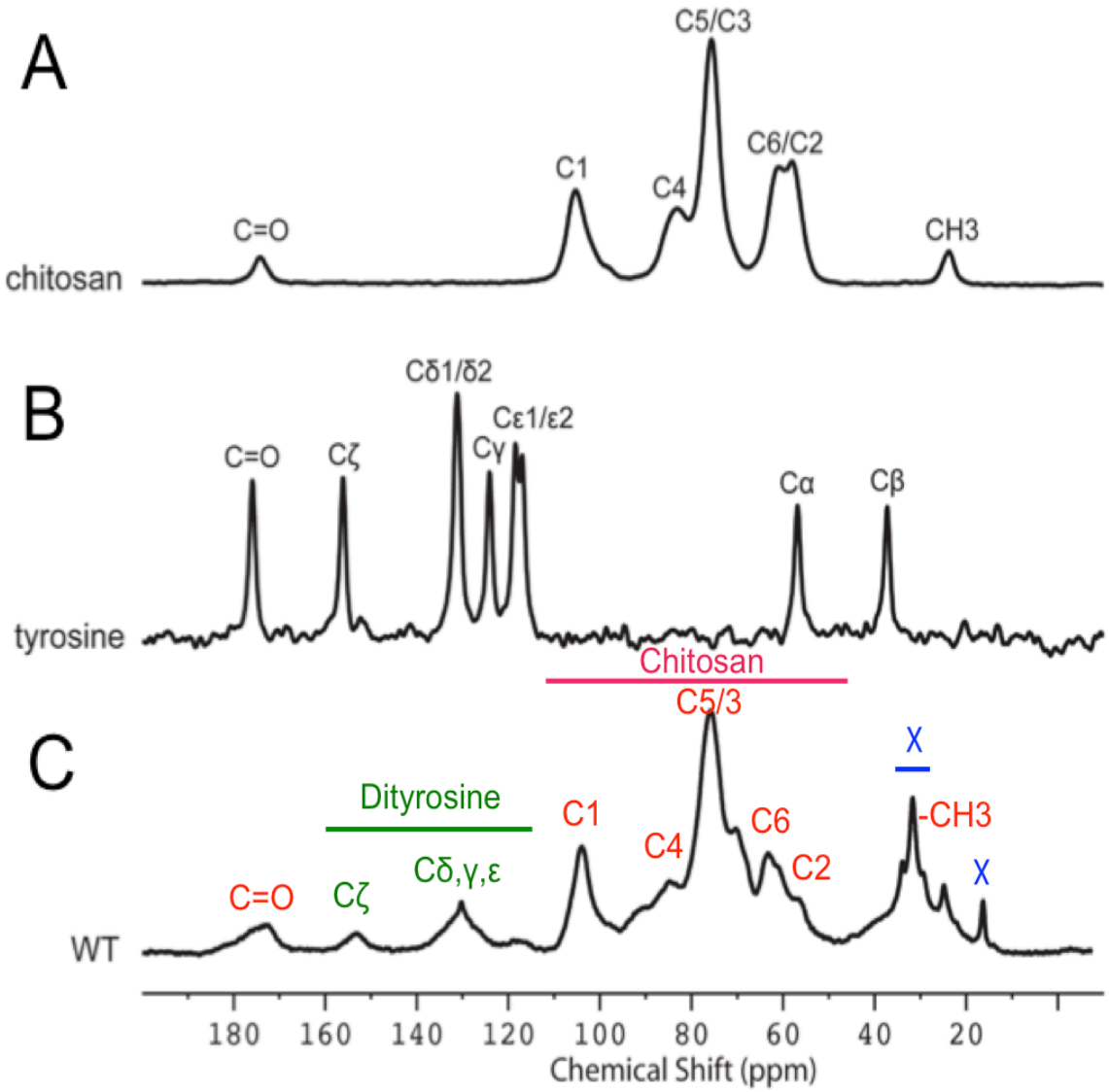

Figure 2.5 Assignment of the components of wild type (C) spore wall unlabeled sample by comparing the chemical shift with standard chitosan (A) and amino acid tyrosine (B).

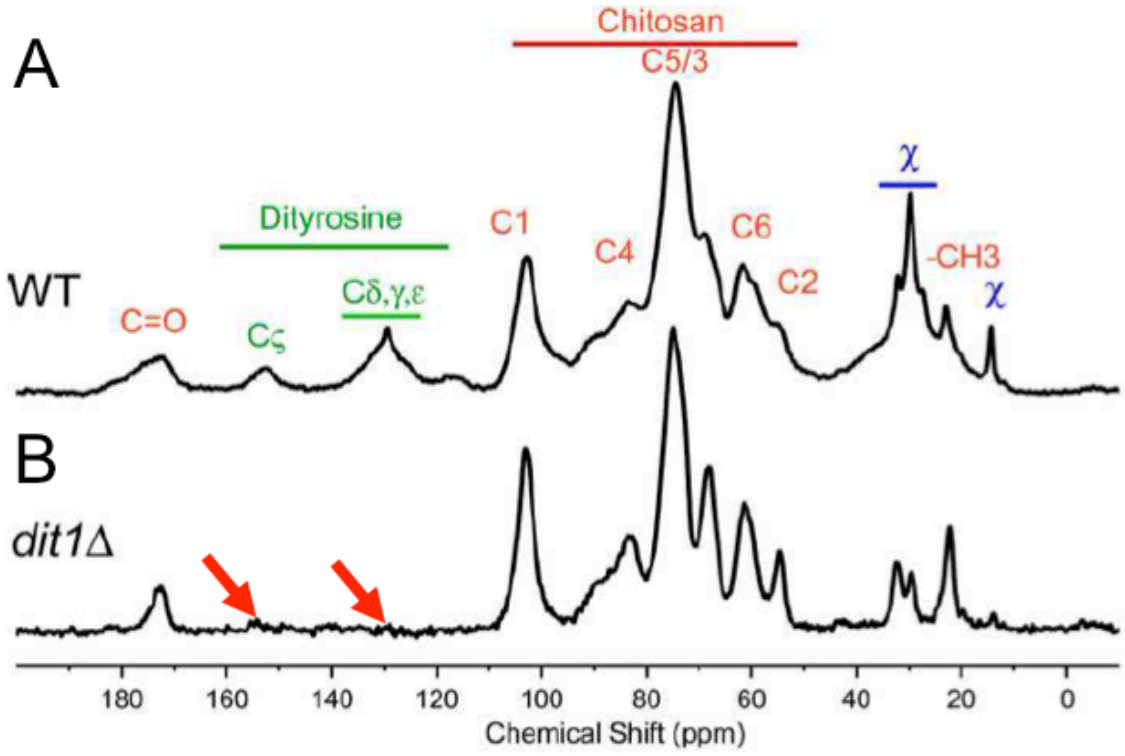

Figure 2.6 NMR ^{13}C CP-MAS spectra of WT and *dit1Δ* spore wall. (A) Wild type spore wall consists of chitosan (labeled with red color), dityrosine (labeled with green) and unknown component χ (labeled in blue). (B) *dit1Δ* strain, which lacks dityrosine layer, spore wall spectra represent no peaks at dityrosine Cδγε (129 ppm) and Cζ (154 ppm) (red arrows), and reduced signal from component χ.

2.3.2 ^{13}C-observed, ^{15}N-dephased REDOR NMR spectra of WT and *dit1*Δ outer spore wall

Next, we wanted to know the ^{13}C-^{15}N correlations among these components. The REDOR difference of *dit1*Δ sample reveals that the direct ^{13}C-^{15}N bonds located at C2 and C=O of residual chitin (Figure 2.7B). However, these two peaks are missing on the REDOR difference profile of WT sample (Figure 2.7A), which may indicate that the modifications are on chitin for dityrosine incorporation. In both WT and *dit1*Δ spectra, the weak correlations to –CH3 and to chitosan C1 suggest that the linkage information provided by REDOR spectra is not only ^{13}C-^{15}N direct binding but also the distal linkages of one carbon distance from ^{15}N. Notably, two REDOR difference peaks appear on WT spectra indicating that the unknown component χ_E (see below and the nomenclature in Figure 2.9B) and dityrosine Cγ may directly link to N.

2.3.3 Investigation of ^{13}C-^{13}C through bond interactions

As the 1D CP spectra of our spore wall preparation show relatively uncomplicated peaks, we wanted to detect the direct linkages among these components. Refocused INADEQUATE experiments were carried out using (U- ^{13}C, ^{15}N)-labeled wild type and *dit1*Δspore wall sample. Figure 2.8 shows the full spectrum and cross-links of the *dit1*Δ sample. In the 2D spectrum, two directly bonded ^{13}C share a common frequency in the double quantum dimension. By comparing with the peak assignment from CP spectra, we were able to identify the cross linkages. In the 2D map, we can unambiguously assign all links from chitosan/chitin. C5/C6 has correlation peaks at 225 ppm in the double quantum frequency dimension. The cross peak of C3/C4 locates at 258 ppm (of double quantum frequency dimension). Both C4/C5 and C2/C3 correlation peaks are at 275 ppm. Finally, C1/C2 is at 310 ppm. The similar chitosan connectivity pattern can also be observed in wild type refocused INADEQUATE spectrum (Figure 2.9A).

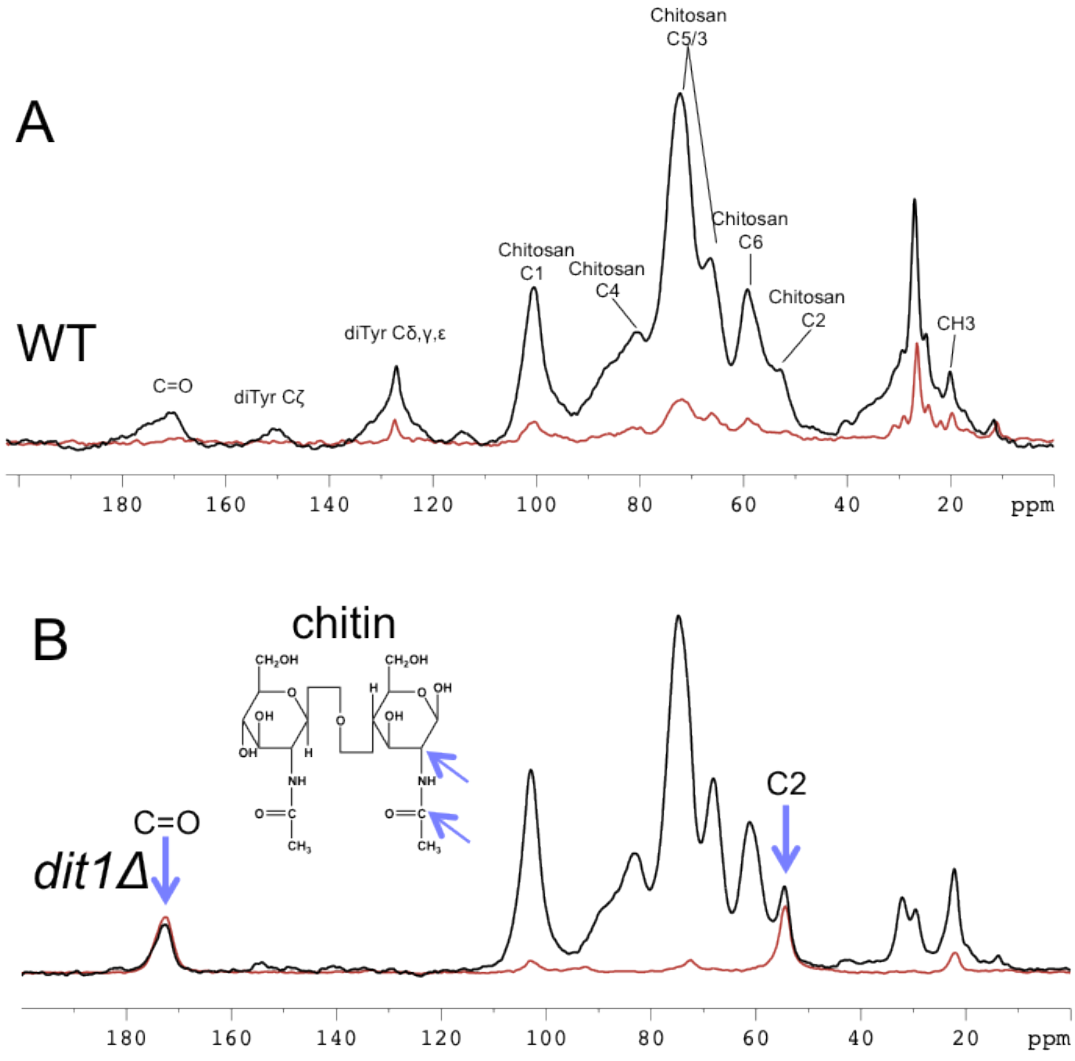

Figure 2.7 ^{13}C-observed, ^{15}N-dephased REDOR spectra of WT(A) and *dit1*Δ(B) yeast outer spore wall. The full echo spectra (S_0, without ^{13}C π pulses) are shown in black lines, while the REDOR difference signal is shown in red lines.

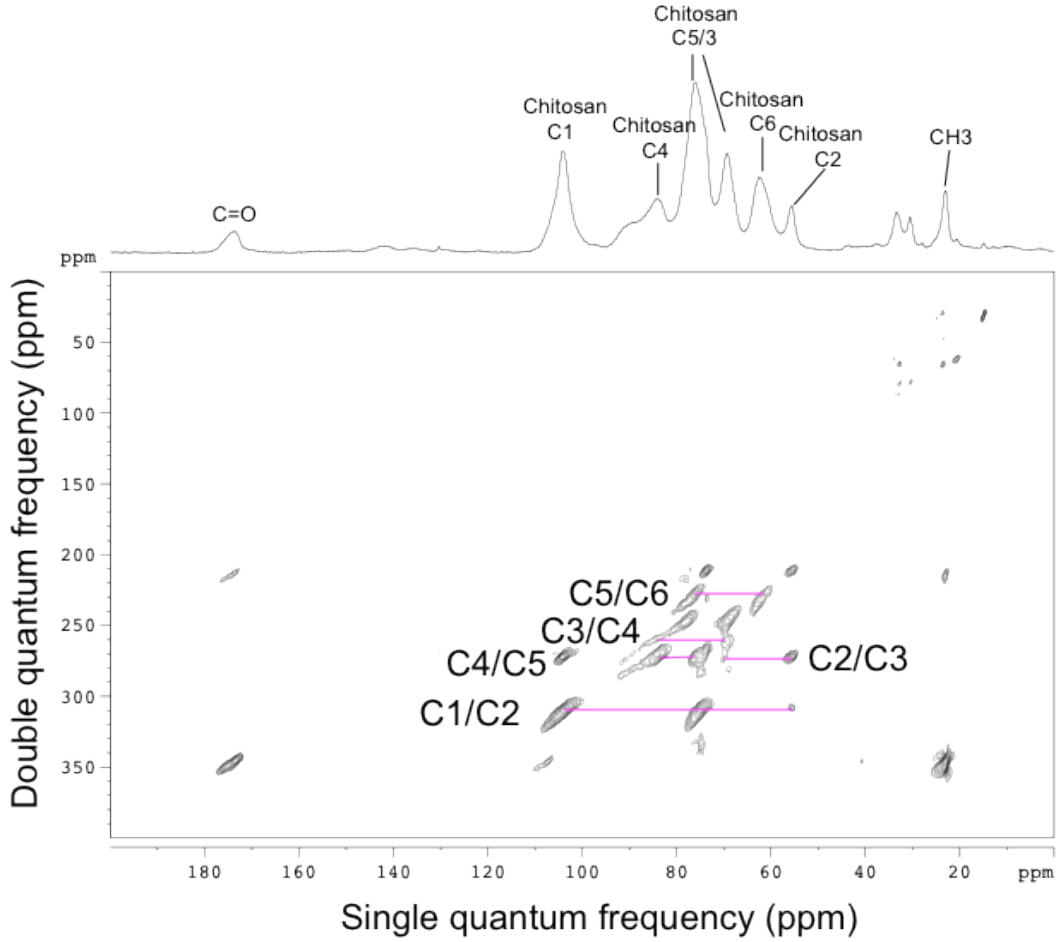

Figure 2.8 Refocused INADEQUATE spectrum of *dit1Δ* spore wall sample. Above, the 1D ^{13}C CP-MAS spectrum is showing chemical shift with the corresponding assignments. Below, 2D refocused INADEQUATE map showing specific ^{13}C-^{13}C through bond connectivity. By following the connectivity pattern through the entire ^{13}C skeleton, as marked with pink lines, the chitosan/chitin carbon ring backbone can be fully assigned.

Remarkably, the correlations of methyl group and the unknown component χ located at 15 to 38 ppm can be distinguished. Starting from the resonance of CH_3 at 24ppm, we were able to assign the carbon spectrum sequentially (Figure 2.9B). First, we denote the 7 peaks from χ -C_A to χ -C_G (shown in blue). Methyl carbon has two correlations with χ -C_A and χ –C_F with the chemical shift on double quantum dimension at 29 and 67 ppm, respectively. χ -C_E connects to three other ^{13}C, with χ –C_c at 64 ppm, with χ –C_D at 69 ppm, and with χ –C_F at 78 ppm. Another correlation identified from the spectrum is χ –C_G/C_B, which is located at 62 ppm. There are two more sets of linkages: χ –C_G/C_A at 36 ppm and χ –C_B/C_E at 78 ppm (Figure 2.9B, shown in dash lines). With the high connectivity for the low chemical shift peaks, including χ and methyl group, it likely represents a ring-like chemical structure. Also, if we consider the peak of REDOR difference spectrum from wild type spore wall (Figure 2.7A), it seems that we can draw a 5-carbon/1-nitrogen ring structure. The real χ structure needs to be further identified and confirmed by other biochemical techniques, such as mass spectrometry.

The other significant linkage is the correlation between dityrosine-$C_{\delta,\gamma,\varepsilon}$ and χ –C_D, which we don't see in *dit1*Δ sample. This is a direct evidence showing the cross linkage between dityrosine layer and χ. The result rises high possibility that χ may play roles for yeast making intact outer spore wall layers.

2.3.4 Detection of spore wall through space interactions by 2D DARR experiments

Other than direct bonded information by REDOR and refocused INADEQUATE NMR experiments, we wanted to know the ^{13}C-^{13}C dipolar correlations in through space interactions. Figure 2.10 shows the spectra of DARR experiments from a wild type uniformly ^{13}C, ^{15}N- labeled spore wall sample. In the 2D map, the peaks representing the isotropic chemical shifts can be seen along the diagonal. The cross peaks indicate that the

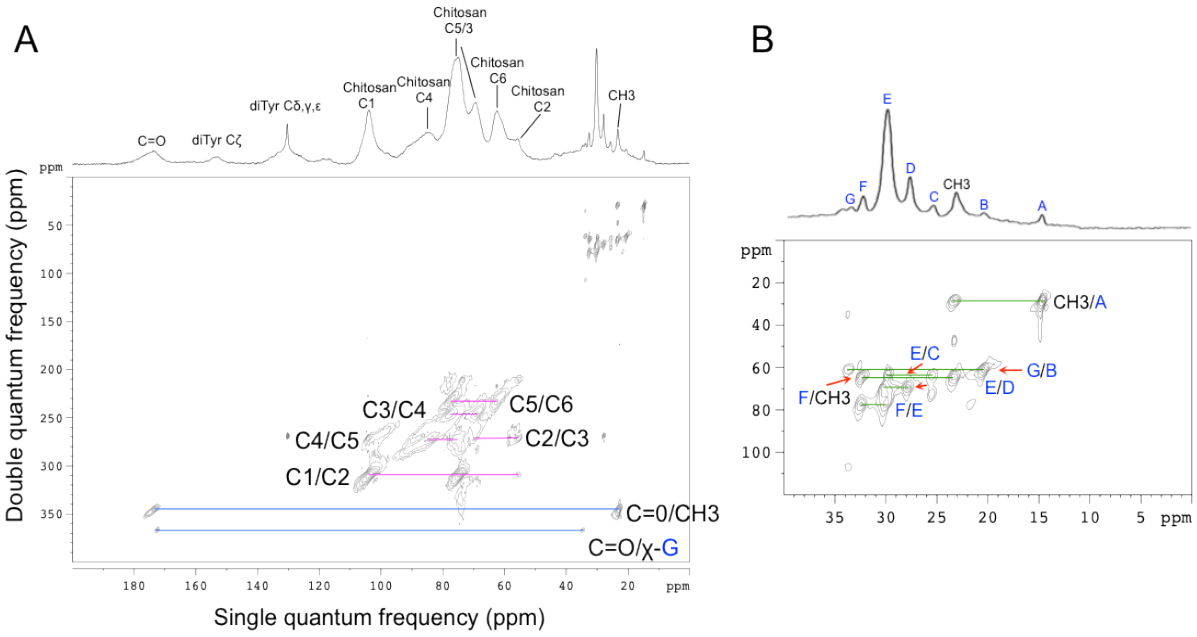

Figure 2.9 Refocused INADEQUATE spectrum of wild type spore wall sample. (A) Full spectrum of the 2D correlation map with the 1D projection of the single quantum axis and chemical shift assignment on the top. The correlations of chitosan/chitin ^{13}C backbone are shown with pink lines. The pattern is same as the *dit1Δ* spectrum (Figure 2.8). (B) The connectivity of component χ. The highly connected spectrum may potentially indicate a ring-like structure for this unknown molecule.

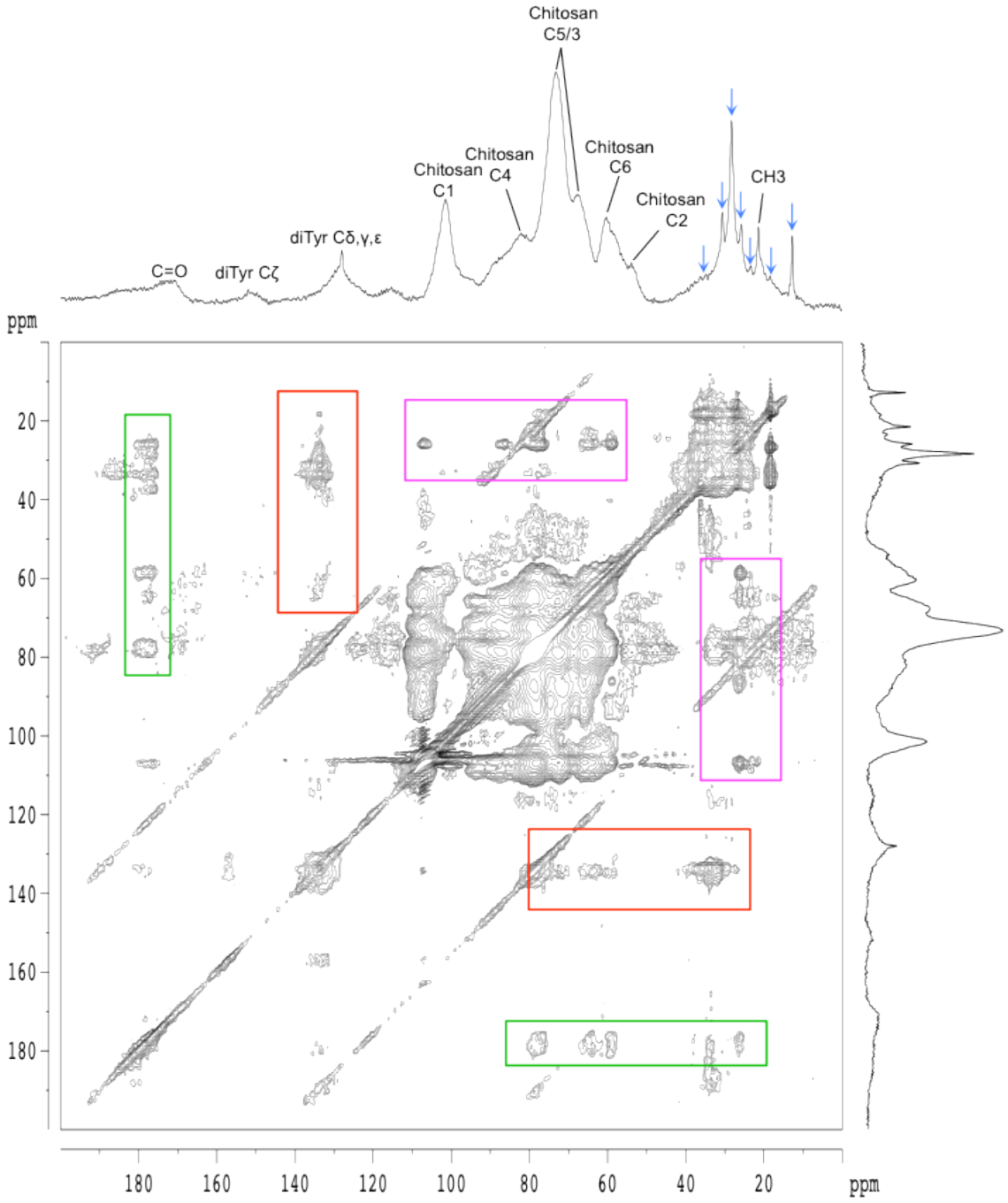

Figure 2.10 DARR NMR spectra. 1D ^{13}C spectrum on top showing chemical shift assignment for wild type spore wall components. χ components χ –C_A to C_G are denoted by blue arrows. The two dimensional map showing ^{13}C-^{13}C dipolar coupling between carbony and χ components/ chitosan (green boxes), dityrosine-$C_{\delta,\gamma,\varepsilon}$ and χ components/ chitosan (red boxes), and methyl group and chitosan (purple boxes).

distance of dipolar coupled ^{13}C nuclei pairs are less than 6 Å. Generally speaking, a strong cross peak typically represents the distance of 4.5 Å or less; a weak cross peak indicates the distance between 4.5 to 6.0 Å. Significantly, intense cross peaks arise from dityrosine-$C_{\delta,\gamma,\varepsilon}$ and unknown component χ- C_E indicating the close linking relationship between dityrosine and χ (Figure 2.10, red box). For comparison, same experiments were performed on labeled *dit1*Δ sample (Figure 2.11). The cross peak pattern from C=O and chitosan is quite similar (shown with green and purple boxes, respectively, in Figure2.10 and 2.11).

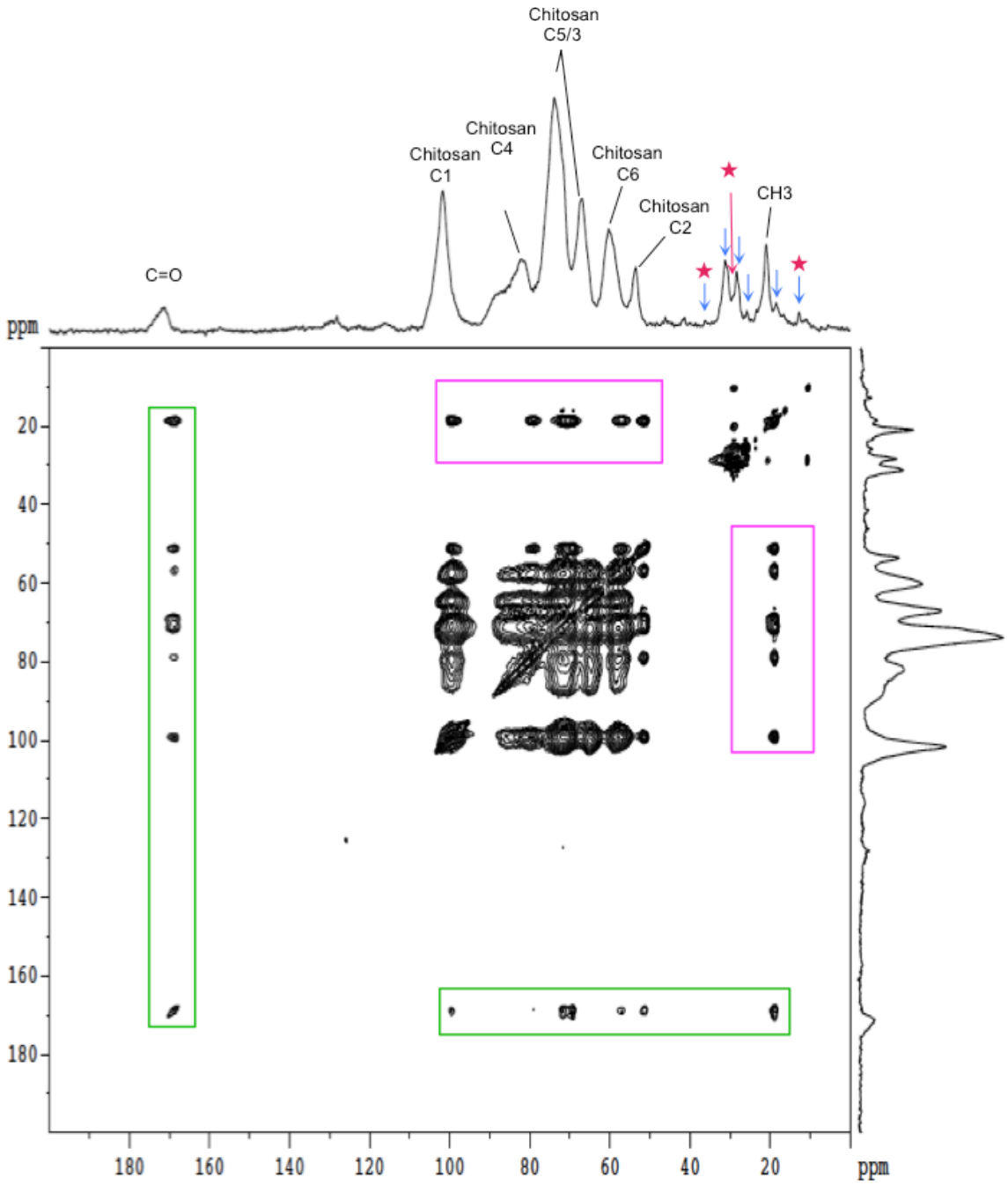

Figure 2.11 DARR spectra of U-^{13}C, ^{15}N-labeled *dit1*Δspore wall sample. Upper panel, 1D ^{13}C spectrum with chemical shift assignments. χ components χ –C_A to C_G are denoted by blue arrows. Red star indicates reduced content compare to wild type spectrum. Red arrow denotes the missing peak of χ –C_E from the *dit1*Δ spectrum. Lower panel, 2D DARR spectrum showing ^{13}C-^{13}C dipolar coupling between carbonyl and methyl group/ chitosan (green boxes), and methyl group and chitosan (purple boxes).

2.4 Discussion

To investigate the properties of the dityrosine layer and reveal proteins involved in the assembly process, many biochemical studies have been done (Briza et al., 1986; Briza et al., 1990; Briza et al., 1996). These previous works provide a schematic idea how the dityrosine precursor is made and transported from the cytosol to the surface of the spore wall (Briza et al.,1990; Briza et al., 1994; Felder et al.,2002). Due to the insolubility of spore wall samples, getting a pure dityrosine portion by conventional chromatography methods is challenging but not impossible. This has been done by solubilizing spore wall samples by acid hydrolysis followed by reverse phase HPLC. Although this can generate pure samples, the harsh treatment raises questions about whether any intermediate components are real. With this consideration, to figure out the proteins involved in dityrosine layer assembly and possible mechanisms, keep spore wall samples on natural status while analyzing the properties is very critical.

In this study, we take advantage of the tough dityrosine structure and insoluble spore wall property to get insight into the native connectivity by solid state NMR methods. Partially purified spore wall samples were treated with a series of lytic enzymes. The 1D ^{13}C NMR chemical shifts reveal the components of spore wall samples. CP spectra give us a big picture for individual sample without complicated preparation or purification steps. It is also a great tool to analyze the spore wall components from different mutant strains. The wild type CP spectrum reveals the relatively uncomplicated components, including dramatic resonance peaks coming from the six ^{13}C of the glucosamine of chitin/chitosan layer located at 50 to 110 ppm, dityrosine $C_{\delta,\gamma,\varepsilon}$ and C_{ζ} at 130 and 154 ppm, repectively, and unknown component χ ranging at 15 to 40 ppm.

The directly bonded ^{13}C-^{13}C information can be revealed by refocused INADEQUATE experiments. Our data show clear and unambiguous intact connectivity of the resonances from chitosan. Although we were able to see the cross peak from

dityrosine to χ and potential connections between dityrosine and chitosan, the signal is still too weak to let us draw the connectivity with other spore wall components completely. Besides carbon backbone connectivity, the cross linkages between nitrogen and carbon are also important to elucidate the correlations between carbons and nitrogens. As amino groups from dityrosine and chitosan are relatively active and may take part in chemical reactions, spectra obtained from REDOR experiments are valuable for the structure determination. Interestingly, two REDOR difference peaks of chitosan C2 and carbonyl observed in *dit1*Δ sample disappear in wild type spectrum, raising the possibility that acetyl group of chitin and amino group of chitosan may be modified during the dityrosine incorporation process and therefore form an intact layer. The χ –C_E peak coming from REDOR difference spectrum of wild type sample is also quite interesting. The χ –C_E peak is even missing in the *dit1*Δ sample. The data not only suggest the linkage between χ –C_E and nitrogen, but also point out the close linking relationship between χ –C_E and dityrosine layer.

Although 2D DARR spectra provide through space contact information, the cross peak between dityrosine $C_{\delta,\gamma,\varepsilon}$ and χ –C_C, C_D, C_E, C_F, which we were not able to see on INADEQUATE spectrum, still gave us the hint for the intimate correlation between dityrosine and χ. Are they directly linked to each other? Since we can only see direct linkage between dityrosine and χ –C_D in the INADEQUATE spectrum, a better protocol for sample preparation to remove residual polysaccharide signal coming from chitosan and get better resolution from dityrosine layer will be the critical step to deconvolute the connectivity.

Chapter 3

A highly redundant gene network controls assembly of the outer spore wall in *S. cerevisiae*

(Reformatting of manuscript submitted to *PLOS genetics*)

(Figure 3.12 is contributed by Carey Kim)

(plasmid pRS426-Spo20$^{51-91}$-mTagBFP was constructed by Liang Jin)

The spore wall of Saccharomyces cerevisiae is a multilaminar extracellular structure that is formed de novo in the course of sporulation. The outer layers of the spore wall provide spores with resistance to a wide variety of environmental stresses. The major components of the outer spore wall are the polysaccharide chitosan and a polymer formed from the di-amino acid dityrosine. Though the synthesis and export pathways for dityrosine have been described, genes directly involved in dityrosine polymerization and incorporation into the spore wall have not been identified. A synthetic gene array approach to identify new genes involved in outer spore wall synthesis revealed an interconnected network influencing dityrosine assembly. This network is highly redundant both for genes of different activities that compensate for the loss of each other and for related genes of overlapping activity. Several of the genes in this network have paralogs in the yeast genome and deletion of entire paralog sets is sufficient to severely reduce dityrosine fluorescence. Solid-state NMR analysis of partially purified outer spore walls identifies a novel component in spore walls from wild type that is absent in some of the paralog set mutants. Localization of gene products identified in the screen reveals an unexpected role for lipid droplets in outer spore wall formation.

3.1 Introduction

All cells surround themselves with some form of extracellular matrix that provides structural integrity to the cell and protection from the environment. While the composition of these extracellular matrices varies, they present all cells with a common problem – how to assemble a complex macromolecular structure in an extracellular milieu. In fungi, the extracellular matrix is referred to as the cell wall and serves as the interface between a fungal cell and its environment. The composition and structure of the wall can determine the ability of cells to survive under different conditions. As a result, cell wall synthesis is an important target for antifungal drugs for the treatment of fungal infections (DENNING 2003).

The cell wall of fungi is composed primarily of long chain polysaccharides and heavily glycosylated proteins. In addition, many fungi also contain polyphenolic compounds such as melanin in their walls, though relatively little is known about how these polyphenols are incorporated into the wall (EISENMAN and CASADEVALL 2012). The vegetative cell wall of Saccharomyces cerevisiae has been used extensively as a model for studies of fungal cell walls, though it lacks components such as the polyphenols that are found in other fungi (ORLEAN 2012). These constituents are found, however, in the wall of S. cerevisiae spores.

Starvation can induce diploid cells of *S. cerevisiae* to undergo meiosis and differentiate to form haploid spores (NEIMAN 2011). Spores are formed by an unusual cell division in which four daughter cells are generated within the cytoplasm of the mother cell. Intracellular membranes termed prospore membranes engulf and eventually enclose each of the four nuclei generated by meiosis, giving rise to the daughter cells (Figure 3.1). Closure of a prospore membrane envelops a nucleus within two membranes; the plasma membrane of the spore and an outer membrane that separates the spore plasma membrane from the mother cell cytoplasm. After prospore membrane closure a spore wall is formed

de novo around each spore (Figure 3.1).

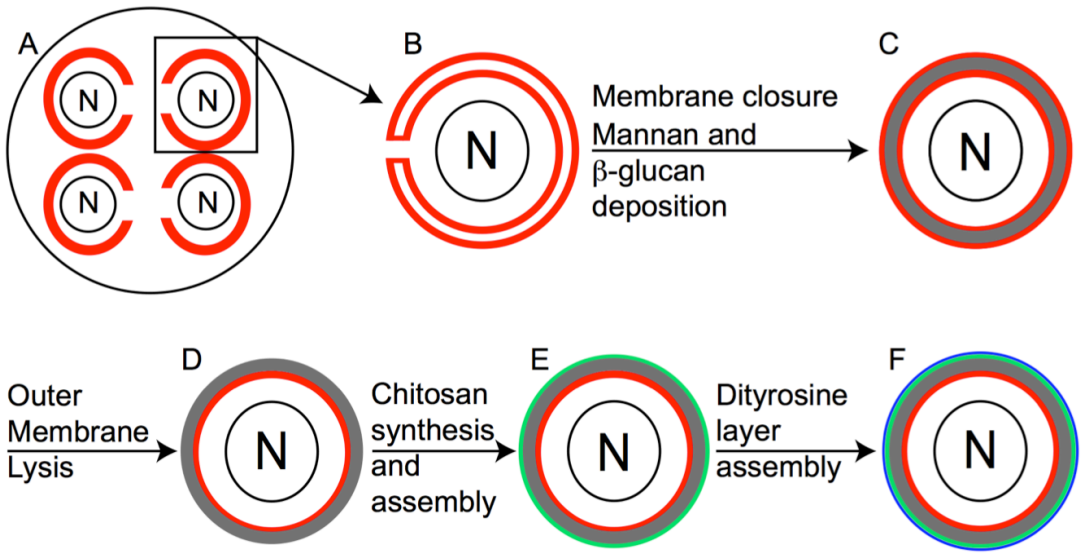

Figure 3.1 Overview of spore wall formation. A) Each of the four nuclei (N) in a sporulating cell are engulfed by a prospore membrane (red). B) A single prospore membrane prior to closure. C) After closure of the prospore membrane, mannans and β-glucans (gray) are deposited in the lumen between the spore plasma membrane and outer membrane derived from the prospore membrane (both in red). D) The outer membrane disappears, exposing spore wall material to the ascal cytoplasm. E) Chitosan is synthesized and assembled as a discrete layer (green) on the outside of the β-glucan. F) The dityrosine layer (blue) is formed on the outside of the chitosan layer.

The completed spore wall consists of four distinct layers (KREGER-VAN RIJ 1978). The first two layers are composed of mannan and β-glucan and are similar in composition to the vegetative cell wall (KLIS *et al.* 2002). These two layers are formed in the lumen between the spore plasma membrane and the outer membrane (Figure 3.1C). After the β-glucan layer is completed, the outer membrane is lost exposing the spore wall directly to the cytoplasm of the surrounding ascus (Figure 3.1D) (COLUCCIO *et al.* 2004a). The two outer layers of the spore wall are made from components unique to the spore (BRIZA *et al.* 1986; BRIZA *et al.* 1988; BRIZA *et al.* 1990b). First, a layer of chitosan is formed on top of the β- glucan layer after outer membrane lysis (Figure 3.1E) (COLUCCIO *et al.* 2004a). Chitosan is a polymer of β-1,4 linked glucosamine moieties and is generated by the combined action of the chitin synthase Chs3 and the sporulation-specific chitin deacetylases Cda1 and Cda2. Chs3 generates and extrudes from the spore chitin, a β-1,4 linked N-acetylglucosamine polymer and the Cda1/2 enzymes then convert the N-acetylglucosamine subunits in the nascent chitin chains to glucosamine (PAMMER *et al.* 1992; CHRISTODOULIDOU *et al.* 1999). Once assembled, the chitosan layer forms a surface on which the outermost layer of the spore wall assembles. The major component this outer layer is the cross-linked amino acid N,N-bis-formyldityrosine (hereafter, dityrosine) (Figure 3.1F) (BRIZA *et al.* 1988).

Dityrosine is formed in the spore cytoplasm by the Dit1 and Dit2 enzymes (BRIZA *et al.* 1986; BRIZA *et al.* 1990a; BRIZA *et al.* 1994; BRIZA *et al.* 1996). These dityrosine molecules are then moved to the spore wall by the action of transporters localized in the spore plasma membrane. The primary transporter is encoded by *DTR1*, however *dtr1*Δ cells still display dityrosine fluorescence indicating that alternative transporters exist (FELDER *et al.* 2002). Once exported, dityrosine is incorporated into a large, insoluble polymer, the chemical structure of which remains to be determined (BRIZA *et al.* 1990b).

Together, the outer spore wall chitosan and dityrosine layers confer enhanced

resistance to environmental stresses on the spore, including the ability to pass through the digestive tracts of insects, permitting dispersal in the environment (BRIZA *et al.* 1990a; PAMMER *et al.* 1992; COLUCCIO *et al.* 2004a). The composition of the spore wall and its construction in a constrained developmental window make it an excellent model system for the study of fungal cell wall assembly.

Dityrosine in the spore wall is fluorescent and screens for mutants that lack this fluorescence have identified a variety of genes involved in sporulation, including *DIT1* and *DIT2* (BRIZA *et al.* 1990a). However, no genes specifically involved in assembly of the dityrosine polymer have been reported. To search for such genes, a synthetic genetic array approach was used to identify mutants that display reduced dityrosine fluorescence in combination with a mutant in the dityrosine transporter *DTR1*. Double mutant analysis of the genes identified in the primary screen reveal a highly interconnected network of genes contributing to dityrosine assembly. Strikingly, many of the major nodes in this network were found to have paralogs in the yeast genome. For several of these 4 paralogous gene sets, deletion of all the paralogs leads to loss of dityrosine from the spore wall. These results reveal a highly redundant network of genes that regulate the assembly of the dityrosine polymer.

3.2 Materials and Methods

3.2.1 Strains and media

Yeast strains used in this study are listed in Table 3.1. Unless otherwise indicated, standard yeast media and growth conditions were used (BURKE *et al.* 2005). For synthetic medium containing Geneticin (G418), monosodium glutamate (Sigma) was added as a nitrogen source instead of ammonium sulfate. Drug concentrations used were 200 mg/L G418, 3 mg/L cycloheximide, 1g/L 5-FOA, and 300 mg/L Hygromycin B. Strain CL62 was derived from the ybr180wΔ strain from the systematic yeast knockout collection (WINZELER *et al.* 1999) by selection for growth on plates containing cycloheximide. To construct the paralog deletion strains (CL6, CL7, CL15, CL26, and CL57) *lds1*Δ, *dtr1*Δ, *gat4*Δ, *osw7*Δ, and *npp2*Δ strains from the SK1 knockout collection (RABITSCH *et al.* 2001) were crossed to *rrt8*Δ, *qdr3*Δ, *gat3*Δ, *she10*Δ, and *npp1*Δ strains from the BY4741 knockout collection (WINZELER *et al.* 1999), respectively. After sporulation and dissection of the resulting diploids, double mutanthaploids were identified by marker segregation, confirmed by PCR, and CL15, CL26 and CL57 were constructed by mating of appropriate segregants. The single gene deletion strains CL38, CL43, CL44, CL47, and CL59 were also obtained as segregants from these crosses. All knockout alleles were confirmed by PCR. For construction of CL6 and CL7, deletion of the third paralog was achieved by PCR-mediated gene disruption in double mutant haploids (RABITSCH *et al.* 2001). For CL6 primers SGA-11-F/SGA-11-R (all primers sequences available upon request to the authors) and pAG32 (GOLDSTEIN and MCCUSKER 1999) as template were used to generate deletion of *LDS2*. For CL7, primers QDR1-KO-F and QDR1-KO-R were used to delete QDR1. Single deletions of *OSW4* and *OSW6* (strains CL52 and CL54) were generated using the primer sets ANO262/ANO262-B for *OSW4* and ANO263/ANO263-B for *OSW6* and pFA6a-HIS3MX6 as the template to generate

deletions in strains AN117-4B and AN117-16D followed by mating of the haploids. Simultaneous deletion of both *OSW4* and *OSW6* (strain CL35) was achieved using the same strategy but ANO262 and ANO263 were used as primers. CL50 was constructed by using the primers CDA1&2-KO-F and CDA1&2-KO-R to simultaneously delete both *CDA1* and *CDA2* in AN117-4B and AN117-16D.

3.2.2 Plasmids

Prospore membranes were visualized using pRS426-Spo20$^{51-91}$-mTagBFP, which expresses a fusion of amino acids 51 to 91 of Spo20 to the N-terminus of mTagBFP under the control of the TEF2 promoter. To construct this plasmid, a yeast codon-optimized version of mTagBFP (SUBACH *et al.* 2008) flanked by PacI and AscI sites was synthesized (GeneWiz Inc., New Jersey) and cloned into pUC57. A PacI-AscI fragment was then used to replace the mCherry sequence in pRS426-Spo20$^{51-91}$-mCherry.

3.2.3 Screen for synthetic interactions with *dtr1*Δ

A 48-pin replicator was used to transfer a collection of 301 deletions of sporulation-induced genes in the SK1 background (RABITSCH *et al.* 2001) onto 90 mm YPD plates. All strains were arrayed in triplicate. Because the strains in this collection are *HO*, the arrayed patches were replica plated to SPO plates to generate haploid spores. CL62 cells (*MAT**a** dtr1*Δ *cyh2*) were crossed to these haploid spores by replica plating the sporulated patches to YPD plates spread with CL62. Diploids from this cross were selected on SD-Ura -Trp -His plates. To obtain double deletion mutants, the patches were then transferred to SPO medium and then to SD(MSG) -His +G418 +cycloheximide +5-FOA plates. On this medium, -His and G418 select for the presence of the two knockouts while the cycloheximide and 5-FOA select against any unsporulated diploid cells. Patches containing the double deletion cells were allowed to grow and spontaneously diploidize

Table 3.1
Yeast strains used in this study

Strain	Genotype	Source
AN117-4B	*MATα ura3 leu2 his3ΔSK trp1Δ::hisG arg4-NspI lys2 hoΔ::LYS2 rme1Δ::LEU2*	Neiman et al., 2000
AN117-16D	*MAT**a** ura3 leu2 his3ΔSK trp1Δ::hisG lys2 hoΔ::LYS2*	Neiman et al., 2000
AN120	*MAT**a**/MATα ura3/ura3 leu2/leu2 his3ΔSK/his3ΔSK trp1Δ::hisG/trp1Δ::hisG ARG4/arg4-NspI lys2/lys2 hoΔ::LYS2/hoΔ::LYS2 RME1/rme1Δ::LEU2*	Neiman et al., 2000
AN262	*MAT**a**/MATα ura3/ura3 leu2/leu2 his3ΔSK/his3ΔSK trp1Δ::hisG/trp1Δ::hisG ARG4/arg4-NspI lys2/lys2 hoΔ::LYS2/hoΔ::LYS2 RME1/rme1Δ::LEU2 chs3Δ::HIS3MX6/chs3Δ::HIS3MX6*	Coluccio et al., 2004
AN264	*MAT**a**/MATα ura3/ura3 leu2/leu2 his3ΔSK/his3ΔSK trp1Δ::hisG/trp1Δ::hisG ARG4/arg4-NspI lys2/lys2 hoΔ::LYS2/hoΔ::LYS2 RME1/rme1Δ::LEU2 dit1Δ::HIS3MX6/dit1Δ::HIS3MX6*	Coluccio et al., 2004
K8409	*MATa/MATa HO/HO his3/his3 trp1/trp1 lys2/lys2 LEU2::P_{URA3}-tetR-GFP/LEU2::P_{URA3}-tetR-GFP REC8::HA3-URA3/REC8::HA3-URA3 URA3::tetO224/URA3::tetO224*	Rabitsch et al., 2001
BY4741	*MAT**a** his3Δ1 leu2Δ0 met15Δ0 ura3Δ0*	(WINZELER *et al.* 1999)
MYA-1801	as K8409, plus *lds1Δ::HIS3MX6/lds1Δ::HISMX6*	Rabitsch et al., 2001
MYA-1810	as K8409, plus *dtr1Δ::HIS3MX6/dtr1Δ::HISMX6*	Rabitsch et al., 2001
MYA-1867	as K8409, plus *npp2Δ::HIS3MX6/npp2Δ::HISMX6*	Rabitsch et al., 2001
MYA-1890	as K8409, plus *osw7Δ::HIS3MX6/osw7Δ::HISMX6*	Rabitsch et al., 2001
MYA-1941	as K8409, plus *gat4Δ::HIS3MX6/gat4Δ::HISMX6*	Rabitsch et al., 2001
MYA-1976	as K8409, plus *gat3Δ::HIS3MX6/gat3Δ::HISMX6*	Rabitsch et al., 2001

MYA-2046	as K8409, plus *lds2Δ::HIS3MX6/lds2Δ::HISMX6*	Rabitsch et al., 2001
LDS1-GFP	as BY4741, plus *LDS1::GFP::HIS3*	Huh et al., 2003
LDS2-GFP	as BY4741, plus *LDS2::GFP::HIS3*	Huh et al., 2003
RRT8-GFP	as BY4741, plus *RRT8::GFP::HIS3*	Huh et al., 2003
CL6	*MAT**a**/MATα HO/HO leu2/leu2 lys2/lys2 URA3::tet0224/URA:3:tet0224 lds1Δ::HIS3/ lds1Δ::HIS3 rrt8Δ::kanMX6/rrt8Δ::kanMX6 lds2Δ::HphMX6/ lds2Δ::HphMX6*	This study
CL7	*MAT**a**/MATα HO/HO leu2/leu2 lys2/lys2 URA3::tet0224/ URA3::tet0224 dtr1Δ::HIS3/dtr1Δ::HIS3 qdr3Δ::kanMX6/qdr3Δ::kanMX6 qdr1Δ::HphMX6/qdr1Δ::HphMX6*	This study
CL11	*MAT**a**/MATα ho/ho ura3/ura3 leu2/leu2 trp1-hisG/trp1-hisG his3ΔSK/his3ΔSK lys2/lys2 RME1/rme1Δ::LEU2 ARG4/arg4-Nsp1 hoΔ::LYS2/hoΔ::LYS2 osw4,6Δ::HIS3/osw4,6Δ::HIS3 URA3::P_{SPR1}-GFP-OSW4(URA3)/ URA3::P_{SPR1}-GFP-OSW4(URA3)*	This study
CL15	*MAT**a**/MATα HO/HO leu2/leu2 trp1/trp1 lys2/lys2 URA3::tet0224/URA3::tet0224 gat4Δ::HIS3/ gat4Δ::HIS3 gat3Δ::kanMX6/ gat3Δ::kanMX6*	This study
CL26	*MAT**a**/MATα HO/HO leu2/leu2 URA3::tet0224/ URA3::tet0224 osw7Δ::HIS3/osw7Δ::HIS3 she10Δ::kanMX6/she10Δ::kanMX6*	This study
CL35	*MAT**a**/MATα ura3/ura3 leu2/leu2 his3ΔSK/his3ΔSK trp1Δ::hisG/trp1Δ::hisG ARG4/arg4-NspI lys2/lys2 hoΔ::LYS2/hoΔ::LYS2 RME1/rme1Δ::LEU2 osw4,6Δ::HIS3MX6/osw4,6Δ::HIS3MX6*	This study
CL38	*MAT**a**/MATα HO/HO his3/his3 trp1/trp1 LEU2::P_{URA3}-tetR-GFP/LEU2::P_{URA3}-tetR-GFP URA3::tetO224/URA3::tetO224 rrt8Δ::kanMX6/rrt8Δ::kanMX6*	This study
CL43	*MAT**a**/MATα HO/HO his3/his3 lys2/lys2 LEU2::P_{URA3}-tetR-GFP/LEU2::P_{URA3}-tetR-GFP URA3::tetO224/URA3::tetO224 qdr1Δ::kanMX6/qdr1Δ::kanMX6*	This study

CL44	*MAT**a**/MATα HO/HO his3/his3 trp1/trp1 leu2/leu2 URA3::tetO224/URA3::tetO224 qdr3Δ::kanMX6/ qdr3Δ::kanMX6*	This study
CL47	*MATa/MATα HO/HO his3/his3 trp1/trp1 LEU2::P_{URA3}-tetR-GFP/LEU2::P_{URA3}-tetR-GFP URA3::tetO224/URA3::tetO224 she10Δ::kanMX6/she10Δ::kanMX6*	This study
CL50	*MATa/MATα ura3/ura3 leu2/leu2 his3ΔSK/his3ΔSK trp1Δ::hisG/trp1Δ::hisG ARG4/arg4-NspI lys2/lys2 hoΔ::LYS2/hoΔ::LYS2 RME1/rme1Δ::LEU2 cda1,2Δ::HygB/cda1,2Δ::HygB*	This study
CL52	*MAT**a**/MATα ura3/ura3 leu2/leu2 his3ΔSK/his3ΔSK trp1Δ::hisG/trp1Δ::hisG ARG4/arg4-NspI lys2/lys2 hoΔ::LYS2/hoΔ::LYS2 RME1/rme1Δ::LEU2 osw4Δ::HIS3MX6/osw4Δ::HIS3MX6*	This study
CL54	*MAT**a**/MATα ura3/ura3 leu2/leu2 his3ΔSK/his3ΔSK trp1Δ::hisG/trp1Δ::hisG ARG4/arg4-NspI lys2/lys2 hoΔ::LYS2/hoΔ::LYS2 RME1/rme1Δ::LEU2 osw6Δ::HIS3MX6/osw6Δ::HIS3MX6*	This study
CL57	*MAT**a**/MATα HO/HO leu2/leu2 TRP1/TRP1 lys2/lys2 URA3:tet0224/ URA3:tet0224 npp2Δ::HIS3 npp1Δ::kanMX6/npp2Δ::HIS3 npp1Δ::kanMX6*	This study
CL59	*MAT**a**/MATα HO/HO leu2/leu2 URA3::tetO224/URA3::tetO224 npp1Δ::kanMX6/npp1Δ::kanMX6*	This study
CL62	*MAT**a** his3Δ1 leu2Δ0 met15Δ0 ura3Δ0 cyh2*	This study

(all patches should contain both mating types due to the presence of the *HO* gene) and then replica plated onto nitrocellulose membranes on SPO plates for dityrosine fluorescence detection under UV_{302}.

3.2.4 Construction of double mutants for pairwise interactions

To examine synthetic interactions between different genes implicated in outer spore wall assembly, individual strains carrying deletions of each gene examined (listed in Table 3.3) were taken from the SK1 knockout collection and crossed to a set of strains from the BY4741 knockout collection carrying deletions of all the remaining genes analyzed. Each double mutant combination was constructed twice, once with each gene as the *MAT**a*** parent in the initial mating (i.e. from the yeast knockout collection) and once with each gene as the *MAT**a*** parent (from the SK1 knockouts). Construction of the initial diploids, isolation of the double mutants, and scoring of dityrosine fluorescence was performed similarly to the *dtr1*Δ synthetic screen described above except that no selection for cycloheximide resistance was used. Three separate isolates for each SK1 knockout were crossed to the other deletions and reduction of dityrosine fluorescence intensity in two of the three replicates was considered a synthetic interaction.

3.2.5 Visualization for pairwise genetic interaction networks

The network in Figure 3.2 was created using Cytoscape (version 2.8.3) (SHANNON *et al.* 2003).

3.2.6 Analysis of dityrosine fluorescence by patch assay

Cells to be assayed were grown as patches on YPD plates for 1 day and then replica- plated onto nitrocellulose membranes (Whatman Optitran BA-S 85) on

YPD plates. After two days growth, the membranes were transferred to SPO plates and incubated for 3 days at 30 °C. The membranes were then transferred to petri dishes containing 200 µl of water, 50 µl of 10 mg/ml zymolyase and 15 µl of β-mercaptoethanol at 30 °C for 5 hrs. Finally, the membranes were wetted with 0.1 M NaOH solution to raise the pH and exposed to short wave UV light for the detection of dityrosine fluorescence.

3.2.7 Microscopy and image processing

All images were collected on a Zeiss Axio-Observer Z1 microscope using a Hamamatsu ER-G camera. Images were collected and fluorescence intensity was measured using Zeiss Axiovision software (version 4.7).

- ***Quantitative analysis of dityrosine fluorescence***

Dityrosine fluorescence from the spore wall was quantified as described (SUDA *et al.* 2009). Briefly, cells were sporulated in liquid SPO medium for three days, centrifuged, washed once with water, re-suspended in 5% ammonia solution to raise the pH, and finally transferred onto microscope slides. Images were collected with a dityrosine fluorescence-specific filter set (Ex. 320 nm/Em. 410 nm) at fixed exposure times. The dityrosine fluorescence intensity (in arbitrary units) was calculated for each cell by taking the average intensity at two points in the spore wall and subtracting the background fluorescence outside of the spore.

-***Calcofluor White and Eosin Y staining***

Sporulated cells were harvested and washed with 1 ml McIlvaine's buffer (0.2 M Na_2HPO_4 /0.1 M citric acid [pH 6.0]) followed by staining with 30 µl Eosin Y disodium salt (Sigma) (5 mg/ml) in 500 µl McIlvaine's buffer for 10 min at room temperature in the dark. Cells were then washed twice in McIlvaine's buffer to remove residual dye and resuspended in 200 µl McIlvaine's buffer. One microliter of a 1mg/ml Calcofluor White

solution (Sigma) was then added to the Eosin Y-stained cells before transfer to microscope slides. Fluorescence of Calcofluor White and Eosin Y stains was examined using DAPI and FITC filter sets, respectively.

-BODIPY TR methyl ester staining

Sporulating cells were stained with 5µM of BODIPY TR methyl ester (Life Technologies) in PBS buffer at room temperature for 10 min and washed twice with PBS buffer. BODIPY TR fluorescence was visualized using a Rhodamine filter set.

3.2.8 Electron microscopy

Sporulating yeast cells were collected and processed for electron microscopy as described in (NEIMAN 1998).

3.2.9 Test of ether resistance

Cells were sporulated in liquid SPO medium at 30 °C for 2 days. All cultures displayed at least 75% sporulation. Serial dilutions (1, 10^{-1}, 10^{-2}, 10^{-3}) of sporulated cells were spotted on two YPD plates. One plate served as an ether-negative control. The other plate was inverted over ether-soaked filter paper (Whatman #3, 1003-090) for 45 min. Plates were incubated at 30 °C for one to two days and photographed.

3.2.10 NMR methods

-Spore wall sample preparation

Isolation of spore walls was performed similarly to that previously described [50]. ~25 g (wet weight) of sporulated wild type (AN120) cells were collected (2.5 L of SPO medium at 75% sporulation frequency), resuspended and washed with 0.1 M sodium phosphate buffer (pH 7.2) and then resuspended in 60 ml of 0.1 M sodium phosphate buffer (pH 7.2) containing 20 mg of Zymolyase (US Biologicals, Salem, MA) as well as

0.04 % of β-mercaptoethanol. The suspension was incubated with shaking at 30 °C for 2 hr until spores were released from asci. To remove ascal debris, spore pellets were washed three times at 4,000 rpm for 10 min in a swinging bucket rotor with 0.5 % Triton X-100 solution and then resuspended in a small volume (around 10 ml) of 0.5% TX-100, layered onto a 30 ml Percoll (MP Biomedicals, Santa Ana, CA) step gradient [Percoll/TX-100/2.5 M sucrose; from bottom to top 0.8/ 0.0005/ 0.1à0.7/ 0.001/ 0.1à 0.6/ 0.0015/ 0.1 à 0.5/ 0.002/ 0.1] and spun at 10,000 rpm for 45 min at 4 °C in a Sorvall SS34 rotor to separate spores from vegetative cells. Spores were collected from the bottom layer and washed three times with 0.5% TX-100 at 6,000 rpm for 5 min. The collected spores were then mixed with 20 ml of 0.5 % Triton X-100 solution and 20 ml of 0.5 mm zirconium/silica beads (BioSpec, Bartlesville, OK) for lysis by bead beating. Spores were disrupted in a BeadBeater (BioSpec, Bartlesville, OK) with pulses of 20 sec ON /40 sec OFF until 80% of spores were disrupted (as determined by light microscopy). The spore wall fragments were separated from intact spores and spore cytoplasm bylayering onto a cushion of 60% Percoll/ 2% TX-100/ H_2O and centrifugation at 23,000 rpm in a Beckman SW41 rotor at 4 °C for 1 hr. Spore wall fragments form a visible band within the Percoll cushion and this band was collected, the Percoll diluted by addition of 35 ml of 0.5% Triton TX-100 and the fragments were pelleted by centrifugation at 6,000 rpm in a Sorvall SS-34 rotor for 5 min. The wall pellets were then washed three times with distilled water. Spore walls from mutant strains appear to have a somewhat lower density and so the concentration of Percoll used in the purifications had to be adjusted. For AN264, CL35, CL7, CL15, and CL26, the steps in the Percoll gradient at the first stage were 0.5→0.4→0.3→0.2. The cushion used in the second stage was 40% Percoll/ 2% TX-100/ H_2O. For CL6, the Percoll gradient was 0.35→0.25→0.15→0.05 and the Percoll cushion was 35% Percoll/ 2% TX-100/ H_2O.

To remove the inner spore wall layers, collected spore wall fragments were first

resuspended in 5 ml of 50 mM Tris (pH 8.0) containing 1% SDS and 5 mM DTT. The sample was heated at 95 °C for 1 hr and then 1 mg of protease K (US Biologicals) was added and the solution incubated at 50 oC for 24 hr. After the protease K reaction, the samples were again heated to 95 °C for 1 hr to inactivate the protease K and then washed 3 times with 0.5% TX-100 followed by 3 washes with 0.1 M sodium phosphate buffer. Samples were then resuspended in 2 ml of 0.1 M sodium phosphate buffer (pH 7.2) containing 0.04% of ß-mercaptoethanol. 1.5 mg of zymolyase (US Biologicals) was added and samples were incubated at 37 °C for 24 hr. After zymolyase digestion, samples were washed 3 times with 0.5% TX-100 and then 3 times with H_2O before desiccation in a speed vacuum concentrator at low temperature.

-Solid-state NMR analys

Spore wall solid-state NMR experiments were carried out on a 500 MHz Bruker AVANCE spectrometer using an HX magic angle spinning (MAS) probe. For analysis, 50-100 mg of dried spore wall samples were packed into 4 mm rotors. All experiments were performed at room temperature. The MAS speed was between 10 and 13 kHz to eliminate the overlap of relevant resonances with MAS sidebands. A ramped-amplitude cross polarization (CP) sequence was used to record the 1D ^{13}C chemical shift spectra with proton decoupling. The experimental conditions were as follows: a 4 µs ^{1}H 90° pulse was followed by 2 ms simultaneous ^{13}C and ^{1}H contact pulses and an acquisitiontime of 27 ms. The repetition delay was 3 s. 2000 to 6000 scans were recorded for each spectrum. The data were processed with exponential line broadening of 100 Hz. The carbonyl resonance of powdered glycine at 176.46 ppm relative to tetramethylsilane was used as an external ^{13}C reference.

3.3 Results

3.3.1 A sensitized screen identifies new genes important for dityrosine fluorescence

The transporter Dtr1 functions in the export of dityrosine from the spore cytoplasm, but deletion of *DTR1* results in only a modest reduction in dityrosine incorporation into the spore wall, presumably due to the presence of alternative transporters (FELDER *et al.* 2002). We reasoned that extracellular dityrosine might nonetheless be limiting in *dtr1*Δ mutants and so this mutant might be more sensitive to additional perturbations in outer spore wall assembly. Thus, we performed a screen to identify mutants that result in loss of dityrosine fluorescence in combination with *dtr1*Δ.

Using a modified synthetic genetic array protocol a *dtr1*Δ strain was crossed to a collection of knockout mutants (TONG *et al.* 2004). As high sporulation frequency is required, we used a set of 301 knockouts of sporulation-induced genes that was previously constructed in the efficiently sporulating SK1 background (RABITSCH *et al.* 2001). Diploids homozygous for *dtr1*Δ and *mutX*Δ were tested for fluorescence after sporulation on plates by a patch assay. Fluorescence was monitored by sporulating cells on nitrocellulose filters and then exposing the filters to shortwave UV light. For each gene, homozygous *mutX*Δ *DTR1* diploids were also examined using the same assay. Mutants that displayed wild-type fluorescence in the *DTR1* background but reduced fluorescence in combination with *dtr1*Δ in at least two of three replicates, were considered to have a genetic interaction with *dtr1*Δ.

Mutants in 38 genes that displayed reduced dityrosine fluorescence only in combination with *dtr1*Δ were identified (Table 3.1). Most of these genes were not identified in previous screens of this same collection of knockouts in SK1 for other phenotypes associated with outer spore wall defects including ether sensitivity, spore wall permeability, and sensitivity to digestion by *Drosophila* indicating that the synthetic screen worked to uncover new genes with possible roles in outer spore wall

assembly (COLUCCIO *et al.* 2004a; COLUCCIO *et al.* 2008; SUDA *et al.* 2009). Several of the mutants identified were in uncharacterized ORFs with no gene designation. For reasons explained below, we have named some of these ORFs. The acronym for *OSW6* (*IRC18*/*YJL038w*) and *OSW7* (*YFR039c*) stands for Outer Spore Wall), while the acronm for *LDS1* (*YAL018w*), and *LDS2* (*YOL047c*) stands for Lipid Droplet in Sporulation.

Table 3.2 Mutants displaying synthetic dityrosine defects with *dtr1*Δ.

ORF	Gene	Found in earlier spore wall screens[a]	Comments[b]
YAL018c	*LDS1*		paralog of *LDS2*
YBR134w		Ether	dubious ORF/overlaps *HSL7*
YBR250w	*SPO23*		
YCR010c	*ADY2*		acetate transporter
YDL076c	*RXT3*		HDAC complex subunit
YDR108w	*TRS85*		TRAPP subunit
YDR273w	*DON1*		leading edge complex protein
YDR480w	*DIG2*		
YDR506c	*GMC1*		synaptonemal complex assembly
YDR525w	*API2*		dubious ORF
YEL016c	*NPP2*		nucleotide pyrophosphorylase
YER106w	*MAM1*	Permeable	kinetochore protein
YER182w	*FMP10*		mitochondrial protein
YFR023w	*PES4*		RNA binding motif
YFR039c	*OSW7*	Fly	signal peptide
YGL096w	*TOS8*		putative transcription factor
YGL144c	*ROG1*		putative lipase
YHR153c	*SPO16*		synaptonemal complex assembly
YIR013c	*GAT4*		putative transcription factor
YJL037w	*IRC18*/*OSW6*	Fly	paralog of *OSW4*
YJL038c	*LOH1*/*OSW4*	Permeable	paralog of *OSW6*
YJL162c	*JJJ2*		DNAJ domain
YJR036c	*HUL4*		E3 ligase
YJR099w	*YUH1*		ubiquitin hydrolase
YKL121w	*DGR2*		
YLL030c	*RRT7*		dubious ORF
YLL054c			

YLR030w			
YLR238w	*FAR10*		FAR complex subunit
YLR373c	*VID22*	Ether	
YML119w			
YMR147w			
YMR148w	*OSW5*	Permeable	
YMR262w			
YOL047c	*LDS2*		paralog of *LDS1*
YOR350c	*MNE1*		mitochondrial protein
YPL033c	*SRL4*	Permeable	
YPL184c	*MRN1*		RNA binding

[a]Whether a mutation in the gene was identified in earlier screens of the same collection for ether sensitive spores (COLUCCIO *et al.* 2004a), spores with permeable spore walls (SUDA *et al.* 2009), or spores with lowered resistance to digestion by *Drosophila* (COLUCCIO *et al.* 2008).

[b]Information from the SGD: www.yeastgenome.org

3.3.2 A highly redundant network of genes is involved in dityrosine layer assembly

A significant fraction of the genes examined in the screen (~13%) displayed fluorescence defects in the sensitized *dtr1*Δ background. This suggests that the process is somehow buffered so that individual mutants have only modest effects. One possible explanation for the failure of individual mutants to produce strong effects on dityrosine would be the presence of redundant pathways leading to dityrosine incorporation. If so, combining mutants in genes involved in two separate pathways might lead to decreased dityrosine fluorescence even in the presence of *DTR1*. This hypothesis was tested by constructing double mutants between genes identified in our screen and examination of dityrosine fluorescence.

As gene products directly involved in assembly of polymerized dityrosine are likely localized to the spore wall, we focused on those with predicted signal peptides or transmembrane domains, or with predicted enzymatic activities. In addition, we also included the genes *OSW3* and *YEL023c* since these genes have been implicated in outer spore wall formation in other studies [our unpublished results and (SUDA *et al.* 2009)]. Most double mutant combinations were constructed twice and each strain was tested in triplicate for dityrosine fluorescence. Double mutants exhibiting a reduction in dityrosine fluorescence in two at least two of the three replicates were scored as a genetic interaction (Table 3.3).

Reduced dityrosine fluorescence was observed for many different mutant combinations. Most of the mutants tested displayed interactions with at least seven other mutants. The extent of these interactions can be seen in graphic representation of the interaction network which shows a highly interconnected set of genes with relatively few outliers having limited synthetic interactions (Figure 3.2). This architecture suggests that an assembly of the dityrosine layer is accomplished through a number of alternative processes with overlapping function. Major hubs of the network, such as *OSW6* or *LDS2*,

Table 3.3 Analysis of double mutants.
Three biological replicates were examined for each indicated double mutant. Numbers indicate fraction of replicates that displayed reduced dityrosine fluorescence. Double mutants scored as interactions and used in Figure 3.2 are highlighted in yellow.
"+" indicates no loss of fluorescence observed.
n.d. not determined.

	lds1	*gmc1*	*spo23*	*api2*	*npp2*	*hul4*	*rog1*	*osw7*	*osw5*	*yml119w*	*lds2*	*gat4*	*pes4*	*ymr147w*	*ymr262w*	*osw6*	*osw4*	*osw3*	*yel023c*	*dtr1*
lds1 test1		2 of 3	2 of 3	2 of 3	3 of 3	2 of 3	+	+	+	+	3 of 3	+	2 of 3	+	2 of 3	2 of 3	+	+	+	n.d
lds1 test2		3 of 3	2 of 3	2 of 3	3 of 3	2 of 3	1 of 3	+	+	3 of 3	3 of 3	1 of 3	2 of 3	+	1 of 3	2 of 3	1 of 3	+	1 of 3	n.d
gmc1	3 of 3		+	+	+	2 of 3	+	+	+	+	1 of 3	1 of 3	+	+	1 of 3	2 of 3	1 of 3	+	1 of 3	n.d
api2	1 of 3	+	+		2 of 3	+	+	+	+	2 of 3	2 of 3	+	+	+	+	2 of 3	+	+	+	+
npp2	1 of 3	+	+	+		1 of 3	+	+	+	2 of 3	3 of 3	3 of 3	2 of 3	+	+	3 of 3	3 of 3	2 of 3	+	3 of 3
hul4	3 of 3	+	+	+	+		1 of 3	+	+	1 of 3	3 of 3	1 of 3	3 of 3	+	+	3 of 3	+	+	2 of 3	1 of 3
rog1	2 of 3	+	+	+	2 of 3	1 of 3		+	+	2 of 3	3 of 3	1 of 3	+	+	+	2 of 3	+	+	1 of 3	3 of 3
osw7	2 of 3	2 of 3	+	+	+	+	+		+	2 of 3	3 of 3	3 of 3	+	+	+	3 of 3	+	+	1 of 3	3 of 3
osw5	1 of 3	+	+	+	1 of 3	1 of 3	+	+		+	2 of 3	+	+	+	+	3 of 3	+	+	2 of 3	n.d
yml119w	2 of 3	2 of 3	+	+	2 of 3	1 of 3	+	+	1 of 3		2 of 3	2 of 3	+	+	1 of 3	2 of 3	+	+	2 of 3	2 of 3
lds2	2 of 3	+	1 of 3	+	1 of 3	2 of 3	2 of 3	1 of 3	1 of 3	1 of 3		3 of 3	2 of 3	2 of 3	1 of 3	2 of 3	3 of 3	1 of 3	1 of 3	2 of 3
gat4	2 of 3	2 of 3	+	1 of 3	+	+	+	+	+	2 of 3	3 of 3		2 of 3	+	+	2 of 3	1 of 3	3 of 3	+	3 of 3
pes4	2 of 3	1 of 3	1 of 3	1 of 3	1 of 3	3 of 3	+	+	2 of 3	2 of 3	3 of 3	+		+	+	2 of 3	+	+	1 of 3	+
ymr147w	2 of 3	+	+	+	2 of 3	2 of 3	+	+	+	2 of 3	3 of 3	+	+		+	2 of 3	1 of 3	+	3 of 3	+
ymr262w	1 of 3	+	+	+	+	1 of 3	+	+	+	+	3 of 3	3 of 3	2 of 3	+		3 of 3	3 of 3	3 of 3	3 of 3	3 of 3
osw4	2 of 3	+	1 of 3	1 of 3	1 of 3	+	+	+	+	+	1 of 3	2 of 3	2 of 3	+	+	2 of 3		2 of 3	1 of 3	2 of 3
osw3	3 of 3	3 of 3	2 of 3	+	2 of 3	3 of 3	3 of 3	+	+	+	3 of 3	3 of 3	+	+	+	2 of 3	1 of 3		2 of 3	3 of 3
yel023c	+	1 of 3	1 of 3	2 of 3	1 of 3	2 of 3	1 of 3	1 of 3	+	+	3 of 3	3 of 3	3 of 3	+	1 of 3	3 of 3	3 of 3	2 of 3		2 of 3
dtr1	2 of 3	1 of 3	+	2 of 3	2 of 3	2 of 3	1 of 3	+	+	2 of 3	3 of 3	3 of 3	3 of 3	3 of 3	+	3 of 3	3 of 3	3 of 3	2 of 3	

show interactions with most of the other genes and might represent particularly important functions in assembly of the outer spore wall.

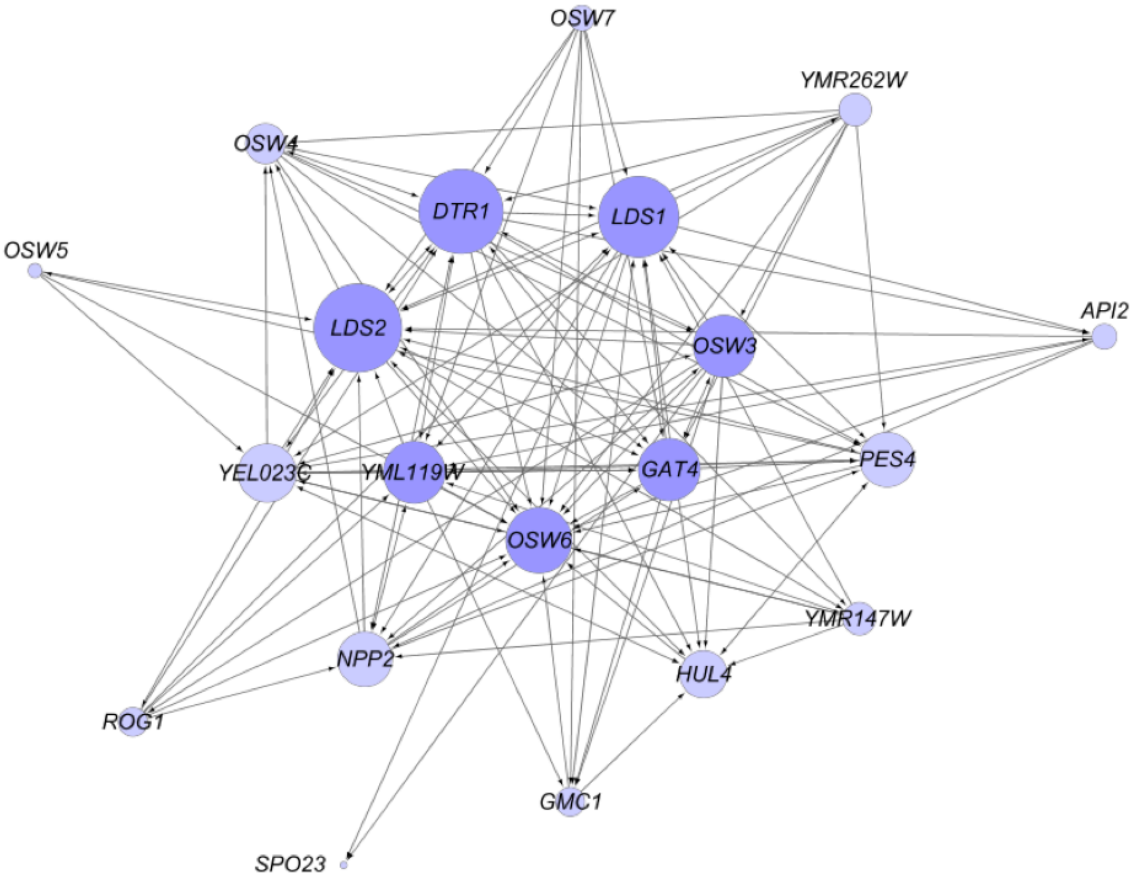

Figure 3.2 Genetic interactions between genes involved in dityrosine layer formation. Cytoscape was used to represent the genetic interactions listed in Table 3.3. Lines between the circles indicate reduction of dityrosine fluorescence in the double mutant. Double mutants were constructed from two independent pairs of parental strains and tested in three biological replicates (see Methods). Arrowheads indicate whether the interaction was seen in one (one arrowhead) or both (two arrowheads) double mutant strains. Circles in darker purple indicate genes with >10 interacting partners. The size of the circles increases with the number of genetic interactions seen for each gene.

3.3.3 Paralogous genes are redundant for dityrosine assembly

The double mutant analysis suggests that different processes can compensate for each other in spore wall assembly. Another type of redundancy results when different genes encode proteins with the same function. Of the 20 genes shown in the network in Figure 3.2, 11 are genes with potential paralogs in the *S. cerevisiae* genome (Table 3.4). If the paralogous genes are functionally redundant, then mutation of all the genes within a set should lead to a more severe phenotype. This idea was tested by construction of diploids homozygous for deletions of all of the genes within the first six paralog sets listed in Table 3.4 (attempts to construct deletions for the other three sets were unsuccesful). These diploids were then examined for dityrosine fluorescence both by patch assay and quantitatively using fluorescence microscopy (SUDA *et al.* 2009) (Figure 3.3). Multiple mutants in all six of the paralog sets displayed reduced dityrosine fluorescence relative to single mutants, supporting the idea that these genes encode functionally redundant proteins. Quantitatively, dityrosine fluorescence was reduced by at least 45%, in deletions of all the paralog sets. The most severe defects were seen in the *lds1*Δ *lds2*Δ *rrt8*Δ and *osw4*Δ *osw6*Δ mutant strains where the fluorescence signal was reduced the levels of a *dit1*Δ, which lacks dityrosine.

3.3.4 Paralogous genes are not required for the presence of a chitosan layer

The deletion of the paralogous pairs (and triples) is distinct from the combination with *dtr1*Δ or other mutants in that these mutations likely remove a single function (e.g. Osw4/6 function) rather than weakening two different aspects of assembly (e.g. Osw4 function and Lds1 function). For this reason, the strains carrying deletions of all the genes for a particular paralog set were phenotypically characterized to determine what role each paralogous group plays in outer spore wall assembly. For simplicity, each multiple mutant strain will be indicated by the name of the paralog set given in Table 3.4, e.g. the

*lds1*Δ *lds2*Δ *rrt8*Δ strain will be referred to as the Lds mutant.

Table 3.4 Paralogous gene sets implicated in outer spore wall formation

ORF	Gene	Sporulation-induced[a]	% Similarity[b]
YAL018c	*LDS1*	Y	53% w/*RRT8*
YOL047c	*LDS2*	Y	38% w/*LDS1*
YOL048c	*RRT8*	Y	58% w/*LDS2*
YJL038c	*OSW4*/*LOH1*	Y	50% w/*OSW6*
YJL037w	*OSW6*/*IRC18*	Y	
YBR180w	*DTR1*	Y	59% w/*QDR3*
YIL120w	*QDR1*	N	48% w/*DTR1*
YBR043c	*QDR3*	N	48% w/*QDR1*
YLR013w	*GAT3*	Y	70% w/*GAT4*
YIR013c	*GAT4*	Y	
YFR039c	*OSW7*	Y	48% w/*SHE10*
YGL228w	*SHE10*	N	
YCR026c	*NPP1*	N	57% w/*NPP2*
YEL016c	*NPP2*	Y	
YDR506c	*GMC1*	Y	52% w/*FET5*
YMR058w	*FET3*	N	50% w/*GMC1*
YFL041w	*FET5*	Y	65% w/*FET3*
YGL144c	*ROG1*	Y	63% w/*ROG1*
YDL109c		N	

[a]Indicates whether the transcript is induced during sporulation (CHU *et al.* 1998)
[b]% similarity is based on comparison of the two sequences using BLASTP (ALTSCHUL *et al.* 1990).

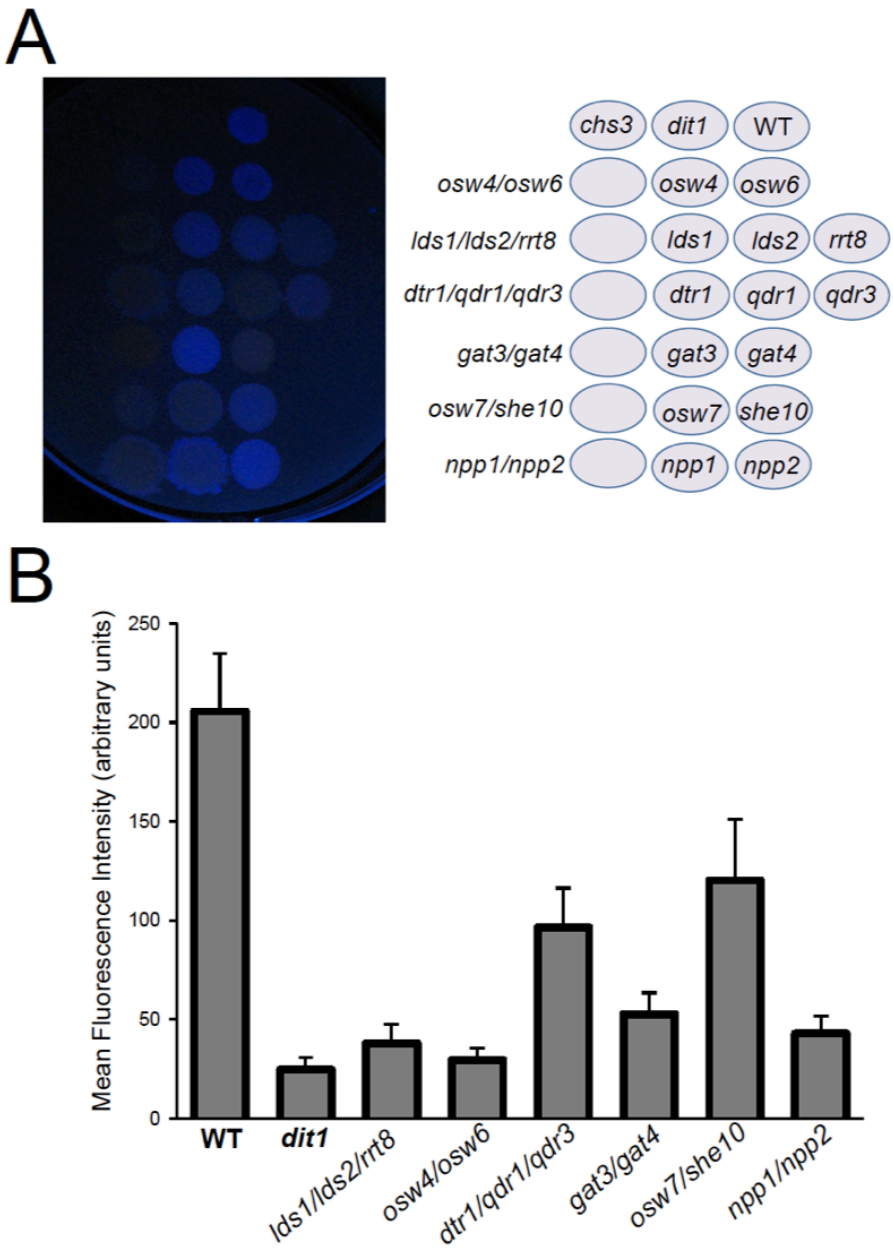

Figure 3.3 The effect of deletion of paralog sets on dityrosine fluorescence. A) Patch assay of dityrosine fluorescence. Single and multiple mutant diploid cells of the indicated genotypes were sporulated on filters and the filter was exposed to UV light to detect dityrosine fluorescence. B) Quantitation of dityrosine fluorescence in the paralog mutant strains. Dityrosine fluorescence from the spore wall was quantified for strains of the indicated genotypes using a fluorescence microscopy assay. For each strain, the fluorescence value represents the average of twenty individual cells. Error bars indicate one standard deviation.

Assembly of the dityrosine layer requires the underlying chitosan layer, so loss of dityrosine fluorescence could be an indirect effect of loss of chitosan (CHRISTODOULIDOU *et al.* 1999). Each paralog set mutant strain was stained with the chitin/chitosan binding dye Calcofluor White as well as the chitosan specific dye Eosin Y and examined in the fluorescence microscope.

In wild-type cells, spores stain weakly with Calcofluor White because the dityrosine layer blocks the dye from binding the underlying chitosan (TACHIKAWA *et al.* 2001). By contrast, Eosin Y binds efficiently to the chitosan in the wild-type spores (BAKER *et al.* 2007) (Figure 3.4, top row). Deletion of the *CDA1* and *CDA2* genes encoding chitin deacetylases results in spore walls that contain chitin instead of chitosan, resulting in the absence of a dityrosine layer (CHRISTODOULIDOU *et al.* 1999). Consistent with this fact, *cda1*Δ *cda2*Δ spores stain with Calcofluor White but not with Eosin Y (Figure 3.4, 2nd row). A *chs3*Δ mutant lacks both chitin and chitosan and as a result stains with neither dye (Figure 3.4, 3rd row). A *dit1*Δ mutant contains chitosan but lacks dityrosine and binding of both dyes is seen (Figure 3.4, 4th row).

None of the paralog sets is required for formation of the chitosan layer, as all of the parologous mutant strains stained with Eosin Y. However, staining of the Lds mutant strain was noticeably less intense than in *dit1*Δ, suggesting that this mutant may have some loss of chitosan in addition to dityrosine. Compared to wild type, the Lds, Osw4/6, Dtr, and Gat mutants all displayed increased Calcofluor White staining consistent with reduced levels of dityrosine in the wall. The Osw/She and Npp strains did not show clear increases in Calcofluor White staining. For Osw/She this is perhaps consistent with the quantitatively modest reduction in dityrosine fluorescence in the double mutant (Figure 3.3B).

3.3.5 Paralogous genes are required for functional spore walls

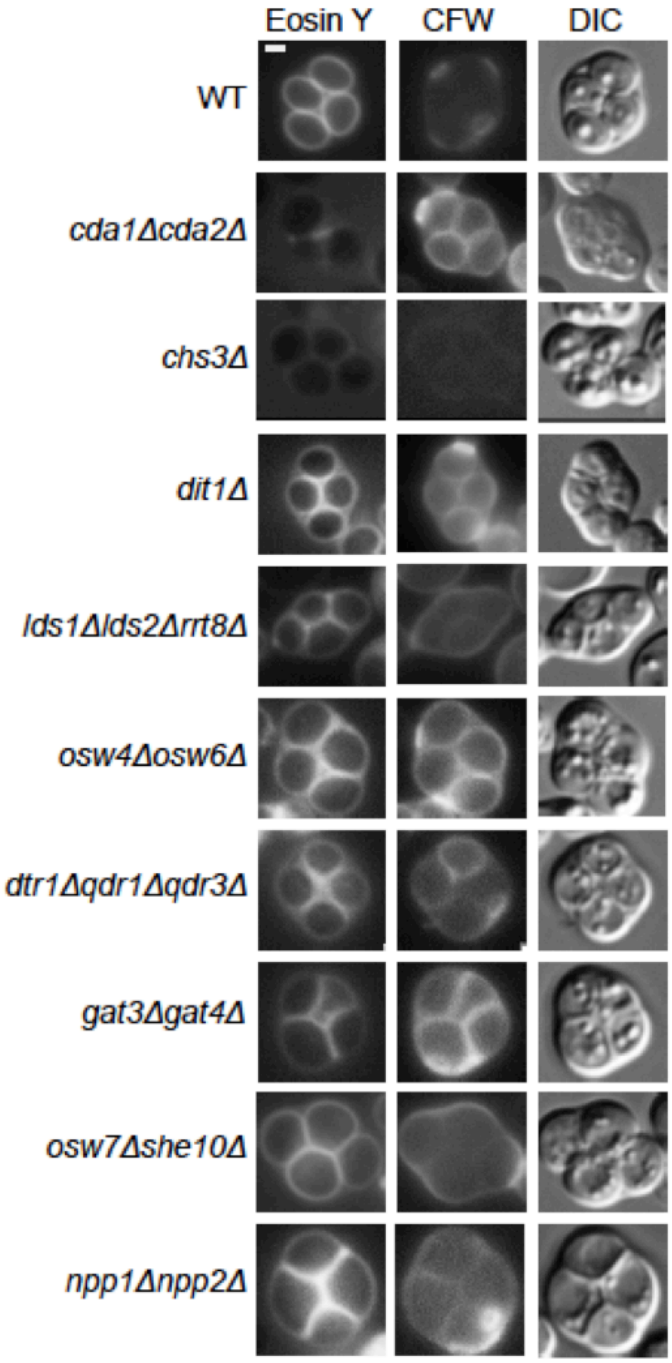

Figure 3.4 The effect of deletion of paralog sets on chitosan. Strains of the indicated genotype were sporulated and stained with both Eosin Y and Calcofluor White (CFW) to visualize the chitosan layer. The *cda1*Δ *cda2*Δ, *chs3*Δ, and *dit1*Δ strains provide standards for the conditions chitin /no chitosan/no dityrosine, no chitin/no chitosan/ no dityrosine, and chitin/chitosan/no dityrosine, respectively. For all strains > 30 cells were examined and > 60% display the staining patterns shown here. DIC = differential interference contrast. Scale bar = 1 micron.

Spore walls function to protect cells form various exogenous stresses. One assay that is commonly used for spore wall function is sensitivity to ether vapor. Ether is toxic to vegetative cells but the outer layers of the spore wall confer resistance to ether exposure (DAWES and HARDIE 1974). To test whether the various paralog sets are required not just for wild-type levels of dityrosine fluorescence but also for making functional spore walls, diploids containing deletions of each set were tested for ether sensitivity. The outer layers of the spore wall contribute to ether resistance, but to different extents so that *dit1*Δ mutants, which lack dityrosine, are sensitive but less so than *chs3*Δ mutants, which lack both chitosan and dityrosine (Figure 3.5). All of the paralog set mutants showed increased sensitivity to ether. In fact, all of the combinations appeared more sensitive to ether than a *dit1*Δ strain, suggesting that the spore wall defect in these mutants may be more significant than just the loss of dityrosine. In the case of the Osw4/6 and Osw/She mutants, deletion of both paralogs is necessary to reveal the sensitive phenotype. In the other paralog sets, however, deletion of one of the genes is sufficient to account for much of the sensitivity. This is most obvious in the Lds set where the *rrt8*Δ single mutant is as ether sensitive as the *lds1*Δ *lds2*Δ *rrt8*Δ triple mutant. The patterns of dityrosine fluorescence in the individual mutants (Figure 3.3A) do not necessarily reflect the patterns of ether sensitivity. Thus, the mechanistic link between ether resistance and outer spore wall structure is unclear. However, the ether tests reveal that the spore walls in all of the paralog mutants are compromised in their ability to confer stress resistance to the spore.

3.3.6 Solid state NMR identifies a novel component of the spore wall

The hypothesis that multiple assembly routes are used for dityrosine incorporation into the spore wall suggests that different mutants might accumulate different intermediates in the biosynthetic pathway. Solid state nuclear magnetic resonance (NMR)

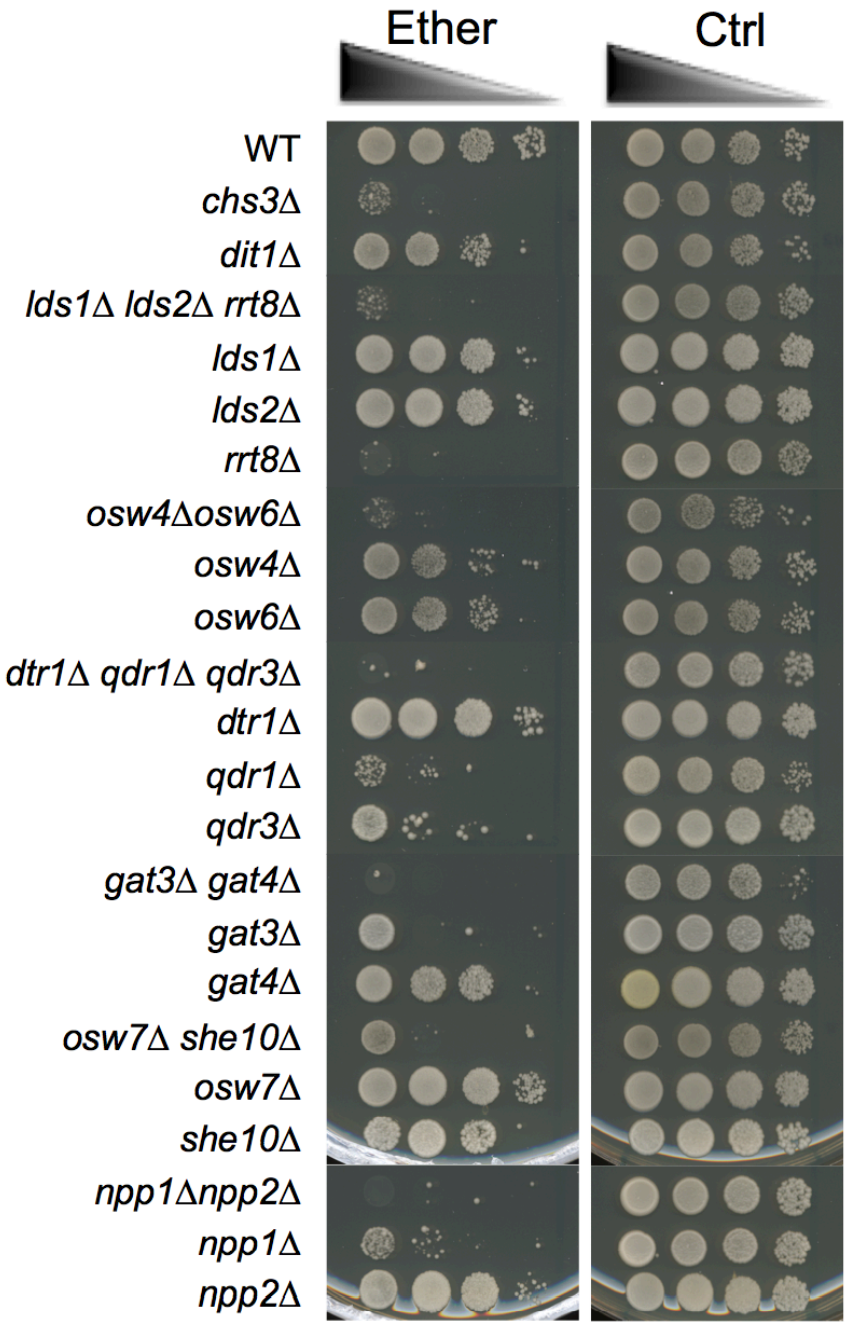

Figure 3.5 The effect of deletion of paralog sets on ether resistance of spores. Strains of the indicated genotypes were sporulated in liquid to >70% asci and then 10-fold serial dilutions were spotted onto YPD plates. Left panels, plates exposed to ether vapor for 45 minutes before incubation at 30 °C. Right panels, no ether control.

has been proven to be an effective tool for the analysis of intact bacterial cell walls (SHENOUDA *et al.* 1996; KERN *et al.* 2008) and we sought to apply this technology to analyze the spore wall. An established protocol for purification of spore walls was adapted to isolate large quantities of spore wall fragments enriched for just the outer spore wall layers. These purified outer spore walls from wild type spores were analyzed using ^{13}C solid state NMR spectroscopy. The samples were not isotopically enriched but relied on the natural abundance of ^{13}C in the wall components. The ^{13}C spectrum from a wild-type spore wall prepared in this way is shown in Figure 3.6. The identities of many of the chemical shifts were confirmed by comparison to spectra prepared using purified chitosan and tyrosine (Figure 3.7). The strongest resonances are from the six carbons of the glucosamine ring of chitosan (labeled in red in Figure 3.6). The conversion of chitin to chitosan is incomplete during spore wall formation as shown by the unique resonance at 22 ppm that corresponds to the methyl carbon of the acetyl moiety on N-acetyl-glucosamine groups present in the polymer (indicated by –CH3 in Figure 3.6). The carbonyl resonance associated with the N-acetyl-glucosamine groups is also observed at ~174 ppm, but overlaps with the carbonyl resonance of dityrosine. A similar incomplete conversion of chitin to chitosan has been reported in cell walls of other fungi (FUKAMIZO *et al.* 1992). Small resonances at chemical shifts between 130 ppm and 155 ppm (labeled in green) correspond to the carbons of the dityrosine rings as confirmed by the loss of these signals when the spore wall of a *dit1*Δ mutant was examined (Figure 3.6, lower spectrum). As expected, the resonances corresponding to chitosan (and the residual N-acetyl- glucosamine groups of chitin) are still observed in the *dit1*Δ spore walls. In the spectrum of the *dit1*Δ mutant, the integrated intensities of carbonyl and methyl resonances of N- acetyl-glucosamine groups is close to 1:1, indicating that the shoulder on the C=O resonance in the wild-type spectrum is primarily due to dityrosine. In addition, a number of significant resonances in the range of 25 to 35 ppm were observed

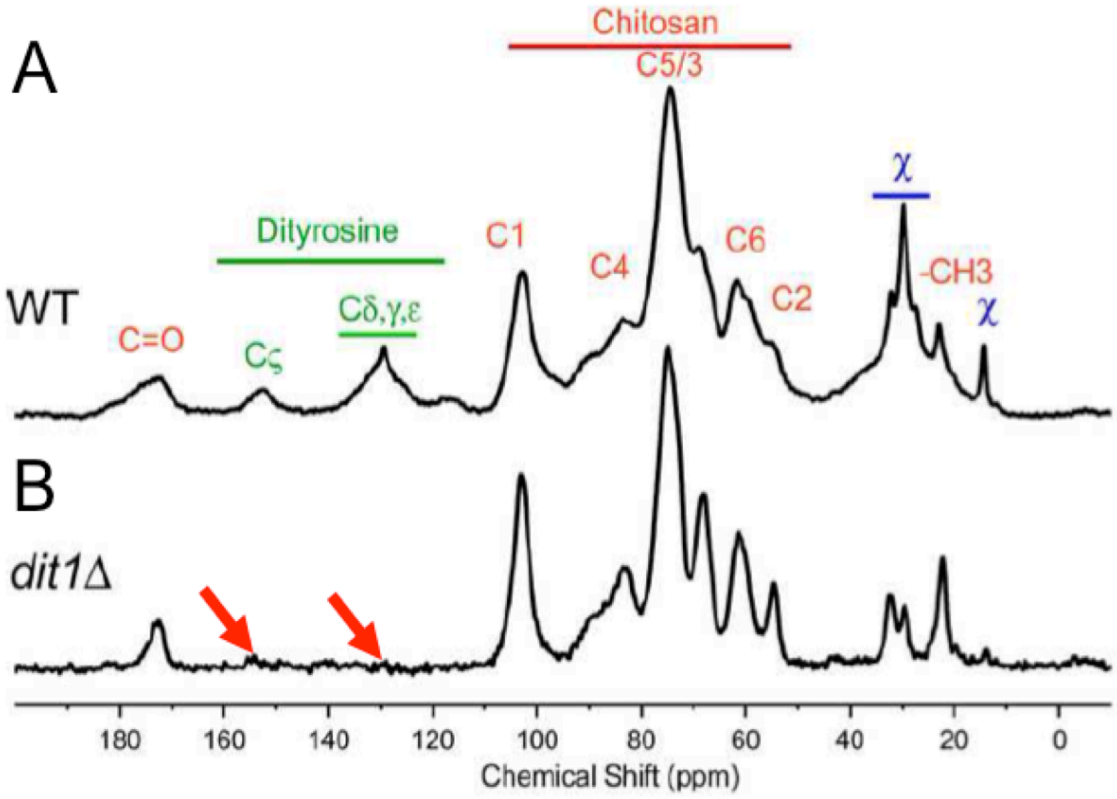

Figure 3.6 NMR analysis of the outer spore wall. Outer spore walls were purified from wild type (AN120) or *dit1*Δ cells and then analyzed by solid state ^{13}C NMR. Resonances assigned to chitosan carbons are designated by red labels and resonances from dityrosine are indicated by green labels. Unassigned chemical shifts from component χ are indicated in blue. Upper spectrum, spore wall from wild type. Lower, spectrum, spore wall from *dit1*Δ. For comparison, spectra are scaled so the C5/3 resonance of chitosan is of constant height.

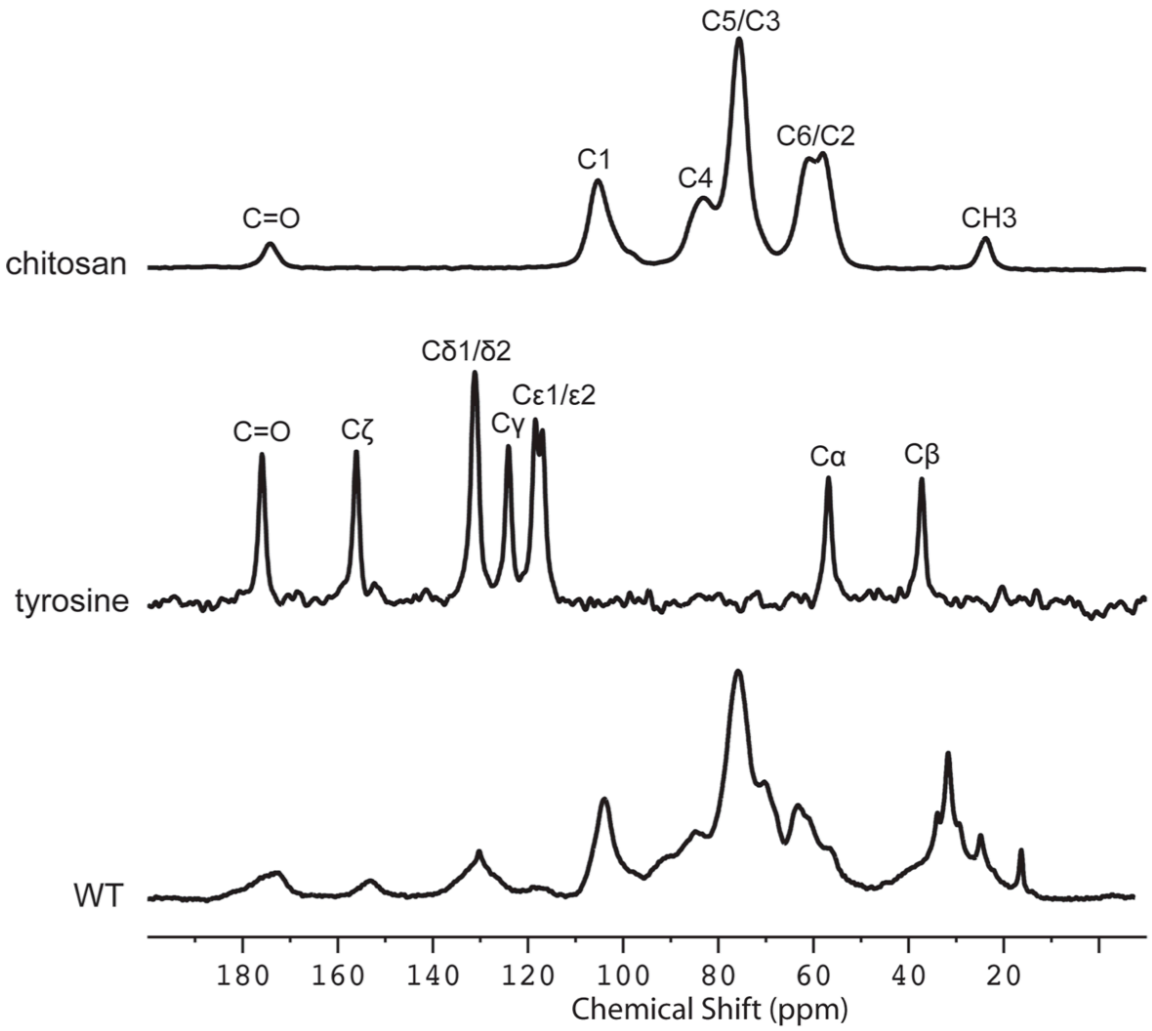

Figure 3.7 Solid state ^{13}C NMR spectra for chitosan, L-tyrosine, and wild-type spore walls. Spore walls were prepared as described in Methods. Chitosan and L-tyrosine are from Sigma (Chicago, Illinois).

that are not from chitosan or dityrosine and, thus, represent an unknown component of the outer spore wall, which we designate as component χ (labeled in blue) (Figure 3.6).

3.3.7 Solid state NMR reveals distinct outer spore wall defects in the paralog mutants

Spore walls prepared from six different paralog mutant strains were similarly analyzed by solid state NMR. Complete spectra for each strain are shown in Figure 3.8. The dityrosine and component χ regions of the spectra are shown in Figure 3.9. The relative heights of the carbonyl and C_ζ resonances can be used to assess the amount of dityrosine in the spore wall (Figure 3.9A). For component χ, the height of the resonances relative to the -CH_3 peak provides an indicator of its abundance (Figure 3.9B). The phenotypes of the various mutants fell on a spectrum with respect to their severity: the Npp mutant showed no strong effect on dityrosine or component χ incorporation; the Osw4/6 mutant had reduced dityrosine but not component χ incorporation; the Osw/She mutant showed reduced dityrosine and a modest reduction component χ incorporation; the Gat and Dtr mutant strains had strong reductions in both dityrosine and component χ; and the Lds mutant appeared to completely lack resonances for both dityrosine and component χ. This NMR analysis confirms the effect of the paralog set mutants on dityrosine incorporation. In addition it identifies a new component of the outer spore wall, and shows that the Lds family proteins are essential for incorporation of both dityrosine and component χ into the wall.

3.3.8 The Lds proteins are localized to a specific population of lipid droplets

The possible role of the Lds proteins in component χ synthesis led us to examine the localization of these proteins. In sporulating cells, Lds1-GFP, Lds2-GFP, and Rrt8- GFP displayed similar localizations, concentrating in discrete patches or puncta along the

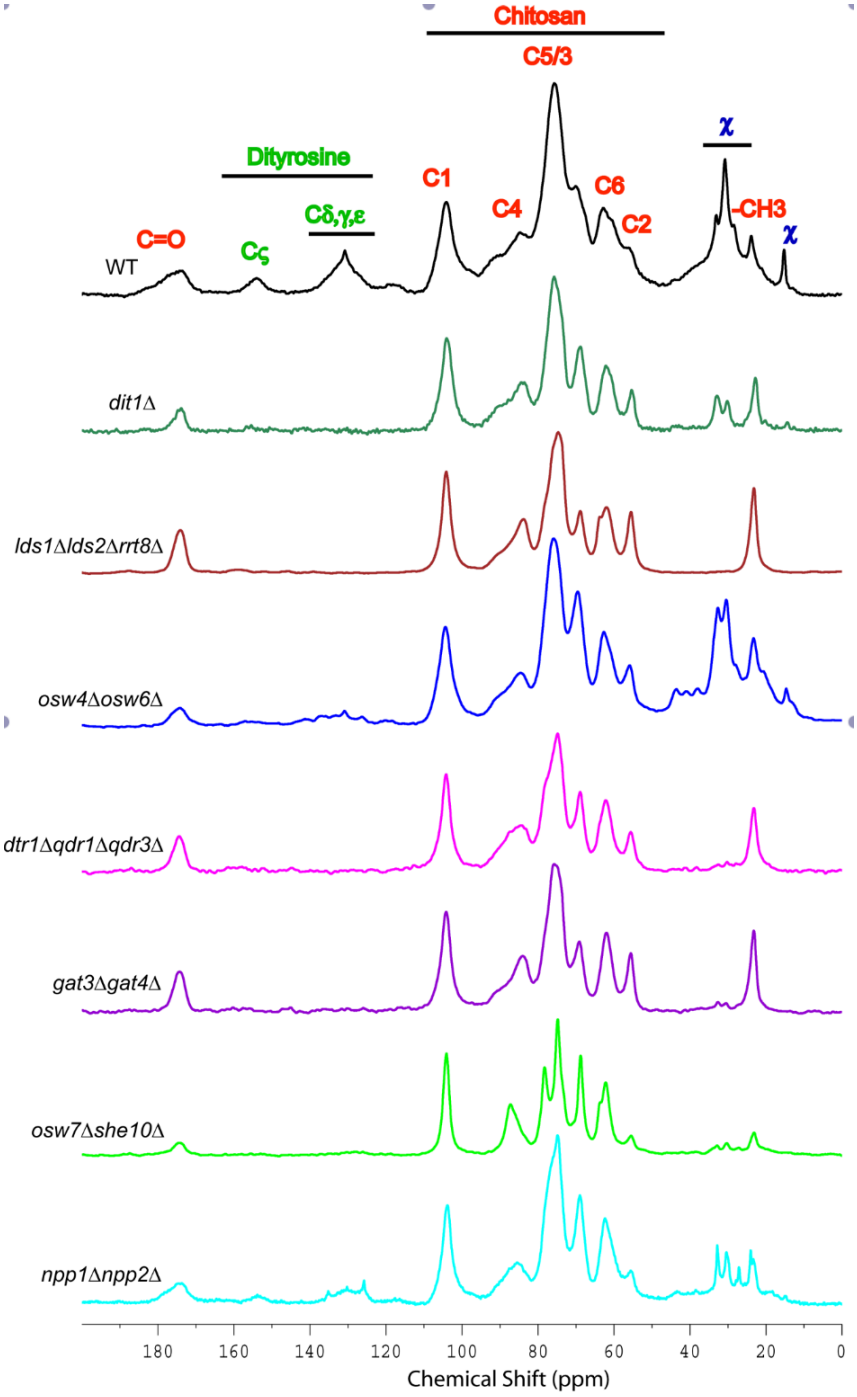

Figure 3.8 Complete NMR spectra for the strains shown in Figure 3.9. Resonances assigned to chitosan, dityrosine and component χ are indicated above the wild type spectrum. For comparison, all the spectra have been scaled to have the same height of the Chitosan C1 peak.

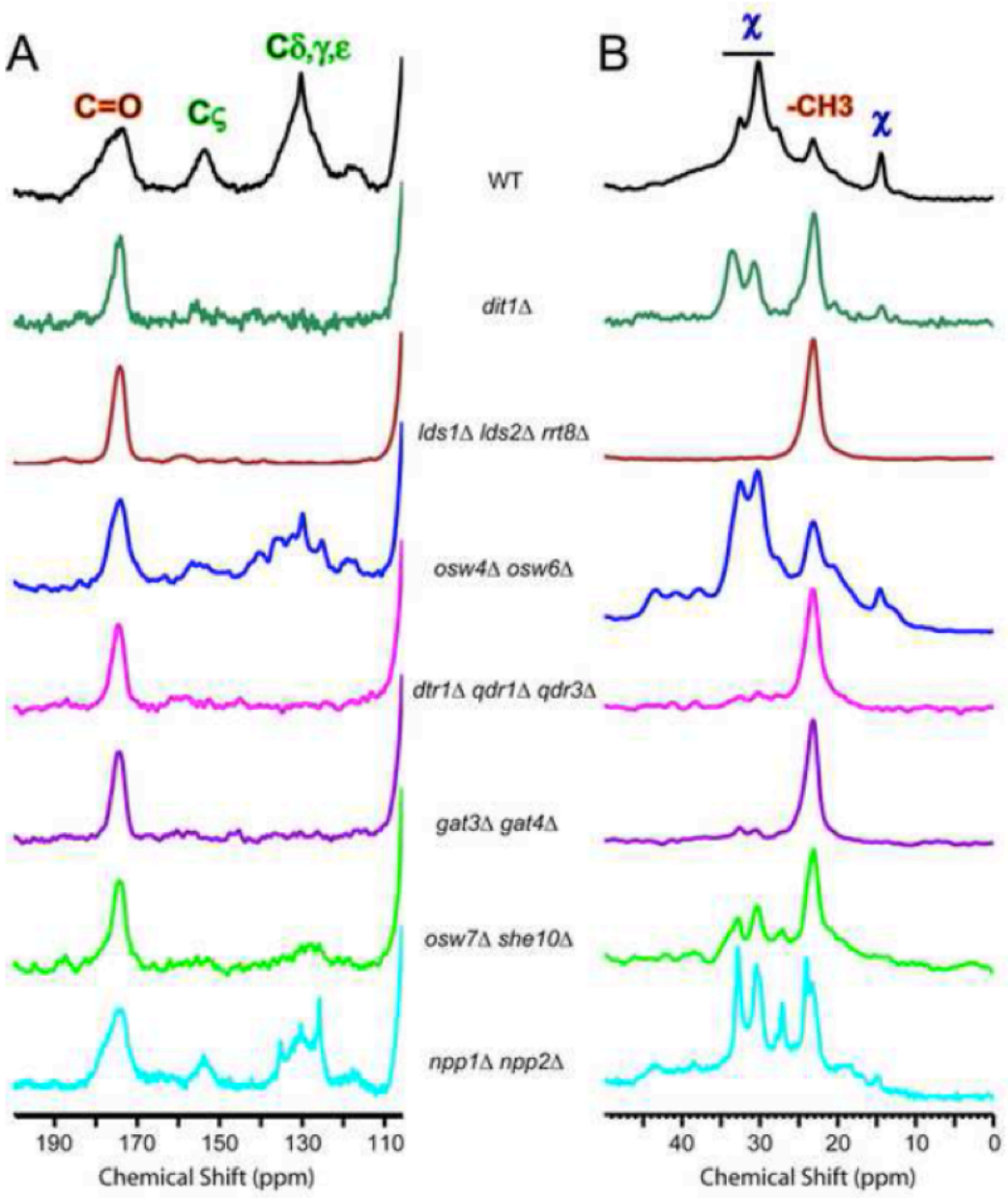

Figure 3.9 NMR analysis of outer spore walls in the paralog mutant strains. A) The dityrosine region of the ^{13}C NMR spectrum is shown for spore walls from wild type, *dit1*Δ and the indicated paralog mutant strains. Positions of the dityrosine chemical shifts and chitin carbonyl chemical shifts are indicated above the wild type spectrum. The spectra have been scaled so the height of the carbonyl resonance is constant. B) The component χ region of the ^{13}C NMR spectrum is shown for spore walls from wild type, *dit1*Δ and the indicated paralog mutant strains. Positions of the component χ chemical shifts and chitin methyl groupshifts are indicated above the wild type spectrum. The spectra have been scaled to the C5/3 resonance.

ascal sides of the growing prospore membranes in cells in mid-Meiosis II. In post-meiotic cells, the proteins localized more uniformly around the outside of spores, consistent with localization to the spore wall (Figure 3.11A).

An Rrt8-GFP fusion protein has previously been reported to localize to lipid droplets in vegetative cells, and an association of lipid droplets with the prospore membrane has been previously reported in electron microscopy studies (LYNN and MAGEE 1970). To determine if the foci observed for Lds set proteins during sporulation are lipid droplets, the localization of this organelle in sporulating cells was investigated. BODIPY 493/503, which has a green fluorescence, can be used to stain lipid droplets in yeast (SZYMANSKI *et al.* 2007). However, because the Lds proteins are fused to GFP that also fluoresces green, an alternative method for visualizing lipid droplets was required for co-localization experiments. Red fluorescent BODIPY TR displayed an identical staining pattern to BODIPY 493/503 in vegetative yeast cells making it a good alternative to BODIPY 493/503 (Figure 3.10). When cells in Meiosis II were stained with BODIPY TR, bright staining lipid droplets were seen inside of the prospore membrane with smaller but clear staining of droplets outside of the prospore membrane as well (Figure 3.11B). In post-meiotic cells, lipid droplets are seen inside of the spores, but the BODIPY TR staining outside of the prospore membrane is lost. As BODIPY stains lipid droplets by

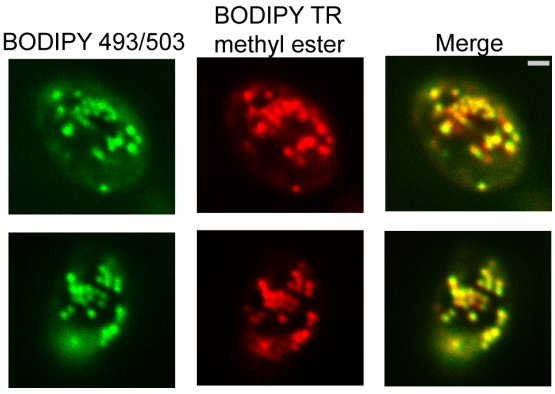

Figure 3.10 Two examples of wild type vegetative yeast cells co-stained with BODIPY 495/503 (green) and BODIPY TR (red).

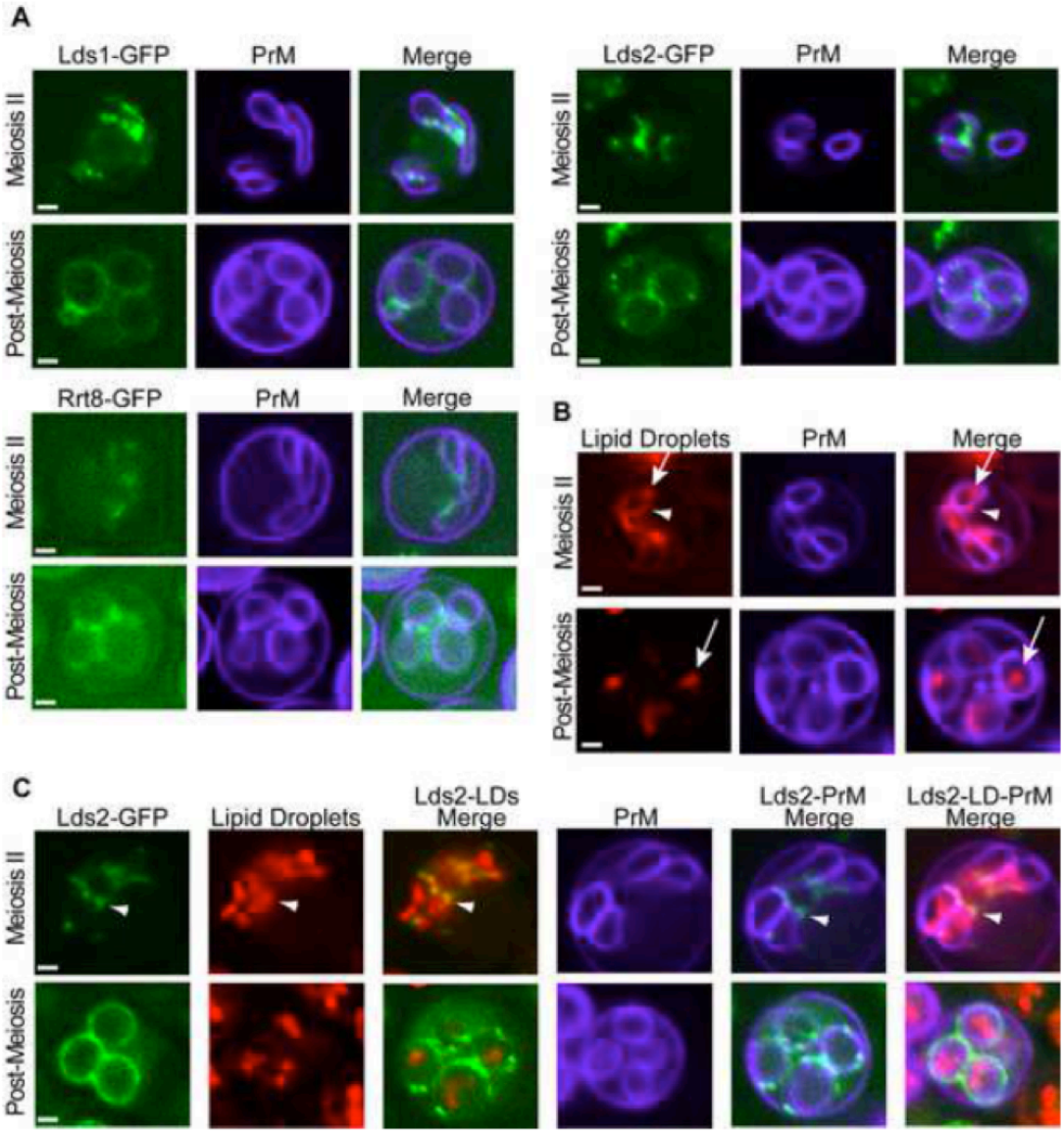

Figure 3.11 Localization of the Lds proteins involved in outer spore wall synthesis. A) Diploids expressing GFP fusions to the indicated protein as well as mTag-BFP-Spo20$^{51-91}$ as a prospore membrane (PrM) marker were sporulated and examined by fluorescence microscopy. Examples of a cell in the middle of Meiosis II and a post-meiotic cell are shown. B) Sporulating wild-type cells expressing mTag-BFP-Spo20$^{51-91}$were stained with the lipid droplet marker Bodipy TR. Arrowheads indicate lipid droplets associated with the ascal side of the prospore membrane. Arrows indicate lipid droplets within the prospore membrane C) Cells expressing both Lds2-GFP and mTag-BFP-Spo20$^{51-91}$ were stained with Bodipy TR. Arrowheads indicate localization of Lds2-GFP to a lipid droplet outside of the prospore membrane. For all experiments at least 20 cells at the indicated stage were scored and 100% of the cells displayed patterns similar to those shown here. Scale bars = 1 micron.

partitioning into the hydrophobic core of the droplet, this loss of staining suggests that the lipid constituents of the droplets outside of the prospore membrane are consumed during the process of spore wall development.

To determine whether the Lds proteins are present in lipid droplets, cells expressing both a blue fluorescent marker for the prospore membrane and Lds2-GFP were sporulated and stained with BODIPY TR. In mid-Meiosis II cells, Lds2-GFP puncta overlapped with or were directly adjacent to a subset of the lipid droplets that appear to be outside of the prospore membrane. No localization of Lds2-GFP to lipid droplets inside of the prospore membrane was observed (Figure 3.11C). In post-meiotic cells, no overlap of GFP with BODIPY TR staining was seen, indicating that the lipid droplets to which Lds2-GFP localizes are the ones consumed during spore wall formation. Thus, the Lds proteins localize to a specific subset of developmentally- regulated lipid droplets. The fluorescence images suggest that the specific lipid droplets to which the Lds proteins localize are found on or outside of the prospore membrane. However, the resolution of the fluorescence images is not sufficient to clearly determine the position of the lipid droplets relative to the prospore membrane. Transmission electron microscopy was used to examine the behavior of lipid droplets in sporulating wild type cells at higher resolution (Figure 3.12). Consistent with the fluorescence experiments, in mid-Meiosis II cells, lipid droplets can bee seen in close contact with the side of the prospore membrane facing the presumptive ascal cytoplasm (Figure 3.12A, B). These droplets are often irregularly shaped and their surface stains more darkly with permanganate than droplets inside of the prospore membrane. After prospore membrane closure, lipid droplets remain associated with the outer membrane (Figure 3.12C). In more mature asci, where spore wall assembly is nearly complete, lipid droplets in the ascal cytoplasm are rarer, but can still be found associated with the outer spore wall after outer membrane lysis (Figure 3.12D). Thus, there is a sub-population of lipid droplets that remain associated with the

exterior surface of the spore throughout spore wall formation. The localization of the Lds proteins to these lipid droplets positions the proteins so that they may contribute directly to outer spore wall morphogenesis.

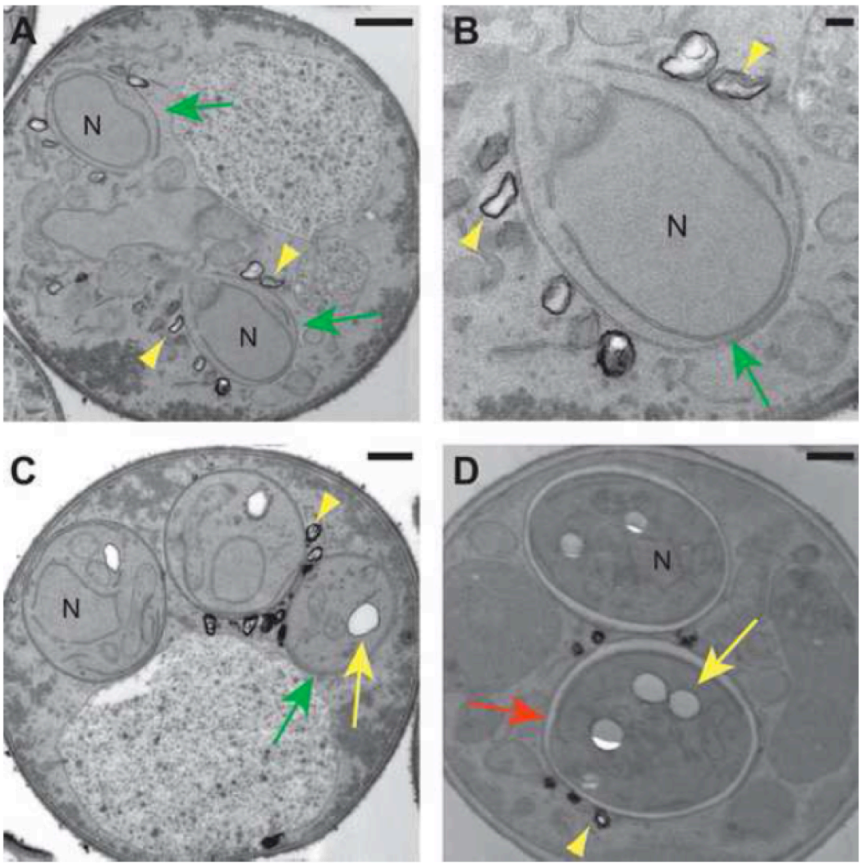

Figure 3.12 Electron microscopy of lipid droplets in sporulating cells. Electron micrographs of wild type cells. A) A cell in Meiosis II showing two prospore membranes (green arrows) engulfing nuclear lobes (N). Lipid droplets can be seen associated with the prospore membrane (yellow arrowheads). Scale bar = 500nm. B) Higher magnification of one of the prospore membranes in A. Scale bar = 100 nm. C) Post meiotic cell showing dark-stained lipid droplets (yellow arrowhead) associated with the outer membrane (green arrow). Lipid droplets inside of the spore (yellow arrow) do not stain as darkly with permanganate. N = nucleus. Scale bar = 500 nm. D) Lipid droplets in the ascus (yellow arrowhead) associated with the outer spore wall (red arrow) of mature spores. Yellow arrow indicated a lipid droplet within the spore cytoplasm. N = nucleus. Scale bar = 500 nm.

3.4 Discussion

Many screens for sporulation defective mutants in *S. cerevisiae* have been published and yet very few genes have been reported to affect the incorporation of dityrosine into the spore wall (RABITSCH *et al.* 2001; BRIZA *et al.* 2002; DEUTSCHBAUER *et al.* 2002; ENYENIHI and SAUNDERS 2003; MARSTON *et al.* 2004). This work shows that two levels of genetic redundancy are utilized in dityrosine assembly, which provides an explanation for the failure of mutant screens to reveal the genes involved. The first level of redundancy is a redundancy of process in which mutations in two genes not related by sequence is required to reveal a phenotype. In these instances, the pair of gene products, e.g. the secreted protease Osw3 and the ubiquitin ligase Hul4, have unrelated functions and yet the presence of one somehow buffers the loss of the other. How this is achieved is unclear. One possibility is that dityrosine might be incorporated into the wall via multiple mechanisms, for example different chemical linkages, and that loss of any individual linkage is insufficient to significantly reduce the fluorescence of the wall. The second level is redundancy of function; many of the genes involved have paralogs of overlapping activities present in the genome and so deletion of multiple paralogs is required to produce a strong phenotype. Paralogous genes are relatively common in *S. cerevisiae* due to a whole genome duplication event that occurred during the evolution of *Saccharomyces* (WOLFE and SHIELDS 1997). Of the paralogs listed in Table 3.2, five pairs (*LDS1/LDS2*, *ROG1/YDL109c*, *NPP1/NPP2*, *OSW7/SHE10*, *PES4/MIP6*) can be assigned to the whole genome duplication (SEOIGHE and WOLFE 1999).

Paralogs with overlapping function are predicted to be lost from the genome without selective pressures for retention of both copies (THOMAS 1993). Several explanations have been advanced to account for redundant paralogs, including compensatory regulation, dosage effects, and incomplete specialization (THOMAS 1993). In particular, redundant genes involved in development in metazoans have been suggested to serve as a

buffering system to protect against error (KRAKAUER and NOWAK 1999; WAGNER 2000). A similar logic may account for the redundancy in spore wall development. Many of the genes involved in spore wall development function only during this one phase of the yeast life cycle and, therefore, cannot be selected for during mitotic growth. Redundancy of these activities may provide "insurance" against loss-of-function mutations arising during vegetative growth.

3.4.1 Functions of the paralog sets

What specific roles do these different gene products play in assembly of the outer spore wall? For several of the genes identified, the function of the proteins is likely indirect. For example, Dtr1 and related transporters are required for delivery of precursors for assembly. Similarly, the Gat3 and Gat4 proteins are DNA-binding proteins and so are likely required for transcription of other genes whose products act on assembly. Very similar consensus binding sites have been defined for both Gat3 and Gat4 (BADIS *et al.* 2008). A search of yeast promoter sequences with these consensus sequences failed to identify any of the genes implicated in outer spore wall assembly (A. M. N., unpublished observations). Identification of the target genes for this pair of transcription factors may, therefore, identify additional genes involved in spore wall development.

Of the genes identified by the screen, *OSW4/OSW6* and *OSW7/SHE10* are the best candidates to encode proteins directly involved in assembly of the dityrosine layer. These genes encode proteins with predicted signal peptides and GFP fusions to Osw4 localized to the prospore membrane consistent with spore wall localization (C. Lin and A. M. Neiman, unpublished observations). Moreover, the ^{13}C NMR spectra of both of the Osw4/6 and Osw/She mutants are similar to that of *dit1*Δ, showing reduced dityrosine, but significant levels of both chitosan and component χ. Thus, these mutants appear somewhat specific in their effects on dityrosine. It remains to be determined if these

proteins play an enzymatic or structural role in the wall.

3.4.2 A role for lipid droplets in spore wall assembly

In vegetative cells, lipid droplets are seen as multiple puncta near the nuclear envelope and ER (SZYMANSKI *et al.* 2007). This distribution is changed in sporulating cells where a subset of lipid droplets is associated specifically with the ascal side of the prospore membrane. The Lds proteins are found on this class of lipid droplets and are essential for outer spore wall assembly, revealing a function for lipid droplets in this process.

The role of the Lds proteins in spore wall assembly is unclear, though the localization of lipid droplets to the surface of the spore wall (after outer membrane lysis) means that the Lds proteins could play a direct role in assembly. In addition to lacking dityrosine, the Lds mutant completely lacks component χ and has reduced Eosin Y and Calcofluor White staining, suggesting that the levels of chitosan may be reduced as well. Thus, the effect on dityrosine may be secondary to these other deficiencies, for instance, incorporation of component χ may be necessary for subsequent dityrosine assembly. Perhaps, some of the reactions in spore wall assembly actually occur on the surface of the lipid droplet, aided by the Lds proteins, before final incorporation of components into the wall. Additionally, both the EM studies and BODIPY staining suggest that the lipid constituents of the prospore membrane-associated lipid droplets are consumed during the course of spore wall assembly. Whether these lipids are used as an energy source for the spore, to expand the prospore membrane, or in some other way contribute to spore wall morphogenesis remains to be determined.

3.4.3 NMR analysis reveals a new component of the spore wall

Our results demonstrate that solid state NMR is an effective assay to examine the

composition of the outer spore wall. The ^{13}C spectrum of the outer spore wall is not overly complex, containing ~20 distinct carbon resonances. This relative simplicity suggests that more sensitive 2-dimensional NMR assays could be effective in defining the structural organization of the spore wall, including how the different components are linked to each other.

In addition, our analysis reveals a previously unknown component of the outer spore wall, which we designate χ. Based on peak height of the NMR resonances, component χ is less abundant in the wall than chitosan, but more abundant than dityrosine. From the analysis of the *dit1*Δ spore wall it is clear that incorporation of component c into the wall does not require dityrosine. Moreover, the Lds mutant spectrum shows that the chitosan layer is still formed in the absence of component χ. These data raise the possibility that component χ might act as a linker between the chitosan and dityrosine components of the spore wall.

The chemical nature of component χ remains to be determined, though based on previous biochemical characterizations of purified outer spore walls, it seems unlikely to be either a polysaccharide or a protein (BRIZA *et al.* 1990b). The lack of a carbonyl resonance associated with component c in the NMR data also indicates that it does not contain amino acids. The positions of the component c chemical shifts are consistent with reduced carbons such as in alkanes. Given that the Lds proteins required for component c incorporation are localized to lipid droplets adjacent to the developing spore wall, perhaps generation of component c requires material that is delivered from the lipid droplets to the spore wall.

It is also noteworthy that levels in the spore wall of component χ are reduced in the *dtr1*Δ *qdr1*Δ *qdr3*Δ mutant strain. This strain lacks dityrosine in the wall because of a failure to export monomeric dityrosine from the spore cytoplasm (FELDER *et al.* 2002). However, the reduction of component χ in this strain cannot be an effect of reduced

dityrosine because incorporation of component c is unaffected in *dit1*Δ cells that lack dityrosine. One straightforward possibility is that like dityrosine, some precursor to component c is synthesized in the spore cytoplasm and exported to the wall by Dtr1 and related transporters.

3.4.4 Implications for other fungi

Genomic sequencing has revealed that many pathogenic fungi possess the enzymes for the production of chitosan and dityrosine. This is true even of fungi that do not form spores, such as *Candida albicans*. In fact, dityrosine has been found in the vegetative cell walls of *C. albicans* and mutants in dityrosine synthesis show drug sensitivity consistent with cell wall defects (SMAIL *et al.* 1995; MELO *et al.* 2008). Chitosan is also an important component of the wall of the pathogen *Cryptococcus neoformans*, where it is required for cell wall integrity and for virulence (BAKER *et al.* 2007; BAKER *et al.* 2011). While *Cryptococcus* does not synthesize dityrosine, it incorporates an analogous polyphenolic compound, melanin, into the cell wall and melanization is important for resistance of the fungus to various environmental stresses and may play an important role in the evasion of host immune responses during infection (CASADEVALL *et al.* 2000; EISENMAN and CASADEVALL 2012). Interestingly, *C. neoformans* mutants lacking chitosan display a "leaky melanin" phenotype, suggesting that chitosan is required for proper incorporation of melanin into the cell wall (BAKER *et al.* 2007). The nature of the connection between the carbohydrate and polyphenol components of the spore wall is, therefore, an important general issue in understanding the structure of the fungal cell wall. Assembly of the outer spore wall in *S. cerevisiae* provides a tractable model to address this issue. Our results identify several new genes intimately involved in construction of the outer spore wall. Further analysis of these gene products should provide insights into the structure of the spore wall and the mechanisms of its assembly.

Chapter 4

Conclusions and future prospects

Assembly of the fungal cell wall to form an extracellular matrix (ECM) outside of the cell plasma membrane is not only a challenging task for fungal cells, but also provides an attractive model for studying cell wall developmental processes. In addition, since cell walls are essential for cell integrity and also often cause the virulence effects by pathogenic fungi, fungal cell walls can be the potential target for antifungal drug development.

The outermost layers of spore wall are composed of a dityrosine polymer connected to a polysaccharide layer containing N-acetyl glucosamine, which give rise to spores resistance to varied environmental stresses. This thesis describes a highly redundant gene network for outer spore wall assembly. Because of the redundancy, the dityrosine assembly pathway is difficult to dissect and therefore the detailed mechanism is not clear so far. From this work, we found six groups of paralogous genes that are closely related to outer spore wall formation. By solid-state NMR analysis, the spore wall of these paralogous gene set deletion strains present different patterns, although they all represented a common theme of spore wall defect. For the purpose of figuring out the mechanisms for outer spore wall assembly, the combinations of redundant gene sets and the paralogous gene groups are excellent candidates for further study. Here, I list the mutants which reveal significant outer spore wall defects and may provide as powerful tools for further biochemical and cell biological studies.

Lds set: *lds1Δ lds2Δ rrt8Δ*

The observation of direct (physical) association between lipid droplets and prospore membranes can be traced to early TEM studies of sporulating cells (Lynn and Magee, 1970). However, the lipid droplet proteins described in this thesis is the first discovery showing the direct evidence that lipid droplet proteins contribute functional roles for spore wall development. LDs (lipid droplets) are highly dynamic cytoplasmic organelles in yeast cells. They are composed of a core of neutral lipids, such as triacylglycerols (TAGs) and sterol esters (SEs), surrounded by a monolayer of phospholipids (Tauchi-Sato *et al*. 2002) and associated proteins. In vegetative cells, LDs are catabolized during the exponential growth stage due to the increased need for phospholipids while cell are dividing, and during the stationary phase, LDs are found more abundant. LDs are found close to ER, where LDs are formed, in vegetative stage (Szymanski et al., 2007). During sporulation, the distribution of LDs is different. One subset of LDs is associated with the ascal cytoplasm of the prospore membrane, and locates at spore wall after complete the meiotic division. The Lds proteins are found to localize on this group of LDs.

The NMR signals of lds1Δ lds2Δ rrt8Δ spore wall samples show dramatically reduced dityrosine, component χ, and moderately reduced chitosan signal. Protein sequence analysis reveals multiple hydrophobic patches/ transmembrane (TM) domains in these Lds proteins: Lds1p contains 5 TM segments, Lds2p has 4 TM regions, and Rrt8p harbors 5 TM fragments. Although these proteins don't look like enzymes, the possible roles may be the assistance for the outer spore wall formation. Indeed, the hydrophobic environment provided by LDs may assist key reactions for the wall assembly, and these proteins my serve as scaffold for the happening of the key steps. Noticeably, rrt8Δ single deletion spores already show severe phenotypically defects, it will be interesting to analyze more detail biochemically in this strain, say TEM and solid-state NMR analysis.

Osw4/6 set: *osw4Δ osw6Δ*

The NMR spectra from *osw4Δ osw6Δ* spores reveal the specific reducing signals from dityrosine fractions, and the chitosan and component χ are consistently similar with the spectra from WT spores. Osw4p and Osw6p are predicted to contain signal peptide. The functional GFP fusion proteins are clearly localized to the prospore membrane, indicating that they are directly involved in the dityrosine layer assembly. A high copy suppressor screening performed on *osw4Δ osw6Δ* cells found several interesting candidates which may provide extended idea for dityrosine layer assembly: *YEL023c*, *QDR3*, *YBR042c*, and *FAT1*. Since Dit1p, Dit2p and Dtr1p serve the early steps for the dityrosine synthesis, an in silico algorithm designed to find candidates which are coevolved with these three proteins was done, and *YEL023c* was found by this method (L Carey and A. Neiman unpublished data). Therefore, *YEL023c* found from this screen reveals the evolutional rational for dityrosine formation. *QDR3* is one of the members of **multidrug transporter of the major facilitator superfamily** contains 12 TM domains. Since dityrosine layer assembly required Dtr1p to transport to outer spore wall, Qdr3p may also serve similar roles. This result is also consistent with the data from synthetic genetic screen described in previous chapter.

Dtr set: *dtr1Δ qdr1Δ qdr3Δ*

As described previously, Dtr1p plays the role as dityrosine transporter. However, in a *DTR1* gene deletion, the spore wall dityrosine layer is still formed. By contrast, spores of the triple deletion of the three paralogous transporters reveal not only dityrosine defects, but also the reducing of component χ, based on NMR spectra. This result indicates that component χ is synthesized in the cytoplasm and then, by the assist of dityrosine transporter, transfer to the outer spore wall. To further identify the chemical structure of component χ, it is worthy to apply the strategy of metabolomics for this deletion strain.

Ideally, we can compare the difference of cytoplasmic extracts in late sporulating cells between the triple deletion and WT strains. Without the assist of multiple drug transporters, component χ and dityrosine would be dramatically accumulated in the cytosol.

Gat set: *gat3Δ gat4Δ*

The NMR spectra of *gat3Δ gat4Δ* spore wall show dramatically erased of dityrosine and component χ signals. Gat3p and Gat4p are DNA binding proteins carrying GATA family zinc finger motifs. They may regulate the transcription of other genes and those regulated gene products may contribute for outer spore wall assembly. It will be interesting to apply microarray and ribosome-profiling studies for both WT and *gat3Δ gat4Δ* strains to compare the genes which are turned on during sporulation.

Appendix:

Spore wall sample preparation for LC-MS/MS analysis

Methods:

After bead-beating to disrupt the intact ascospores, the spore wall materials first go through SDS extraction steps. The spore walls are washed with 1M NaCl three times and then resuspended into SDS-containing buffer with 50 mM Tris-HCl (pH 7.8), 2% SDS, 100mM EDTA, and 40 mM β-mercaptoethanol at 100°C for 5 minutes followed by washing with water for three times. The SDS extraction steps should be repeated for five times. The speed applied for spinning samples down is 8,000 rpm. The spore wall samples are dried with speed vacuum concentrator under low temperature. The second step is washing by methanol solution with 50% methanol (with HPLC grade), 20 mM di-AP (diammonium phosphate), pH 8.0. As SDS will interfere with the signal in LC-MS/MS, this step is critical to get rid of residue SDS from the spore wall samples. The samples are resuspended in methanol solution and vortex for 15 to 30 minutes at room temperature and repeated the step for 5 times. Then, resuspend sample in the solution and vortex overnight at 4°C following with 30 to 60 minutes of vortex at room temperature for 3 times. Again, freeze dry the sample before start next step. The third step is reduction by resuspending samples in 100 mM ammonium bicarbonate (NH_4HCO_3) containing 10 mM DTT, and incubated at 56°C for 1 hour. The fourth step is alkylation by resuspending samples in 100 mM ammonium bicarbonate containing 55 mM iodoacetamide (C_2H_4INO) at room temperature for 45 minutes **in the dark**. Then samples are washed 3 times with 50 mM ammonium bicarbonate following by drying under vacuum. The fifth step is trypsin digestion. Samples are resuspended in 50 mM ammonium bicarbonate, and incubated overnight at 37°C adding sequencing-grade

trypsin (Promega, V511A) with a protein/enzyme ratio of 50: 1. The supernatants containing the solubilized peptides are collected and completely dried by speed vacuum concentrator under low temperature. The sixth step is pre-ZipTip step. The dried samples are resuspended in 50 µl of 0.5% TFA solution following by sonication for 10 minutes and centrifugation with 13,000 rpm for 10 minutes to precipitate undissolved particles and collect supernatant. The seventh step is ZipTip C18 (EMD Millipore) clean up. Place ZipTip on P20 pipetman and set volume for 20 µl. Washing twice with 20 µl of 95% acetonitrile containing 0.1% formate for activation of the ZipTip as well as washing twice with 20 µl of 0.1% formate for balance.

Bibliography

AESCHBACH, R., R. AMADO and H. NEUKOM, 1976 Formation of dityrosine cross-links in proteins by oxidation of tyrosine residues. Biochim Biophys Acta **439:** 292-301.

AHMED, N. T., D. BUNGARD, M. E. SHIN, M. MOORE and E. WINTER, 2009 The Ime2 protein kinase enhances the disassociation of the Sum1 repressor from middle meiotic promoters. Mol Cell Biol **29:** 4352-4362.

ALTSCHUL, S. F., W. GISH, W. MILLER, E. W. MYERS and D. J. LIPMAN, 1990 Basic local alignment search tool. J Mol Biol **215:** 403-410.

ANDERSEN, S. O., 1964 The Cross-Links in Resilin Identified as Dityrosine and Trityrosine. Biochim Biophys Acta **93:** 213-215.

ANDERSON, S. F., C. M. STEBER, R. E. ESPOSITO and J. E. COLEMAN, 1995 UME6, a negative regulator of meiosis in Saccharomyces cerevisiae, contains a C-terminal Zn2Cys6 binuclear cluster that binds the URS1 DNA sequence in a zinc-dependent manner. Protein Sci **4:** 1832-1843.

BADIS, G., E. T. CHAN, H. VAN BAKEL, L. PENA-CASTILLO, D. TILLO *et al.*, 2008 A library of yeast transcription factor motifs reveals a widespread function for Rsc3 in targeting nucleosome exclusion at promoters. Mol Cell **32:** 878-887.

BAKER, L. G., C. A. SPECHT, M. J. DONLIN and J. K. LODGE, 2007 Chitosan, the deacetylated form of chitin, is necessary for cell wall integrity in Cryptococcus neoformans. Eukaryot Cell **6:** 855-867.

BAKER, L. G., C. A. SPECHT and J. K. LODGE, 2011 Cell wall chitosan is necessary for virulence in the opportunistic pathogen Cryptococcus neoformans. Eukaryot Cell **10:** 1264-1268.

BARTNICKI-GARCIA, S., 1968 Cell wall chemistry, morphogenesis, and taxonomy of fungi. Annu Rev Microbiol **22:** 87-108.

BHATTACHARJEE, S., S. PENNATHUR, J. BYUN, J. CROWLEY, D. MUELLER *et al.*, 2001 NADPH oxidase of neutrophils elevates o,o'-dityrosine cross-links in proteins and urine during inflammation. Arch Biochem Biophys **395:** 69-77.

BRIZA, P., E. BOGENGRUBER, A. THUR, M. RUTZLER, M. MUNSTERKOTTER *et al.*, 2002 Systematic analysis of sporulation phenotypes in 624 non-lethal homozygous deletion strains of Saccharomyces cerevisiae. Yeast **19:** 403-422.

BRIZA, P., M. BREITENBACH, A. ELLINGER and J. SEGALL, 1990a Isolation of two developmentally regulated genes involved in spore wall maturation in Saccharomyces cerevisiae. Genes Dev **4:** 1775-1789.

BRIZA, P., M. ECKERSTORFER and M. BREITENBACH, 1994 The sporulation-specific enzymes encoded by the DIT1 and DIT2 genes catalyze a two-step reaction leading to a soluble LL-dityrosine-containing precursor of the yeast spore wall. Proc Natl Acad Sci U S A **91:** 4524-4528.

BRIZA, P., A. ELLINGER, G. WINKLER and M. BREITENBACH, 1988 Chemical composition of the yeast ascospore wall. The second outer layer consists of chitosan. J Biol Chem **263:** 11569-11574.

BRIZA, P., A. ELLINGER, G. WINKLER and M. BREITENBACH, 1990b Characterization of a DL-dityrosine-containing macromolecule from yeast ascospore walls. J Biol Chem **265:** 15118-15123.

BRIZA, P., H. KALCHHAUSER, E. PITTENAUER, G. ALLMAIER and M. BREITENBACH, 1996 N,N'-Bisformyl dityrosine is an in vivo precursor of the yeast ascospore wall. Eur J Biochem **239:** 124-131.

BRIZA, P., G. WINKLER, H. KALCHHAUSER and M. BREITENBACH, 1986 Dityrosine is a prominent component of the yeast ascospore wall- A proof of its structure. J Biol Chem **261:** 4288-4294.

BURKE, D. J., D. C. AMBERG and J. N. STRATHERN, 2005 *Methods in Yeast Genetics: A Cold Spring Harbor Laboratory Course Manual*. Cold Spring Harbor Laboratory Press, Cold Spring Harbor, N.Y.

CASADEVALL, A., A. L. ROSAS and J. D. NOSANCHUK, 2000 Melanin and virulence in Cryptococcus neoformans. Curr Opin Microbiol **3:** 354-358.

CHRISTODOULIDOU, A., V. BOURIOTIS and G. THIREOS, 1996 Two sporulation-specific chitin deacetylase-encoding genes are required for the ascospore wall rigidity of Saccharomyces cerevisiae. J Biol Chem **271:** 31420-31425.

CHRISTODOULIDOU, A., P. BRIZA, A. ELLINGER and V. BOURIOTIS, 1999 Yeast ascospore wall assembly requires two chitin deacetylase isozymes. FEBS Lett **460:** 275-279.

CHU, S., J. DERISI, M. EISEN, J. MULHOLLAND, D. BOTSTEIN *et al.*, 1998 The transcriptional program of sporulation in budding yeast. Science **282:** 699-705.

CHU, S., and I. HERSKOWITZ, 1998 Gametogenesis in yeast is regulated by a transcriptional cascade dependent on Ndt80. Mol Cell **1:** 685-696.

COLUCCIO, A., E. BOGENGRUBER, M. N. CONRAD, M. E. DRESSER, P. BRIZA *et al.*, 2004a Morphogenetic pathway of spore wall assembly in Saccharomyces cerevisiae. Eukaryot Cell **3:** 1464-1475.

COLUCCIO, A., M. MALZONE and A. M. NEIMAN, 2004b Genetic evidence of a role for membrane lipid composition in the regulation of soluble NEM-sensitive factor receptor function in Saccharomyces cerevisiae. Genetics **166:** 89-97.

COLUCCIO, A. E., R. K. RODRIGUEZ, M. J. KERNAN and A. M. NEIMAN, 2008 The yeast spore wall enables spores to survive passage through the digestive tract of Drosophila. PLoS One **3:** e2873.

DAWES, I. W., and I. D. HARDIE, 1974 Selective killing of vegetative cells in sporulated yeast cultures by exposure to diethyl ether. Mol Gen Genet **131:** 281-289.

DEITS, T., M. FARRANCE, E. S. KAY, L. MEDILL, E. E. TURNER *et al.*, 1984 Purification and properties of ovoperoxidase, the enzyme responsible for hardening the fertilization membrane of the sea urchin egg. J Biol Chem **259:** 13525-13533.

DENNING, D. W., 2003 Echinocandin antifungal drugs. Lancet **362:** 1142-1151.

DEUTSCHBAUER, A. M., R. M. WILLIAMS, A. M. CHU and R. W. DAVIS, 2002 Parallel phenotypic analysis of sporulation and postgermination growth in Saccharomyces cerevisiae. Proc Natl Acad Sci U S A **99:** 15530-15535.

DICKINSON, J. R., 2004 Life cycle and morphogenesis, pp. 1-19 in *Metabolism and Molecular Physiology of Saccharomyces Cerevisiae, 2nd Edition*. CRC Press.

DIJKGRAAF, G. J., M. ABE, Y. OHYA and H. BUSSEY, 2002 Mutations in Fks1p affect the cell wall content of beta-1,3- and beta-1,6-glucan in Saccharomyces cerevisiae. Yeast **19:** 671-690.

EISENMAN, H. C., and A. CASADEVALL, 2012 Synthesis and assembly of fungal melanin. Appl Microbiol Biotechnol **93:** 931-940.

ENYENIHI, A. H., and W. S. SAUNDERS, 2003 Large-scale functional genomic analysis of sporulation and meiosis in Saccharomyces cerevisiae. Genetics **163:** 47-54.

FARKAS, V., 1979 Biosynthesis of cell walls of fungi. Microbiol Rev **43:** 117-144.

FAZZIO, T. G., C. KOOPERBERG, J. P. GOLDMARK, C. NEAL, R. BASOM *et al.*, 2001 Widespread collaboration of Isw2 and Sin3-Rpd3 chromatin remodeling complexes in transcriptional repression. Mol Cell Biol **21:** 6450-6460.

FELDER, T., E. BOGENGRUBER, S. TENREIRO, A. ELLINGER, I. SA-CORREIA *et al.*, 2002 Dtrlp, a multidrug resistance transporter of the major facilitator superfamily, plays an essential role in spore wall maturation in Saccharomyces cerevisiae. Eukaryot Cell **1:** 799-810.

FOERDER, C. A., and B. M. SHAPIRO, 1977 Release of ovoperoxidase from sea urchin eggs hardens the fertilization membrane with tyrosine crosslinks. Proc Natl Acad Sci U S A **74:** 4214-4218.

FRANTZ, C., K. M. STEWART and V. M. WEAVER, 2010 The extracellular matrix at a glance. J Cell Sci **123:** 4195-4200.

FRIEDLANDER, G., D. JOSEPH-STRAUSS, M. CARMI, D. ZENVIRTH, G. SIMCHEN *et al.*, 2006 Modulation of the transcription regulatory program in yeast cells committed to sporulation. Genome Biol **7:** R20.

FRIESEN, H., S. R. HEPWORTH and J. SEGALL, 1997 An Ssn6-Tup1-dependent negative regulatory element controls sporulation-specific expression of DIT1 and DIT2 in Saccharomyces cerevisiae. Mol Cell Biol **17:** 123-134.

FUKAMIZO, T., T. OHKAWA, K. SONODA, H. TOYODA, T. NISHIGUCHI *et al.*, 1992 Chitinous components of the cell wall of Fusarium oxysporum. Biosci Biotechnol Biochem **56:** 1632-1636.

GIULIVI, C., and K. J. DAVIES, 1993 Dityrosine and tyrosine oxidation products are endogenous markers for the selective proteolysis of oxidatively modified red blood cell hemoglobin by (the 19 S) proteasome. J Biol Chem **268:** 8752-8759.

GIULIVI, C., and K. J. DAVIES, 1994 Dityrosine: a marker for oxidatively modified proteins and selective proteolysis. Methods Enzymol **233:** 363-371.

GIULIVI, C., N. J. TRAASETH and K. J. DAVIES, 2003 Tyrosine oxidation products: analysis and biological relevance. Amino Acids **25:** 227-232.

GOLDMARK, J. P., T. G. FAZZIO, P. W. ESTEP, G. M. CHURCH and T. TSUKIYAMA, 2000 The Isw2 chromatin remodeling complex represses early meiotic genes upon recruitment by Ume6p. Cell **103:** 423-433.

GOLDSTEIN, A. L., and J. H. MCCUSKER, 1999 Three new dominant drug resistance cassettes for gene disruption in Saccharomyces cerevisiae. Yeast **15:** 1541-1553.

GOMEZ-ESQUER, F., J. M. RODRIGUEZ-PENA, G. DIAZ, E. RODRIGUEZ, P. BRIZA *et al.*, 2004 CRR1, a gene encoding a putative transglycosidase, is required for proper spore wall assembly in Saccharomyces cerevisiae. Microbiology **150:** 3269-3280.

GROSS, A. J., and I. W. SIZER, 1959 The oxidation of tyramine, tyrosine, and related compounds by peroxidase. J Biol Chem **234:** 1611-1614.

GULLION, T., and J. SCHAEFER, 1989 Rotational-echo double-resonance NMR. J. Magn. Reson. **81:** 196-200.

HARTMANN, S. R., and E. L. HAHN, 1962 Nuclear Double Resonance in the Rotating Frame. Physical Review **128:** 2042-2053.

HUANG, L. S., H. K. DOHERTY and I. HERSKOWITZ, 2005 The Smk1p MAP kinase negatively regulates Gsc2p, a 1,3-beta-glucan synthase, during spore wall morphogenesis in Saccharomyces cerevisiae. Proc Natl Acad Sci U S A **102:** 12431-12436.

INOUE, S. B., N. TAKEWAKI, T. TAKASUKA, T. MIO, M. ADACHI *et al.*, 1995 Characterization and gene cloning of 1,3-beta-D-glucan synthase from Saccharomyces cerevisiae. Eur J Biochem **231:** 845-854.

ISHIHARA, S., A. HIRATA, S. NOGAMI, A. BEAUVAIS, J. P. LATGE *et al.*, 2007 Homologous subunits of 1,3-beta-glucan synthase are important for spore wall assembly in Saccharomyces cerevisiae. Eukaryot Cell **6:** 143-156.

JABS, A., M. WEISSA and R. HILGENFELD, 1999 Non-proline Cis peptide bonds in proteins. J Mol Biol **286:** 291-304.

JANTTI, J., M. K. AALTO, M. OYEN, L. SUNDQVIST, S. KERANEN *et al.*, 2002 Characterization of temperature-sensitive mutations in the yeast syntaxin 1 homologues Sso1p and Sso2p, and evidence of a distinct function for Sso1p in sporulation. J Cell Sci **115:** 409-420.

KADOSH, D., and K. STRUHL, 1998 Targeted recruitment of the Sin3-Rpd3 histone deacetylase complex generates a highly localized domain of repressed chromatin in vivo. Mol Cell Biol **18:** 5121-5127.

KASSIR, Y., D. GRANOT and G. SIMCHEN, 1988 IME1, a positive regulator gene of meiosis in S. cerevisiae. Cell **52:** 853-862.

KERN, T., S. HEDIGER, P. MULLER, C. GIUSTINI, B. JORIS *et al.*, 2008 Toward the characterization of peptidoglycan structure and protein-peptidoglycan interactions by solid-state NMR spectroscopy. J Am Chem Soc **130:** 5618-5619.

KLIS, F. M., A. BOORSMA and P. W. DE GROOT, 2006 Cell wall construction in Saccharomyces cerevisiae. Yeast **23:** 185-202.

KLIS, F. M., P. MOL, K. HELLINGWERF and S. BRUL, 2002 Dynamics of cell wall structure in Saccharomyces cerevisiae. FEMS Microbiol Rev **26:** 239-256.

KNOP, M., and K. STRASSER, 2000 Role of the spindle pole body of yeast in mediating assembly of the prospore membrane during meiosis. EMBO J **19:** 3657-3667.

KOLLAR, R., E. PETRAKOVA, G. ASHWELL, P. W. ROBBINS and E. CABIB, 1995 Architecture of the yeast cell wall. The linkage between chitin and beta(1-->3)-glucan. J Biol Chem **270:** 1170-1178.

KOLLAR, R., B. B. REINHOLD, E. PETRAKOVA, H. J. YEH, G. ASHWELL *et al.*, 1997 Architecture of the yeast cell wall. Beta(1-->6)-glucan interconnects mannoprotein, beta(1-->)3-glucan, and chitin. J Biol Chem **272:** 17762-17775.

KRAKAUER, D. C., and M. A. NOWAK, 1999 Evolutionary preservation of redundant duplicated genes. Semin Cell Dev Biol **10:** 555-559.

KREGER-VAN RIJ, N. J., 1978 Electron microscopy of germinating ascospores of Saccharomyces cerevisiae. Arch Microbiol **117:** 73-77.

KRISAK, L., R. STRICH, R. S. WINTERS, J. P. HALL, M. J. MALLORY *et al.*, 1994 SMK1, a developmentally regulated MAP kinase, is required for spore wall assembly in Saccharomyces cerevisiae. Genes Dev **8:** 2151-2161.

KUPIEC, M., B. BYERS, R. E. ESPOSITO and A. P. MITCHELL, 1997 *11 Meiosis and Sporulation in Saccharomyces cerevisiae*.

LEEUWENBURGH, C., P. A. HANSEN, J. O. HOLLOSZY and J. W. HEINECKE, 1999a Hydroxyl radical generation during exercise increases mitochondrial protein oxidation and levels of urinary dityrosine. Free Radic Biol Med **27:** 186-192.

LEEUWENBURGH, C., P. A. HANSEN, J. O. HOLLOSZY and J. W. HEINECKE, 1999b Oxidized amino acids in the urine of aging rats: potential markers for assessing oxidative stress in vivo. Am J Physiol **276:** R128-135.

LESAGE, A., M. BARDET and L. EMSLEY, 1999 Through-Bond Carbon−Carbon Connectivities in Disordered Solids by NMR. Journal of the American Chemical Society **121:** 10987-10993.

LESAGE, G., and H. BUSSEY, 2006 Cell wall assembly in Saccharomyces cerevisiae. Microbiol Mol Biol Rev **70:** 317-343.

LEVITT, M. H., 2008 *Spin Dynamics: Basics of Nuclear Magnetic Resonance, 2nd Edition*. Wiley.

LYNN, R. R., and P. T. MAGEE, 1970 Development of the spore wall during ascospore formation in Saccharomyces cerevisiae. J Cell Biol **44:** 688-692.

MARSTON, A. L., W. H. THAM, H. SHAH and A. AMON, 2004 A genome-wide screen identifies genes required for centromeric cohesion. Science **303:** 1367-1370.

MATHIESON, E. M., C. SCHWARTZ and A. M. NEIMAN, 2010 Membrane assembly modulates the stability of the meiotic spindle-pole body. J Cell Sci **123:** 2481-2490.

MAZUR, P., and W. BAGINSKY, 1996 In vitro activity of 1,3-beta-D-glucan synthase requires the GTP-binding protein Rho1. J Biol Chem **271:** 14604-14609.

MAZUR, P., N. MORIN, W. BAGINSKY, M. EL-SHERBEINI, J. A. CLEMAS *et al.*, 1995 Differential expression and function of two homologous subunits of yeast 1,3-beta-D-glucan synthase. Mol Cell Biol **15:** 5671-5681.

MCDONALD, C. M., K. F. COOPER and E. WINTER, 2005 The Ama1-directed anaphase-promoting complex regulates the Smk1 mitogen-activated protein kinase during meiosis in yeast. Genetics **171:** 901-911.

MCDONALD, C. M., M. WAGNER, M. J. DUNHAM, M. E. SHIN, N. T. AHMED *et al.*, 2009 The Ras/cAMP pathway and the CDK-like kinase Ime2 regulate the MAPK Smk1 and spore morphogenesis in Saccharomyces cerevisiae. Genetics **181:** 511-523.

MELO, N. R., G. P. MORAN, A. G. WARRILOW, E. DUDLEY, S. N. SMITH *et al.*, 2008 CYP56 (Dit2p) in Candida albicans: characterization and investigation of its role in growth and antifungal drug susceptibility. Antimicrob Agents Chemother **52:** 3718-3724.

MISHRA, C., C. E. SEMINO, K. J. MCCREATH, H. DE LA VEGA, B. J. JONES *et al.*, 1997 Cloning and expression of two chitin deacetylase genes of Saccharomyces cerevisiae. Yeast **13:** 327-336.

MIZUNO, T., N. NAKAZAWA, P. REMGSAMRARN, T. KUNOH, Y. OSHIMA *et al.*, 1998 The Tup1-Ssn6 general repressor is involved in repression of IME1 encoding a transcriptional activator of meiosis in Saccharomyces cerevisiae. Curr Genet **33:** 239-247.

MRSA, V., T. SEIDL, M. GENTZSCH and W. TANNER, 1997 Specific labelling of cell wall proteins by biotinylation. Identification of four covalently linked O-mannosylated proteins of Saccharomyces cerevisiae. Yeast **13:** 1145-1154.

NAKANISHI, H., M. MORISHITA, C. L. SCHWARTZ, A. COLUCCIO, J. ENGEBRECHT *et al.*, 2006 Phospholipase D and the SNARE Sso1p are necessary for vesicle fusion during sporulation in yeast. J Cell Sci **119:** 1406-1415.

NEIGEBORN, L., and A. P. MITCHELL, 1991 The yeast MCK1 gene encodes a protein kinase homolog that activates early meiotic gene expression. Genes Dev **5:** 533-548.

NEIMAN, A. M., 1998 Prospore membrane formation defines a developmentally regulated branch of the secretory pathway in yeast. J Cell Biol **140:** 29-37.

NEIMAN, A. M., 2005 Ascospore formation in the yeast Saccharomyces cerevisiae. Microbiol Mol Biol Rev **69:** 565-584.

NEIMAN, A. M., 2011 Sporulation in the budding yeast Saccharomyces cerevisiae. Genetics **189:** 737-765.

NEIMAN, A. M., L. KATZ and P. J. BRENNWALD, 2000 Identification of domains required for developmentally regulated SNARE function in Saccharomyces cerevisiae. Genetics **155:** 1643-1655.

NICKAS, M. E., C. SCHWARTZ and A. M. NEIMAN, 2003 Ady4p and Spo74p are components of the meiotic spindle pole body that promote growth of the prospore membrane in Saccharomyces cerevisiae. Eukaryot Cell **2:** 431-445.

ORLEAN, P., 2012 Architecture and biosynthesis of the Saccharomyces cerevisiae cell wall. Genetics **192:** 775-818.

PAK, J., and J. SEGALL, 2002 Role of Ndt80, Sum1, and Swe1 as targets of the meiotic recombination checkpoint that control exit from pachytene and spore formation in Saccharomyces cerevisiae. Mol Cell Biol **22:** 6430-6440.

PAMMER, M., P. BRIZA, A. ELLINGER, T. SCHUSTER, R. STUCKA *et al.*, 1992 DIT101 (CSD2, CAL1), a cell cycle-regulated yeast gene required for synthesis of chitin in cell walls and chitosan in spore walls. Yeast **8:** 1089-1099.

PANDEY, N. K., and A. I. ARONSON, 1979 Properties of the Bacillus subtilis spore coat. J Bacteriol **137:** 1208-1218.

PIERCE, M., K. R. BENJAMIN, S. P. MONTANO, M. M. GEORGIADIS, E. WINTER *et al.*, 2003 Sum1 and Ndt80 proteins compete for binding to middle sporulation element sequences that control meiotic gene expression. Mol Cell Biol **23:** 4814-4825.

PINES, A., M. G. GIBBY and J. S. WAUGH, 1973 Proton-enhanced NMR of dilute spins in solids. The Journal of Chemical Physics **59:** 569-590.

PRIMIG, M., R. M. WILLIAMS, E. A. WINZELER, G. G. TEVZADZE, A. R. CONWAY *et al.*, 2000 The core meiotic transcriptome in budding yeasts. Nat Genet **26:** 415-423.

RABITSCH, K. P., A. TOTH, M. GALOVA, A. SCHLEIFFER, G. SCHAFFNER *et al.*, 2001 A screen for genes required for meiosis and spore formation based on whole-genome expression. Curr Biol **11:** 1001-1009.

RIEDEL, C. G., M. MAZZA, P. MAIER, R. KORNER and M. KNOP, 2005 Differential requirement for phospholipase D/Spo14 and its novel interactor Sma1 for regulation of exocytotic vesicle fusion in yeast meiosis. J Biol Chem **280:** 37846-37852.

SARKAR, P. K., M. A. FLORCZYK, K. A. MCDONOUGH and D. K. NAG, 2002 SSP2, a sporulation-specific gene necessary for outer spore wall assembly in the yeast Saccharomyces cerevisiae. Mol Genet Genomics **267:** 348-358.

SCHABER, M., A. LINDGREN, K. SCHINDLER, D. BUNGARD, P. KALDIS *et al.*, 2002 CAK1 promotes meiosis and spore formation in Saccharomyces cerevisiae in a CDC28-independent fashion. Mol Cell Biol **22:** 57-68.

SEOIGHE, C., and K. H. WOLFE, 1999 Updated map of duplicated regions in the yeast genome. Gene **238:** 253-261.

SHANNON, P., A. MARKIEL, O. OZIER, N. S. BALIGA, J. T. WANG *et al.*, 2003 Cytoscape: a software environment for integrated models of biomolecular interaction networks. Genome Res **13:** 2498-2504.

SHENOUDA, N. S., Y. PAN, J. SCHAEFER and G. E. WILSON, 1996 A simple solid-state NMR method for determining peptidoglycan crosslinking in Bacillus subtilis. Biochim Biophys Acta **1289:** 217-220.

SHIN, M. E., A. SKOKOTAS and E. WINTER, 2010 The Cdk1 and Ime2 protein kinases trigger exit from meiotic prophase in Saccharomyces cerevisiae by inhibiting the Sum1 transcriptional repressor. Mol Cell Biol **30:** 2996-3003.

SMAIL, E. H., P. BRIZA, A. PANAGOS and L. BERENFELD, 1995 Candida albicans cell walls contain the fluorescent cross-linking amino acid dityrosine. Infect Immun **63:** 4078-4083.

SMITH, H. E., S. S. SU, L. NEIGEBORN, S. E. DRISCOLL and A. P. MITCHELL, 1990 Role of IME1 expression in regulation of meiosis in Saccharomyces cerevisiae. Mol Cell Biol **10:** 6103-6113.

SMITS, G. J., H. VAN DEN ENDE and F. M. KLIS, 2001 Differential regulation of cell wall biogenesis during growth and development in yeast. Microbiology **147:** 781-794.

STEBER, C. M., and R. E. ESPOSITO, 1995 UME6 is a central component of a developmental regulatory switch controlling meiosis-specific gene expression. Proc Natl Acad Sci U S A **92:** 12490-12494.

STERN, M., R. JENSEN and I. HERSKOWITZ, 1984 Five SWI genes are required for expression of the HO gene in yeast. J Mol Biol **178:** 853-868.

STRICH, R., R. T. SUROSKY, C. STEBER, E. DUBOIS, F. MESSENGUY *et al.*, 1994 UME6 is a key regulator of nitrogen repression and meiotic development. Genes Dev **8:** 796-810.

SUBACH, O. M., I. S. GUNDOROV, M. YOSHIMURA, F. V. SUBACH, J. ZHANG *et al.*, 2008 Conversion of red fluorescent protein into a bright blue probe. Chem Biol **15:** 1116-1124.

SUDA, Y., R. K. RODRIGUEZ, A. E. COLUCCIO and A. M. NEIMAN, 2009 A screen for spore wall permeability mutants identifies a secreted protease required for proper spore wall assembly. PLoS One **4:** e7184.

SZYMANSKI, K. M., D. BINNS, R. BARTZ, N. V. GRISHIN, W. P. LI *et al.*, 2007 The lipodystrophy protein seipin is found at endoplasmic reticulum lipid droplet junctions and is important for droplet morphology. Proc Natl Acad Sci U S A **104:** 20890-20895.

TACHIKAWA, H., A. BLOECHER, K. TATCHELL and A. M. NEIMAN, 2001 A Gip1p-Glc7p phosphatase complex regulates septin organization and spore wall formation. J Cell Biol **155:** 797-808.

TAKEGOSHI, K., S. NAKAMURA and T. TERAO, 2001 13C–1H dipolar-assisted rotational resonance in magic-angle spinning NMR. Chemical Physics Letters **344:** 631-637.

TAKEGOSHI, K., S. NAKAMURA and T. TERAO, 2003 [sup 13]C--[sup 1]H dipolar-driven [sup 13]C--[sup 13]C recoupling without [sup 13]C rf irradiation in nuclear magnetic resonance of rotating solids. The Journal of Chemical Physics **118:** 2325-2341.

THOMAS, J. H., 1993 Thinking about genetic redundancy. Trends Genet **9:** 395-399.

TONG, A. H., G. LESAGE, G. D. BADER, H. DING, H. XU *et al.*, 2004 Global mapping of the yeast genetic interaction network. Science **303:** 808-813.

UFANO, S., P. SAN-SEGUNDO, F. DEL REY and C. R. VAZQUEZ DE ALDANA, 1999 SWM1, a developmentally regulated gene, is required for spore wall assembly in Saccharomyces cerevisiae. Mol Cell Biol **19:** 2118-2129.

VERSHON, A. K., and M. PIERCE, 2000 Transcriptional regulation of meiosis in yeast. Curr Opin Cell Biol **12:** 334-339.

WAGNER, A., 2000 The role of population size, pleiotropy and fitness effects of mutations in the evolution of overlapping gene functions. Genetics **154:** 1389-1401.

WAGNER, M., P. BRIZA, M. PIERCE and E. WINTER, 1999 Distinct steps in yeast spore morphogenesis require distinct SMK1 MAP kinase thresholds. Genetics **151:** 1327-1340.

WILLIAMS, R. M., M. PRIMIG, B. K. WASHBURN, E. A. WINZELER, M. BELLIS *et al.*, 2002 The Ume6 regulon coordinates metabolic and meiotic gene expression in yeast. Proc Natl Acad Sci U S A **99:** 13431-13436.

WINZELER, E. A., D. D. SHOEMAKER, A. ASTROMOFF, H. LIANG, K. ANDERSON *et al.*, 1999 Functional characterization of the S. cerevisiae genome by gene deletion and parallel analysis. Science **285:** 901-906.

WOLFE, K. H., and D. C. SHIELDS, 1997 Molecular evidence for an ancient duplication of the entire yeast genome. Nature **387:** 708-713.

YANG, H. J., H. NAKANISHI, S. LIU, J. A. MCNEW and A. M. NEIMAN, 2008 Binding interactions control SNARE specificity in vivo. J Cell Biol **183:** 1089-1100.